Study on the Effective Screening of Cell-selective Peptides and the Application for Biomaterials

細胞選択的ペプチドの効率的探索と生体材料への応用に関する研究

Kei KANIE

蟹江　慧

Department of Biotechnology, School of Engineering,

Nagoya University, Japan

名古屋大学大学院　工学研究科　化学・生物工学専攻

Contents

Chapter 1

General Introduction

1.1. Tissue engineering with biomaterials for the application of regenerative medicine

Recently, regenerative medicine has been one of the most attracting scientific researches over the world. In 2006, Shinya Yamanaka et al. established the induced pluripotent stem (iPS) cells from mouse fibroblasts [1]. And they also established the human iPS cells from human fibroblasts [2]. From the epoch-making event, the research of iPS cells is advancing very fast in recent few years [3]. iPS cells could be prospective for cell therapy of all our tissues, because it is believed that they have the multi potency to differentiate to all kinds of cells. In additional and important advantage, they have no immunologic rejection because the iPS cells are obtained from our own body.

To make regenerative medicine fit for practical applications, there are two approaches. One therapeutic approach is transplantation of cells (such as stem cells), and the other approach is the tissue engineering with biomaterials. In the transplantation, cells are administrated into the body by the bolus injection or infusion method. However, few cells are retained at the transplanted site and their grafted rate is very low because of their excretion and death. To overcome these problems, it is

necessary to give the cells an environment suitable for their survival and functional achievement. Tissue engineering is based on tissue reconstruction, in which cell scaffolds as environmental surroundings is inevitable materials. The basic concept of biomaterial-based tissue engineering was originally introduced by Langer and Vacanti in 1993 [4]. The key technology of biomaterials-based tissue regeneration is the preparation of cell scaffolds to promote cell adhesion, proliferation and differentiation (**Fig. 1**). The scaffold is generally prepared from biomaterials, while the biomaterial is also used as the delivery carrier of biosignalling molecules as the cell nutrients to biologically activate cells. Cell scaffold and biosignalling molecule delivery technologies with biomaterials have been demonstrated to create cell environments suitable for tissue regeneration [5-7].

Biomaterials play a key role in creating the environment for cells, and many biomaterials are used for many types of medical devices (**Fig. 2**). As the biomaterials, various synthetic and natural materials, such as polymers, ceramics, metals and their composites, have been investigated and used in different manners. In particular, polymers are used for many medical devices and artificial organs, because of its flexibility, lightness and advantage of manufacturing. Many kinds of polymers, such as synthetic biodegradable polymers or natural materials, are used in the form of sponge, fibers or hydrogels for scaffolds to support for cell adhesion, proliferation, differentiation and organization [8, 9]. **Table 1** shows the biodegradable polymers including synthetic or natural polymers. Biodegradable polymers are useful to support the reconstruction of a new tissue without inflammation.

The ultimate goal of biomaterials is to develop synthetic three-dimensional (3D) constructs that restore and enhance the functions of healthy tissues. Developmental studies provide crucial information about the interactions of cells with the extracellular matrix (ECM) that regulate the fate and function of cells.

1.2. The importance of extracellular matrix (ECM)

Basically, tissue is composed of two components that are cells and the surrounding environment. The latter includes the extracellular matrix (ECM) which is required for cell adhesion, proliferation and differentiation (natural scaffold) as the living place of cells and biosignalling molecules as the growth factors of cells. The ECM is a complex of collagens, elastic fibers, glycosaminoglycans, and adhesive glycoproteins [10]. The roles of the ECM are indispensable not only to maintain the structures of tissues but also to control cell adhesion, proliferation, differentiation and fate (**Table 2**). Each tissue is composed of an ECM with a unique composition and topology that is generated during tissue development through a dynamic and reciprocal, biochemical and biophysical relationship between the various types of cells (e.g. epithelial, fibroblast, endothelial elements) and their microenvironment. For example, cartilage ECM, which is highly enriched in large proteoglycans and collagen II, has an additional unique function in resisting compression. By contrast, basement membrane ECMs, which are enriched in the glycoproteins laminin and collagen IV with a lesser amount of proteoglycans and growth factors, regulate cell polarity, separate different tissue types, and have a specialized function as a molecular filter in the kidney [11].

Cells attach with transmembrane integrin receptors that bind to specific motifs on the matrix proteins, such as collagen, laminin, fibronectin and vitronectin [12]. And there are more than 150 proteins that stimulate various cellular functions, including tissue organization, migration, and differentiation [13, 14]. These cellular functions will be revealed by the understanding of cell-ECM communication mechanisms [15].

Collagen is the most abundant protein in the human body which constitutes a heterogeneous class of proteins. Up to now about 20 different collagens have been characterized, and various mechanical and functional properties have been exhibited. Some collagens are specific for a given

tissue. Type II collagen is found in cartilage mentioned above. Types I, II, and III are the most abundant collagens in human body that form fibrils responsible for the tensile strength of the tissue. Types IV, VII, IX, X, and XII are found associated with collagen fibrils or organized in the network as a basement membrane. In addition to mechanical and structural functions, collagens play an important role in determining cell attachment and spreading [16], differentiation and movement [17].

Fibronectin plays an important role in attachment of cells to surrounding surfaces, movement and differentiation [18]. Along the backbone of the molecule there are present multiple RGD (Arg-Gly-Asp), RGDS (Arg-Gly-Asp-Ser), LDV (Leu-Asp-Val), and REDV (Arg-Glu-Asp-Val) sequences that are responsible for cell binding [19], while other domains of fibronectin represent binding sites for other ECM molecules such as collagen, fibrin, heparin sulfate, etc. Due to its broad binding properties, fibronectin is widely used for anchorage dependent cell culture including tissue reconstruction, in order to favor cell adhesion and spreading.

Laminin is found mainly associated with basement membranes. RGD sequences are also present along the backbone of the molecule chains together with other specific sequences, such as PDSGR (Pro-Asp-Ser-Gly-Arg), YIGSR (Tyr-Ile-Gly-Ser-Arg), and IKVAV (Ile-Lys-Val-Ala-Val) sequences that are able to recognize and bind to cell-surface receptors [20]. Given its high cell binding affinity, laminin alone or in combination with other ECM molecules is widely used to coat cell culture dishes and implant materials to enhance cell attachment and spreading.

1.3. The application of ECM as biomaterials

Considering the function of ECM, it is natural to come up with the idea of mimicking ECMs as biomaterials. The ECM is an ideal biological material in nature. The molecules in the ECM provide

the place for adjacent cells which communicate with each other and with the external environment [11, 15]. Individual components of the ECM such as collagen, laminin, fibronectin and hyaluronic acid can be isolated and used both *in vitro* and *in vivo* to facilitate cell growth and differentiation. Various forms of the intact ECM have been used as biological scaffolds to promote the constructive remodeling of tissues and organs. Many ECM materials derived from human and animals have been commercialized for a variety of therapeutic application [21]. The ECM used in these scaffold materials are derived from a variety of tissues, including heart valves, blood vessels, skin, nerves, skeletal muscle, tendons, ligaments, small intestinal submucosa, urinary bladder and liver. **Table 3** shows a partial list of biological scaffold materials currently available for clinical use.

1.4. Peptides as biomimetic materials

To serve as a scaffold for cells, scaffold should mimic the advantageous feature of the natural ECM. Because the tissue regeneration with the tissue engineering process is not exactly the same as the natural developmental or wound healing mechanism, it is difficult for a scaffold to entirely mimic the ECM. There is also an aspect that natural ECMs or its derivatives are not suitable for tissue engineering applications. Since tissue engineering is an accelerated artificial regeneration process compared to the natural development program, natural material might be too moderate. For example, mature tissue matrix seldom possess a macro- or micro-pore structures to allow quick and uniform cell spreading and dispersion, which is essential for regeneration. In addition, the elimination of the infectious pathogen transmission is always a severe demand for natural ECMs. Therefore artificially designed scaffolds are indispensable for accelerated tissue regeneration.

Consequently, a biomimetic scaffold has the demand to be artificially designed for tissue engineering. In other words, the scaffold that mimics partial and effective advantageous features of

the natural ECM is required.

The surface of scaffold is important in tissue engineering, because the surface can directly relate to cellular response and affect ultimately the regeneration [22]. An ideal tissue engineering scaffold should positively interact with cells, including enhanced cell adhesion, proliferation and differentiated function. Although a variety of synthetic biodegradable polymers have been used as biomaterials, they often lack the biocompability.

Extensive studies have been performed to provide biomimetic materials that are recognized by cells as ECMs. The surface modification of biomaterials with bioactive molecules is a simple way to make biomimetic materials. Early works have used long chains of ECM proteins such as fibronectin, vitronectin, and laminin for surface modification. Biomaterials can be coated with these proteins, which promoted cell adhesion and proliferation. In addition, signaling domains that are composed of ECM proteins also accelerate the surface modification of biomaterial. Thus the short peptide fragments which can primarily interact with cell membrane receptors have been used for surface modification in numerous studies [23]. The selective synthetic peptide sequences used in tissue engineering applications are summarized in **Table 4**.

The most commonly used peptide for surface modification is RGD, a signaling domain derived from fibronectin and laminin. Other peptide sequences such as YIGSR, REDV, and IKVAV have been also immobilized on various model materials. A number of materials including metal oxide [24], and polymers [25] have been modified with these peptides and characterized for cellular interaction with surfaces of the materials.

In particular, the use of a short peptide for surface modification is advantageous over the use of the long chain of native ECM proteins. The native ECM protein tends to be randomly folded upon adsorption to the biomaterial surface such that the receptor binding domains are not always statically available. However, the short peptide sequences are relatively more stable from enzymatic

digestion compared to long proteins, therefore availability is considered to be high. In addition, short peptide sequences can be massively synthesized in laboratories more economically. The biomimetic material modified with these bioactive molecules can be used as a tissue engineering scaffold that potentially serves as artificial ECM, which provides suitable biological cues to guide new tissue formation.

1.5. Cell-based functional peptide screening techniques

Peptide is one of the most effective biological molecules that regulate the complex biological mechanism in our body. Recently, interests have been increasing for the cell-interactive peptides as an ideal synthetic biological material in medical and cellular biology. Examples of the potential uses of such peptides include the following: (a) as a stimulating factor for cellular events [26-28], (b) as a scaffold for cell culture [29-31], and (c) as a targeting tag molecule for objective delivery [32-35].

Currently, many types of peptide screening have been developed: the peptide beads library [36], phage display [37] and peptide array [38]. Although the peptide array has long been applied to assay various biological targets [39, 40], there are still few reports on peptide-cell (animal cell) interaction assays. To the best of our knowledge, the work of Otvos et al [41] is the only publication other than our work that clearly indicates the SPOT peptide array's applicability to the cell-stimulation assay. Their pioneering work indicated the applicability of a cellulose-support-type peptide array for the direct stimulation of animal T helper cells. However, most animal cells are composed of anchorage-dependent cells, which require an adhesive surface to be cultured. Peptide array-based interaction assay of solid-bound peptide and anchorage-dependent cells (PIASPAC) method are proposed and applied it to various types of cells (not only animal cells but also human

cells) for assaying (1) cell-adhesion peptides [42, 43] and (2) tumor-inhibition peptides [44, 45].

1.6. Aim of this thesis

In this thesis, the aim is to obtain cell-selective peptide for developing the biomimetic biomaterial by using peptide array. The ultimate goal of this study is to design novel biomaterial, especially ECM mimetic biomaterial having cell-selectivity (**Fig. 3**). Concerning how to screen the cell-selective peptides, we focused on the ECM that has the selectivity and applied for biomaterials. Biomaterials should be suitable for the environment that they are implanted, and suitable for certain tissues and cells. If the biomaterials are not suitable for certain tissues and cells, side effect such as inflammatory response would occur. Hence it is necessary to develop the surface modification molecule that has selectivity for cells in tissue regeneration. The idea for the surface modification is to design cell-selective surface applying the mechanism of natural mechanism (**Fig. 4A**). Basically, natural tissue has the cell-selectivity that correctly generates well-organized tissue by itself. In such construction, ECMs have the key roles including cell adhesion, proliferation, differentiation, tensile strength, boundary between different tissue types (**Table 2**), and have the cell-selectivity to construct correct tissue. Thus the cell-selective peptides that mimic functions of specific ECM are needed to be explored as functional biomaterials. And investigating the cell-selectivity of ECM as peptide level could lead to understand the mechanism of ECM. Thus the possibility of designing the ECM mimetic biomaterials safety and effectively is increasing.

In this thesis, the basic concept of such screening was supported by two hypotheses.

First, we hypothesized that cells could adhere to not only one strict peptide sequence such as

RGD that is very little concentration in one ECM sequence, but also flexible peptide sequences as physicochemical preferences such as electric charge or hydrophobicity. Previous work with fibronectin identified several cell-adhesion peptides were comparable with the conventional RGD ligand [42]. And amino acid substitution revealed that certain flexibility in peptide sequence is possible, but was confined to certain physicochemical parameters [43]. ECM protein also has the physicochemical preference. Considering the conservation of evaluation, the protein is not strictly constructed with exclusive sequences but is rather flexible. For instance, the high homologous proteins are not matched at 100% sequences but their function is often similar to each other. Thus cell could adhere not strictly but flexible.

Second, we hypothesized that ECM-specificity is partially governed by the physicochemical preference. Based on the first hypothesis, if the physicochemical preference of ECM has the cell-selectivity, ECM-specificity is related to the differences of physicochemical preferences. For example, collage type II and IV exist in certain tissues and have the cell-selectivity. Thus there is a possibility that the physicochemical preference in ECM induce the cell-selectivity. We propose that the cell-selectivity of certain ECM types is supported not only by cell receptor ligands but also by peptides that are uniquely enriched in the given ECM type. The focus of the present work is to determine which sequences govern the cellular preferences that are unique to a particular ECM type.

Based on that, to consider mimicking the particular ECM, it is important to use not only one discrete ligand-like peptide but uniquely found within a specific ECM type. Additionally, it is very important to screen a number of cell-selective peptides by understanding the function of ECM.

In this study, the tissue of blood vessel was focused as a model case. Blood vessel mainly has three cell types, endothelial cell (EC), smooth muscle cell (SMC) and fibroblast (FB). To investigate our hypothesis, we used two strategies: (1) Investigation of the cell-selectivity peptides

constructed with the particular amino acids sequences (homo-oligopeptide) and (2) Investigation of the cell-selectivity peptides from certain ECM sequences (ECM-specific peptides) (**Fig. 4B**).

This thesis is constructed with following four chapters.

In Chapter 2, Standardization scheme for datasets obtained from peptide array for comparative cell-selectivity is described. To evaluate "cell-selectivity", several cell types should be compared. In this comparison of array data, the dataset from different cells, and different arrays should be standardized effectively. With peptide array, such comparative analysis methodology has not well being developed. Therefore, I have developed the basic scheme to obtain novel cell-selective peptides effectively by peptide array-based cell assay.

In Chapter 3, the cell-selective preference of simple peptides that composed of particular amino acids is described. Three types of cells (EC, SMC and FB) were selected to be compared for the cellular preference toward different amino acids. Cell adhesion and proliferation was examined in detail with single amino acid peptides (20 kinds of amino acid peptide that are 1-mer, 5-mer, and 7-mer).

In Chapter 4, the cell-selectivity of ECM-specific peptides is described. Two types of cells (EC, SMC) were examined since they both interact with basement membrane that includes aboundingly collagen type IV, the target ECM, in the blood vessel. From the screening, one of the cell-selective peptide was also applied to modify the poly (ε-caprolactone) (PCL) biomaterial, and evaluated its effect *in vitro*.

In Chapter 5, further application of the obtained cell-selective peptide (CAG) as medical biomaterial modification evaluated *in vivo* is described. The biological investigation such as immunostaining, scanning electron microscopy (SEM) and Western blotting, were investigated.

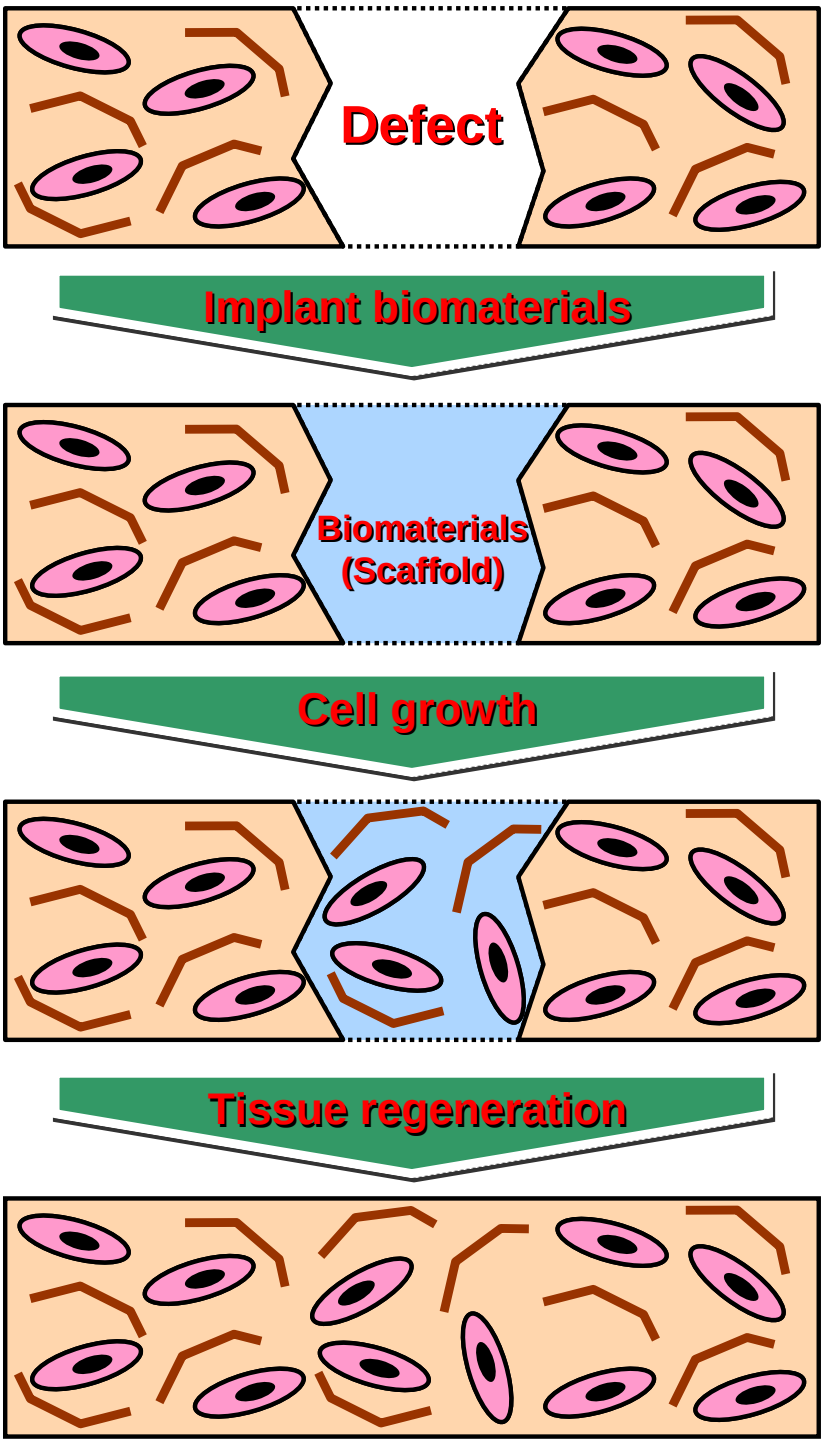

Figure 1. Role of biomaterials in tissue engineering-based regeneration therapy.

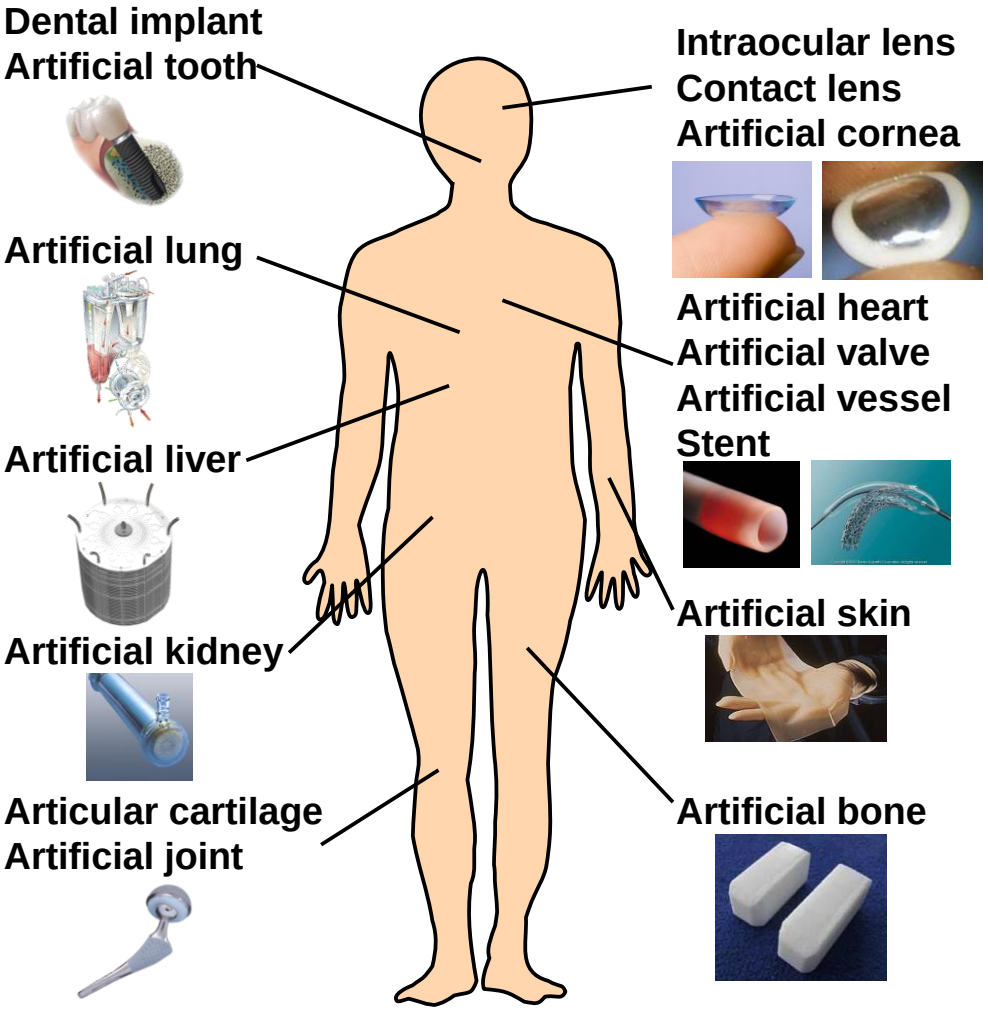

*** The pictures used in this figure referred to the URLs [last accessed Jan 2011]**

http://www.mmt-med.co.jp	http://technologywonk.com	http://www.toyobo.co.jp
http://www.bostonscientific.jp	http://www.chiba-reha.jp	http://www.xconomy.com
http://www.topnews.in	http://www.hopkinsmedicine.org	http://www.jsao.org

Figure 2. The medical devices, prosthetic devices and artificial organs that use the biomaterials.

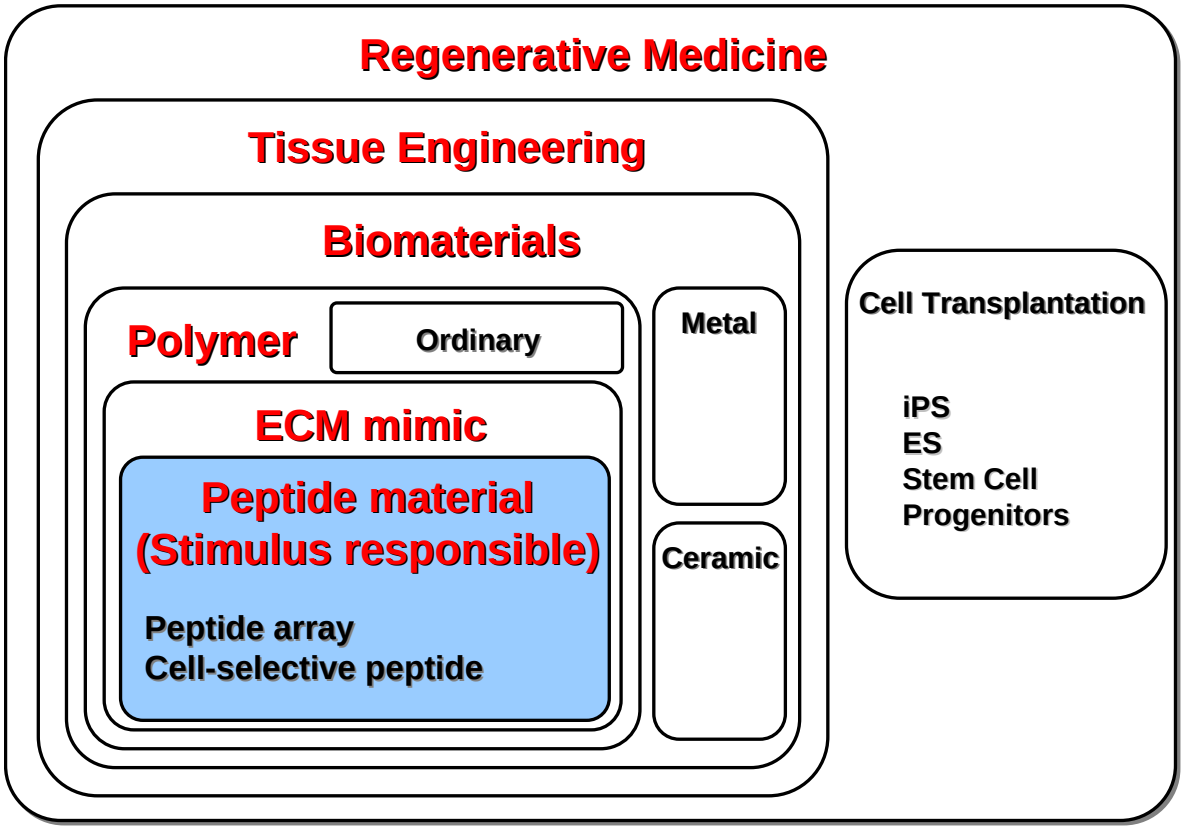

Figure 3. The field of my thesis.

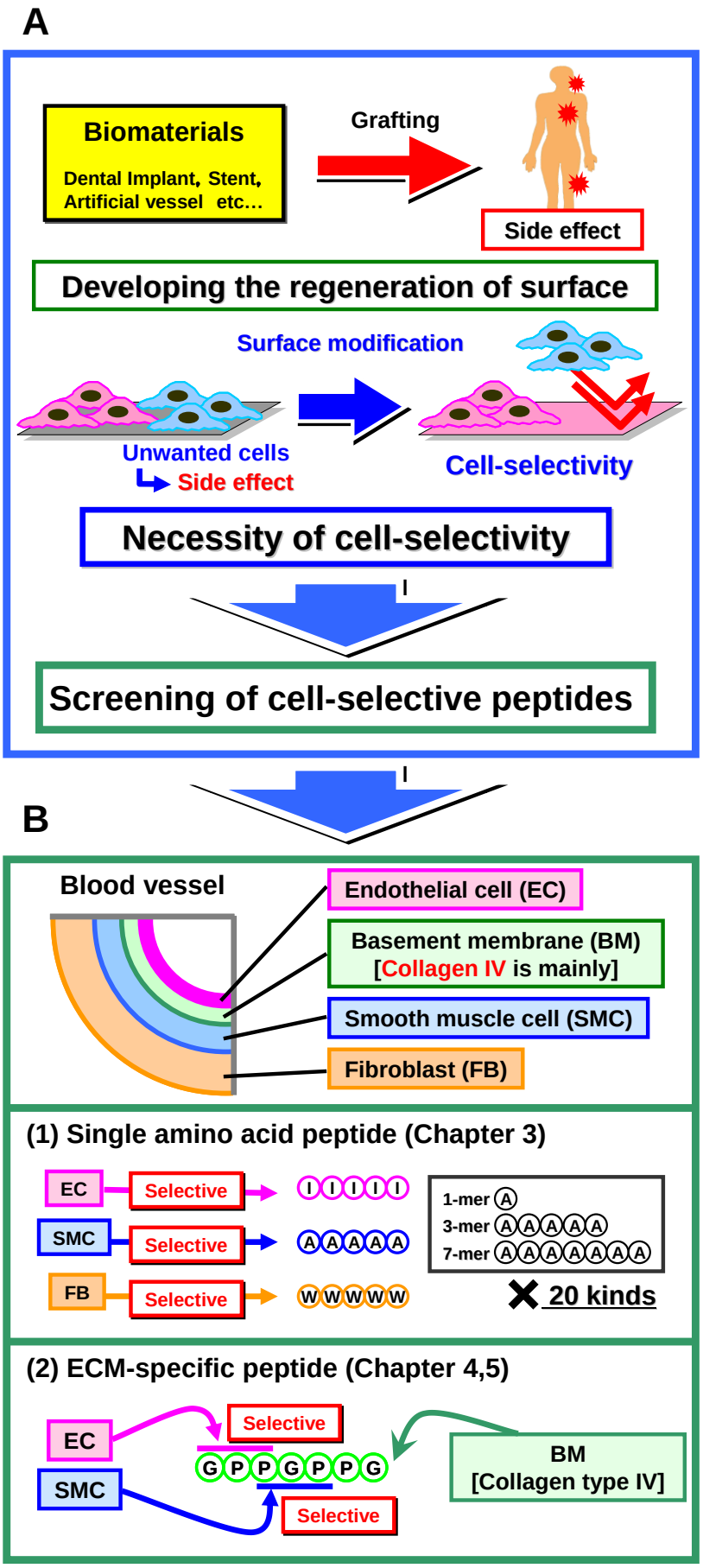

Figure 4. Total concept of my thesis.

Table 1. Biodegradable polymers used for tissue engineering of cell scaffold and biosignalling molecule release [7].

Synthetic polymers	Natural polymers
Poly (L-lactic acid) (PLLA)	Collagen
Poly (glycolic acid) (PGA)	Gelatin
Poly (ε-caprolactone) (PCL)	Fibrin
Poly (etylene glycol) (PEG)	Hyaluronic acid
	Alginate
	Chitosan, Chitin

Table 2. Functions of the ECM [11].

Structural
Scaffold
Tensile strength
Cushioning (cartilage)
Molecular filter (kidney)
Boundary between different tissue types
Storage depot (for growth factors, cytokines and chemokines)
Conformational blocking of cryptic sites
Biological
Cell polarity
Cell adhesion
Morphogenesis/differentiation
Migration
Proliferation
Prevention of apoptosis

Table 3. Commercially available biological scaffold materials [21].

Product	Company	Material	Processing	Form
AlloDerm	Lifecell	Human skin	Natural	Dry sheet
AlloPatch®	Musculoskeletal Transplant Foundation	Human fascia lata	Natural	Dry sheet
Axis™ dermis	Mentor	Human dermis	Natural	Dry sheet
Bard® Dermal Allograft	Bard	Cadaveric human dermis	Natural	Dry sheet
CuffPatch™	Arthrotek	Porcine small intestinal submucosa (SIS)	Cross-linked	Hydrated sheet
DurADAPT™	Pegasus Biologicals	Horse pericardium	Cross-linked	Dry sheet
Dura-Guard®	Synovis Surgical	Bovine pericardium	Cross-linked	Hydrated sheet
Durasis®	Cook SIS	Porcine small intestinal submucosa (SIS)	Natural	Dry sheet
Durepair®	TEI Biosciences	Fetal bovine skin	Natural	Dry sheet
FasLata®	Bard	Cadaveric fascia lata	Natural	Dry sheet
Graft Jacket®	Wright Medical Tech	Human skin	Natural	Dry sheet
Oasis®	Healthpoint	Porcine small intestinal submucosa (SIS)	Natural	Dry sheet
OrthADAPT™	Pegasus Biologicals	Horse pericardium	Cross-linked	Dry sheet
Pelvicol®	Bard	Porcine dermis	Cross-linked	Hydrated sheet
Peri-Guard®	Synovis Surgical	Bovine pericardium	Cross-linked	Dry sheet
Permacol™	Tissue Science Laboratories	Porcine skin	Cross-linked	Hydrated sheet
PriMatrix™	TEI Biosciences	Fetal bovine skin	Natural	Dry sheet
Restore™	DePuy	Porcine small intestinal submucosa (SIS)	Natural	Dry sheet
Stratasis®	Cook SIS	Porcine small intestinal submucosa (SIS)	Natural	Dry sheet
SurgiMend™	TEI Biosciences	Fetal bovine skin	Natural	Dry sheet
Surgisis®	Cook SIS	Porcine small intestinal submucosa (SIS)	Natural	Dry sheet
Suspend™	Mentor	Human fascia lata	Natural	Dry sheet
TissueMend®	TEI Biosciences	Fetal bovine skin	Natural	Dry sheet
Vascu-Guard®	Synovis Surgical	Bovine pericardium	Cross-linked	Dry sheet
Veritas®	Synovis Surgical	Bovine pericardium	Cross-linked	Hydrated sheet
Xelma™	Molnlycke	ECM protein, PGA, water		Gel
Xenform™	TEI Biosciences	Fetal bovine skin	Natural	Dry sheet
Zimmer Collagen Patch®	Tissue Science Laboratories	Porcine dermis	Cross-linked	Hydrated sheet

Table 4. Selective synthetic peptide sequences of ECM proteins used in tissue engineering applications [23]

Synthetic sequences	Origin	Function	References
RGD	Fibronectin, Vitronectin	Cell adhesion	[46]
KQAGDV		Smooth muscle cell adhesion	[47]
YIGSR	Laminin B1	Cell adhesion	[48]
REDV	Fibronectin, Vitronectin	Endothelial cell adhesion	[49]
IKVAV	Laminin	Neurite extension	[48]
RNIAEIIKDI	Laminin B2	Neurite extension	[50]
KHIFSDDSSE	Neural cell adhesion molecules	Astrocyte adhesion	[51]
VPGIG	Elastin	Enhance elastic modulus of artificial ECM	[52]
FHRRIKA	Heparin binding domain	Improve osteoblastic mineralization	[53]
KRSR	Heparin binding domain	Osteoblast adhesion	[54]
NSPVNSKIPKACCVPTELSAI	BMP-2	Osteoinduction	[55]
APGL		Collagenase mediated degradation	[56]
VRN		Plasmin mediated degradation	[56]
AAAAAAAAA		Elastase mediated degradation	[57]

1.7. References

[1] Takahashi K, Yamanaka S. Induction of pluripotent stem cells from mouse embryonic and adult fibroblast cultures by defined factors. Cell. 2006;126:663-76.

[2] Takahashi K, Tanabe K, Ohnuki M, Narita M, Ichisaka T, Tomoda K, et al. Induction of pluripotent stem cells from adult human fibroblasts by defined factors. Cell. 2007;131:861-72.

[3] Lengner CJ. iPS cell technology in regenerative medicine. Ann N Y Acad Sci. 2010;1192:38-44.

[4] Langer R, Vacanti JP. Tissue engineering. Science. 1993;260:920-6.

[5] Silva EA, Mooney DJ. Synthetic extracellular matrices for tissue engineering and regeneration. Curr Top Dev Biol. 2004;64:181-205.

[6] Langer R, Tirrell DA. Designing materials for biology and medicine. Nature. 2004;428:487-92.

[7] Tabata Y. Biomaterial technology for tissue engineering applications. J R Soc Interface. 2009;6 Suppl 3:S311-24.

[8] Smith IO, Liu XH, Smith LA, Ma PX. Nanostructured polymer scaffolds for tissue engineering and regenerative medicine. Wiley Interdiscip Rev Nanomed Nanobiotechnol. 2009;1:226-36.

[9] Subramanian A, Krishnan UM, Sethuraman S. Development of biomaterial scaffold for nerve tissue engineering: Biomaterial mediated neural regeneration. J Biomed Sci. 2009;16:108.

[10] Aumailley M, Gayraud B. Structure and biological activity of the extracellular matrix. J Mol Med. 1998;76:253-65.

[11] Kleinman HK, Philp D, Hoffman MP. Role of the extracellular matrix in morphogenesis. Curr Opin Biotechnol. 2003;14:526-32.

[12] Hynes RO. Integrins: bidirectional, allosteric signaling machines. Cell. 2002;110:673-87.

[13] Gumbiner BM. Cell adhesion: the molecular basis of tissue architecture and morphogenesis. Cell. 1996;84:345-57.

[14] Berrier AL, Yamada KM. Cell-matrix adhesion. J Cell Physiol. 2007;213:565-73.

[15] Rosso F, Giordano A, Barbarisi M, Barbarisi A. From cell-ECM interactions to tissue engineering. J Cell Physiol. 2004;199:174-80.

[16] Prasad N, Topping RS, Decker SJ. Src family tyrosine kinases regulate adhesion-dependent tyrosine phosphorylation of 5'-inositol phosphatase SHIP2 during cell attachment and spreading on collagen I. J Cell Sci. 2002;115:3807-15.

[17] Keely PJ, Fong AM, Zutter MM, Santoro SA. Alteration of collagen-dependent adhesion, motility, and morphogenesis by the expression of antisense alpha 2 integrin mRNA in mammary cells. J Cell Sci. 1995;108 (Pt 2):595-607.

[18] Mostafavi-Pour Z, Askari JA, Parkinson SJ, Parker PJ, Ng TT, Humphries MJ. Integrin-specific signaling pathways controlling focal adhesion formation and cell migration. J Cell Biol. 2003;161:155-67.

[19] Kao WJ. Evaluation of protein-modulated macrophage behavior on biomaterials: designing biomimetic materials for cellular engineering. Biomaterials. 1999;20:2213-21.

[20] El-Ghannam A, Starr L, Jones J. Laminin-5 coating enhances epithelial cell attachment, spreading, and hemidesmosome assembly on Ti-6A1-4V implant material *in vitro*. J Biomed Mater Res. 1998;41:30-40.

[21] Badylak SF, Freytes DO, Gilbert TW. Extracellular matrix as a biological scaffold material: Structure and function. Acta Biomater 2009;5:1-13.

[22] Ma PX. Biomimetic materials for tissue engineering. Adv Drug Deliv Rev. 2008;60:184-98.

[23] Shin H, Jo S, Mikos AG. Biomimetic materials for tissue engineering. Biomaterials. 2003;24:4353-64.

[24] Xiao SJ, Textor M, Spencer ND, Wieland M, Keller B, Sigrist H. Immobilization of the cell-adhesive peptide Arg-Gly-Asp-Cys (RGDC) on titanium surfaces by covalent chemical

attachment. J Mater Sci Mater Med. 1997;8:867-72.

[25] Hersel U, Dahmen C, Kessler H. RGD modified polymers: biomaterials for stimulated cell adhesion and beyond. Biomaterials. 2003;24:4385-415.

[26] Vagner J, Qu H, Hruby VJ. Peptidomimetics, a synthetic tool of drug discovery. Curr Opin Chem Biol. 2008;12:292-6.

[27] Smith-Garvin JE, Koretzky GA, Jordan MS. T cell activation. Annu Rev Immunol. 2009;27:591-619.

[28] Wraith DC. Therapeutic peptide vaccines for treatment of autoimmune diseases. Immunol Lett. 2009;122:134-6.

[29] Khatayevich D, Gungormus M, Yazici H, So C, Cetinel S, Ma H, et al. Biofunctionalization of materials for implants using engineered peptides. Acta Biomater. 2010;6:4634-41.

[30] Hozumi K, Otagiri D, Yamada Y, Sasaki A, Fujimori C, Wakai Y, et al. Cell surface receptor-specific scaffold requirements for adhesion to laminin-derived peptide-chitosan membranes. Biomaterials. 2010;31:3237-43.

[31] Yamazaki CM, Kadoya Y, Hozumi K, Okano-Kosugi H, Asada S, Kitagawa K, et al. A collagen-mimetic triple helical supramolecule that evokes integrin-dependent cell responses. Biomaterials. 2010;31:1925-34.

[32] Crawford M, Woodman R, Ko Ferrigno P. Peptide aptamers: tools for biology and drug discovery. Brief Funct Genomic Proteomic. 2003;2:72-9.

[33] Ramachandran S, Yu YB. Peptide-based viscoelastic matrices for drug delivery and tissue repair. BioDrugs. 2006;20:263-9.

[34] Ezzat K, El Andaloussi S, Abdo R, Langel U. Peptide-based matrices as drug delivery vehicles. Curr Pharm Des. 2009;16:1167-78.

[35] Giordano RJ, Edwards JK, Tuder RM, Arap W, Pasqualini R. Combinatorial ligand-directed

lung targeting. Proc Am Thorac Soc. 2009;6:411-5.

[36] Lebl M, Krchnak V, Sepetov NF, Seligmann B, Strop P, Felder S, et al. One-bead-one-structure combinatorial libraries. Biopolymers. 1995;37:177-98.

[37] Smith GP. Filamentous fusion phage: novel expression vectors that display cloned antigens on the virion surface. Science. 1985;228:1315-7.

[38] Frank R. SPOT-Synthesis: An easy technique for the positionally addressable, parallel chemical synthesis on a membrane support. Tetrahedron. 1992;48:9917-32.

[39] Frank R. The SPOT-synthesis technique. Synthetic peptide arrays on membrane supports--principles and applications. J Immunol Methods. 2002;267:13-26.

[40] Volkmer R. Synthesis and application of peptide arrays: quo vadis SPOT technology. Chembiochem. 2009;10:1431-42.

[41] Otvos L, Jr., Pease AM, Bokonyi K, Giles-Davis W, Rogers ME, Hintz PA, et al. In situ stimulation of a T helper cell hybridoma with a cellulose-bound peptide antigen. J Immunol Methods. 2000;233:95-105.

[42] Kato R, Kaga C, Kunimatsu M, Kobayashi T, Honda H. Peptide array-based interaction assay of solid-bound peptides and anchorage-dependant cells and its effectiveness in cell-adhesive peptide design. J Biosci Bioeng. 2006;101:485-95.

[43] Kaga C, Okochi M, Tomita Y, Kato R, Honda H. Computationally assisted screening and design of cell-interactive peptides by a cell-based assay using peptide arrays and a fuzzy neural network algorithm. Biotechniques. 2008;44:393-402.

[44] Kato R, Okuno Y, Kaga C, Kunimatsu M, Kobayashi T, Honda H. Pentamer peptide from Fas antigen ligand inhibits tumor-growth with solid-bound form found by peptide array. J Pept Res. 2005;66 Suppl 1:146-53.

[45] Kaga C, Okochi M, Nakanishi M, Hayashi H, Kato R, Honda H. Screening of a novel octamer

peptide, CNSCWSKD, that induces caspase-dependent cell death. Biochem Biophys Res Commun. 2007;362:1063-8.

[46] Shin H, Jo S, Mikos AG. Modulation of marrow stromal osteoblast adhesion on biomimetic oligo[poly(ethylene glycol) fumarate] hydrogels modified with Arg-Gly-Asp peptides and a poly(ethyleneglycol) spacer. J Biomed Mater Res. 2002;61:169-79.

[47] Mann BK, Schmedlen RH, West JL. Tethered-TGF-beta increases extracellular matrix production of vascular smooth muscle cells. Biomaterials. 2001;22:439-44.

[48] Ranieri JP, Bellamkonda R, Bekos EJ, Vargo TG, Gardella JA, Jr., Aebischer P. Neuronal cell attachment to fluorinated ethylene propylene films with covalently immobilized laminin oligopeptides YIGSR and IKVAV. II. J Biomed Mater Res. 1995;29:779-85.

[49] Hubbell JA, Massia SP, Desai NP, Drumheller PD. Endothelial cell-selective materials for tissue engineering in the vascular graft via a new receptor. Biotechnology (N Y). 1991;9:568-72.

[50] Schense JC, Bloch J, Aebischer P, Hubbell JA. Enzymatic incorporation of bioactive peptides into fibrin matrices enhances neurite extension. Nat Biotechnol. 2000;18:415-9.

[51] Kam L, Shain W, Turner JN, Bizios R. Selective adhesion of astrocytes to surfaces modified with immobilized peptides. Biomaterials. 2002;23:511-5.

[52] Panitch A, Yamaoka T, Fournier M, Mason T, Tirrell D. Design and biosynthesis of elastin-like artificial extracellular matrix proteins containing periodically spaced fibronectin CS5 domains. Macromolecules. 1999;32:1701-3.

[53] Rezania A, Healy K. Biomimetic peptide surfaces that regulate adhesion, spreading, cytoskeletal organization, and mineralization of the matrix deposited by osteoblast-like cells. Biotechnol Progr. 1999;15:19-32.

[54] Dee K, Andersen T, Bizios R. Design and function of novel osteoblast-adhesive peptides for

chemical modification of biomaterials. Journal of Biomedical Materials Research. 1998;40:371-7.

[55] Suzuki Y, Tanihara M, Suzuki K, Saitou A, Sufan W, Nishimura Y. Alginate hydrogel linked with synthetic oligopeptide derived from BMP-2 allows ectopic osteoinduction *in vivo*. Journal of Biomedical Materials Research. 2000;50:405-9.

[56] West J, Hubbell J. Polymeric biomaterials with degradation sites for proteases involved in cell migration. Macromolecules. 1999;32:241-4.

[57] Mann B, Gobin A, Tsai A, Schmedlen R, West J. Smooth muscle cell growth in photopolymerized hydrogels with cell adhesive and proteolytically degradable domains: synthetic ECM analogs for tissue engineering. Biomaterials. 2001;22:3045-51.

Chapter 2

Standardization scheme for datasets obtained from peptide array for comparative cell-selectivity

2.1. Introduction

Peptide array technique was initially applied to the understanding of molecular recognition events in the immune system using synthetic peptides by Ronald Frank [1]. This technique has become a widespread and essential tool in biology and biochemistry [2]. Until now, many subjects are investigated such as proteins, metals, bacterial and cells. From 1990 until 2009, more than 400 original, peer-reviewed papers relevant to the peptide array technology have been published [3].

A large amount of datasets are obtained from the peptide array method, and it is very important to consider the correction and normalization considering the comparison of the different experiments and different datasets.

First, the correction of peptide array-datasets was considered. The peptide array is a useful method, but experimental errors between the lots of peptide array occur indispensably. To reduce these errors, the control peptides (such as negative control (linker only) or positive control peptides) are used in every experiment. However, the errors are also included in the control itself.

In particular, the indispensable errors are often obtained in cell based-assay, because the cell activities such as cell adhesion, proliferation and differentiation are related to the culture medium, time of passage, and time of culture. Thus more effective correction of peptide array-datasets is required to compare the experimental results equally.

Second, the normalization of each datasets obtained from peptide array method was considered. In this study, it is important to compare different cell types with the same peptide sequence. However, each cell type has the various preferences for adhesion and proliferation. For example, one cell type “A” has the high ability of cell adhesion (“A” cell is easy to adhere), but another cell type “B” has the low ability of cell adhesion. Thus even though “A” cell adheres on certain peptide and “B” cell adheres lower than “A” cell on the same peptide in raw data, there is a possibility that the peptide promotes “B” cell adhesion more strongly than “A” cell to consider the distribution of “A” and “B” through all experimental data. To compare all datasets equally, it is necessary to consider the distribution and to use the idea of normalization.

2.2. Method

2.2.1. Scaling the different lots of peptide array

Two point correction methods with negative and positive control was used to correct the experiment. This idea is referred from the DNA microarray data analysis. In the analysis of DNA microarray, the expression of house-keeping genes is used for the scaling of each gene chip. For cell adhesion or proliferation assay, two spot data on peptide array were used: negative control spot (linker only), and positive control (RGD sequence). RGD peptide is well known peptide that has the ability to adhere the any type of cell. The image of this method is shown in Fig. 1. In this figure, Array 1 and Array 2 are scaled to Array3 using the mathematical expression (Array 1 and Array 3:

y = 1.64x +1.82, Array 2 and Array 3: y = 0.69x – 3.85).

2.2.2. Normalization for comparing the datasets

Each dataset was normalized by using standardization to assess the different cell type's properties. Standardization was carried out by Microsoft excel. The image of the standardization of distribution is shown in Fig. 2. In this figure, the blue distribution is the standard normal distribution, and red and green distributions are standardized to blue distribution (standard normal distribution). This idea is referred from the clustering analysis to assess the different type properties together.

2.3. Summary

Through the standardization, the different lots of peptide array data could be compared, and different properties of cell types could be analyzed. The correction method is applied for "**Chapter 3**" and "**Chapter 4**" to compare the different peptide array experiment, and normalization method is applied for "**Chapter 3**" to compare 3 different types of cell adhesion and proliferation.

This method could be applied for any peptide array assay to compare the interaction of different type molecule. For more secure analysis of peptide array datasets, it is indubitable that the number of internal control has to be increased.

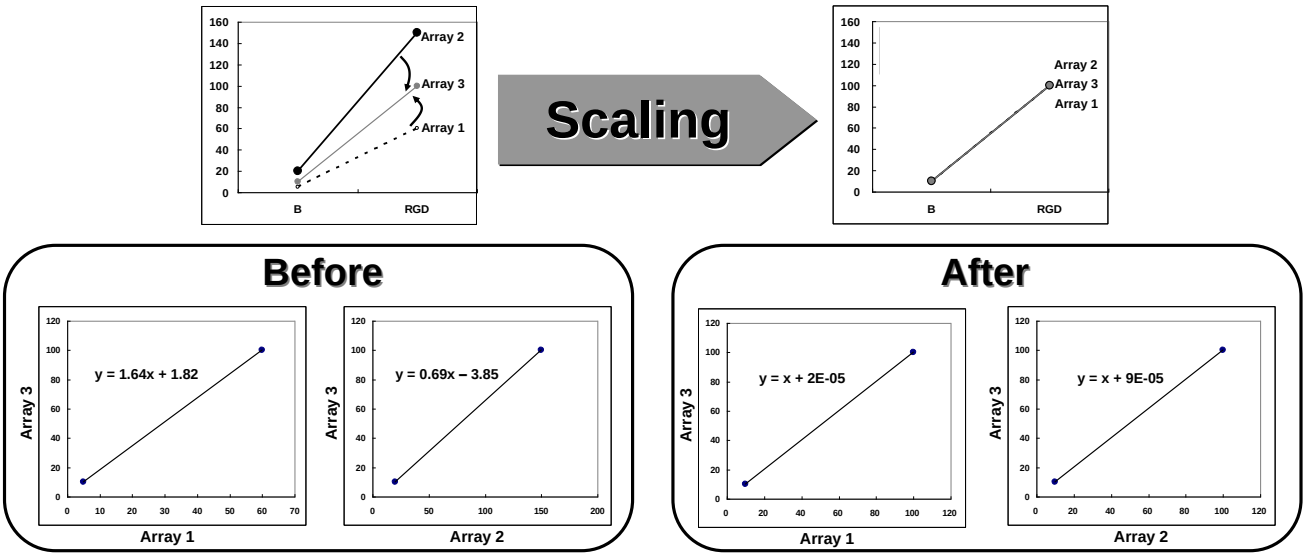

Figure 1. The scaling way of different peptide arrays.

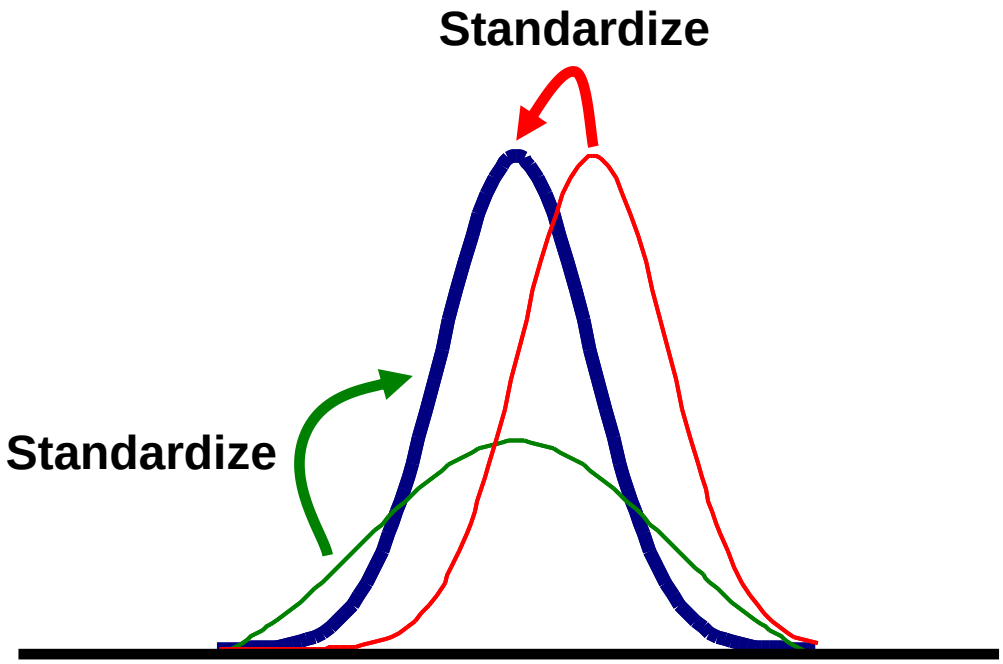

Figure 2. The image of standardization. Blue distribution indicate the standard normal distribution (AV = 0, SD = 1.0). And Red distribution and Green distribution are standardized to Blue distribution (standard normal distribution). Red distribution (AV = 1.0, SD = 1.0), and Green distribution (AV = 0, SD = 2.0).

3.4. References

[1] Frank R. SPOT-Synthesis: An easy technique for the positionally addressable, parallel chemical synthesis on a membrane support. Tetrahedron. 1992;48:9917-32.

[2] Frank R. The SPOT-synthesis technique. Synthetic peptide arrays on membrane supports--principles and applications. J Immunol Methods. 2002;267:13-26.

[3] Volkmer R. Synthesis and application of peptide arrays: quo vadis SPOT technology. Chembiochem. 2009;10:1431-42.

Chapter 3

Amino acid sequence preferences to control cell-selective organization of endothelial cells, smooth muscle cells, and fibroblasts

3.1. Introduction

The life-threatening risks that occur after implantation of medical devices and products are mostly due to the disruption of the biological environment of the location. With medical devices and products for cardiovascular treatments, such disruption-induced side effects could directly end patients' lives. The most common risk with cardiovascular implants is stenosis caused by thrombosis and neointimal hyperplasia [1]. Thrombosis is caused by the atypical attraction of serum proteins, platelet and circulating blood cells to damaged or absent endothelial surfaces [2]. Neointimal hyperplasia, which is characterized by excessive smooth muscle cell growth is also a critical risk caused by damage to the endothelial layer together with expansion pressure in the cases of stent implants [3, 4]. Side effects such as these, which occur with cardiovascular treatments, are commonly contradictory. It is known that when restenosis is effectively suppressed by the elution

of cell growth inhibition reagents, for example by the use of drug eluting stents, proper endothelialization is inhibited [5]. Therefore, to overcome such defects, the ideal surface coating of a cardiovascular implant should inhibit over-growth of smooth muscle cells but also enhance the growth of the endothelial cells for successful endothelialization [4].

One of the most promising strategies in regenerative medicine is to lower the risks of cardiovascular implants by modifying the device surface with biological molecules (such as proteins [6-9], glycosaminoglycan [10], chemokines [11], and protein-derived peptides [12-15]) to mimic the natural biological atmosphere for rapid and prolonged repair by the native cellular system [16]. Fibrin, collagen, fibronectin, and elastin are frequently chosen biological molecules for medical device coating because of the anti-thrombosis effects of these molecules. Because endothelialization is the most critical event involved in both thrombosis and restenosis, biological molecules with the ability to enhance endothelialization have attracted attention. CD34 antibodies have been utilized to coat stent surfaces to capture endothelial progenitor cells for rapid and effective endothelialization [17]. However, most large biological molecules, such as the anti-CD34 antibody, are obtained from non-human hosts; therefore, the risk of unexpected infection is a concern that has led to medical restrictions. Considering this risk, artificially synthesized peptides derived from human proteins could serve as ideal molecules because of their biocompatibility and safety assurance.

Many short peptides have been shown to enhance cellular adhesion by surface conjugation. RGDS (Arg-Gly-Asp-Ser) is the most commonly studied short peptide from extracellular matrix (ECM) and binds to integrins on cells to form strong cellular adhesions [18]. Besides RGDS, short peptides, such as LDV (Leu-Asp-Val) [19], YIGSR (Try-Ile-Gly-Ser-Arg) [20], and PHSRN (Pro-His-Ser-Arg-Asn) [21], have been reported to enhance cellular attraction to the material

surface. These peptides are ideal model peptides and reveal that even short peptides can serve as cell adhesion molecules.

In the natural biological repair system, cells specifically localize to their correct location to form a well-organized cellular system; therefore, there are few chances to explore the above mentioned integrin ligands on the complex ECM surface. As a result, we hypothesized that there might be a cellular preference for more broad candidate molecules with similar physicochemical properties, such as a bias towards certain varieties of amino acid or peptide, on ECM surfaces that could explain cell-selective adhesion and proliferation mechanisms. To investigate our hypothesis, we examined the amino acid preferences that control the cellular organization in cardiovascular tissue. We chose three cell types, endothelial cells (ECs), smooth muscle cells (SMCs), and fibroblasts (FBs), that typically have roles in cardiovascular tissues and compared the relative preferences of these cells for selective amino acids and repeated sequences. For the cell-peptide interaction assay, we introduced a PIASPAC (peptide array-based interaction assay of solid-bound peptides and anchorage-dependent cells) method [22-24], an application of a SPOT peptide array technique [25]. By combinatorial examination of the peptide array, we could compare the cellular preferences in adhesion and proliferation. The accumulation of serum-derived proteins was also examined to determine its effect on cell-selective adhesion to peptides. Finally, to propose a design strategy for biomimetic polymers, we analyzed the relationship between cell selectivity and the physicochemical properties of amino acids by using amino acid indices and multi-variant analysis. To our knowledge, this is the first detailed analysis comparing the amino acid preferences of cardiovascular related cells.

3.2. Materials and Methods

3.2.1. Cells and cell culture

Normal human umbilical vein endothelial cells (Kurabo Industries Ltd., Osaka, Japan) were maintained in HuMedia-EG2 (Kurabo) and designated as ECs. Smooth muscle cells (Cell Applications, Inc., San Diego, CA, USA) were maintained in smooth muscle growth medium (Cell Applications) and designated as SMCs. Normal human dermal fibroblasts (Kurabo) were routinely maintained in Dulbecco's modified Eagle's medium (DMEM) (Life Technologies Corporation, Carlsbad, CA, USA) at 37°C under 5% CO_2 and designated as FBs. Penicillin streptomycin (Life Technologies Corporation) was used as antibiotics in the DMEM. All of the cells were used in assays within four to six passages.

3.2.2. Peptide array synthesis

A cellulose membrane (grade 542; Whatman, Maidstone, UK) was modified using Fmoc-β-Ala-OH (Watanabe Chemical Industries, Ltd., Hiroshima, Japan) as the N-terminal basal spacer by 1-Methylimidazole, redistilled, 99+% (Sigma-Aldrich, St. Louis, MO, USA), and DIPCI (N,N'-Diisopropylcarbodiimide) (Watanabe Chemical Industries). Fmoc-11-aminoundecanoic acid (Watanabe Chemical Industries) was linked as an additional spacer between the candidate peptide and the cellulose by the cocktail of DIPCI and1-hydrozybenzotriazole (HOBt, Anhydrous) (Watanabe Chemical Industries) (volume ratio 1:4), and which was optimized for better interaction with the cells. Fmoc amino acids (0.5 M) (Watanabe Chemical Industries) were also activated by the cocktail of DIPCI and HOBt, and spotted twice with a peptide auto-spotter (ASP222; Intavis Bioanalytical Instruments AG, Köln, Germany) in accordance with the manufacturer's instructions.

Peptides were elongated by conventional Fmoc chemistry using the 20% piperidine (Watanabe Chemical Industries) as the removal agent of side-chain protecting groups. By the repeated numbers of elongation steps, peptide spots were designated as 1-mer (1 elongation step), 5-mer (5 elongation steps), and 7-mer (7 elongation steps). The final deprotection step of side chains were carried out by the cocktail of m-cresol (Wako Pure Chemical Industries, Ltd., Osaka, Japan), thioanisole (Tokyo chemical industry co., LTD., Tokyo, Japan), 1,2-Ethanedithiol (EDT) (Watanabe Chemical Industries) and trifluoroacetic acid (TFA) (Watanabe Chemical Industries) = 1 : 6 : 3 : 40 respectively for 3 h. The synthesized array membrane was then thoroughly washed three times for 2 h with diethyl ether (Wako Pure Chemical Industries), methanol (Wako Pure Chemical Industries), and Dulbecco's PBS (pH 7.2) (Nissui Pharmaceutical Co., Ltd., Tokyo, Japan). Finally, the array was soaked in methanol (Wako Pure Chemical Industries) and dried on a clean bench.

3.2.3. PIASPAC (peptide array-based interaction assay of solid-bound peptides and anchorage-dependent cells)

The cell assay on SPOT arrays was carried out according to a previously described method [22] with slight modifications. Briefly, from the synthesized peptide array, each spot corresponding to different peptides was punched out as a disk and embedded in a 96-well plate, and after soaking the punched disks with the appropriate cell culture medium, 1.5×10^4 cells/well were directly seeded on the disks. Cells and peptide disks were incubated for 1 h for cell adhesion assays and for three days for cell proliferation assays. After three repeat washes of PBS to remove unattached cells by pipetting, the viable cells were stained with calcein AM (Life Technologies Corporation) for 30 min, and fluorescence intensity was measured on a Fluoroskan Ascent (type 374; Labsystems, Helsinki, Finland) with 485 nm excitation and 538 nm emission. For reproducibility, the data of triplicate

spots from two experiments were averaged. To normalize the fluorescence intensities to compare the cellular preferences, each average fluorescence intensity was divided by the average negative control (no peptide, linker only) value, which was set to 1.0, to obtain a relative preference ratio (adhesion or proliferation) for each sequence. The assay scheme is depicted in **Fig. 1**. Peptides that exerted their effects equally in all of the cells were considered to be "peptides with no cell preference (non-selective peptides)", and peptides that indicated a biased effect to particular cell were considered to be "peptides with cell preference (selective peptides to target cells)". For example, when the number of ECs on a peptide spot disk is larger than any other cell types, it is designated as EC-selective peptide.

3.2.4. Protein attraction assay on peptide array

The synthesized peptide arrays were washed 5 times with phosphate-buffered saline (PBS; pH 7.2), and the membranes were allowed to dry under sterile conditions. Arrays were blocked with 1% bovine serum albumin (BSA) in PBS for 12 h at 4°C. After blocking, the arrays were incubated for 1 h at 37°C with DMEM containing 10% fetal bovine serum (Life Technologies Corporation) in order to assay the binding activity of each spot with serum-derived protein such as fibronectin (FN) or vitronectin (VN). After continuous washes with PBS, the arrays were hybridized with anti-rabbit human fibronectin IgG (Novotec, Saint Martin La Garenne, France) or anti-rabbit human vitronectin IgG (Chemicon, Tokyo, Japan) diluted to a concentration of 1/500 or 1/1000 with PBS containing 0.25% BSA for 2 h at 37°C. After several washes with Tris-buffered saline containing 0.05% Tween-20 (T-TBS; pH 7.2), arrays were hybridized with anti-rabbit IgG-conjugated Alexa 488 (Life Technologies Corporation) diluted to a concentration of 2 μg/ml with PBS containing 0.25% BSA for 1 h at 37°C. After several washes with T-TBS at 37°C, the fluorescence intensities

of spots were scanned with a FLA-7000 (Fujifilm, Tokyo, Japan) with 473 nm excitation and 520 nm emission. The scanned spot image was analyzed with ArrayGauge Ver.2.0 (Fujifilm, Tokyo, Japan), and the fluorescence intensity of each spot was calibrated. Each array was designed to contain triplet spots, and two duplicate experiments were averaged as the data. The averaged fluorescence intensity of each sequence was normalized by subtracting the fluorescence intensity of the same sequence without the addition of the first antibody.

3.2.5. Scanning electron microscope (SEM) analysis

Cells were treated according to the cell assay protocol described for the PIASPAC method, and the cells on the peptide disks were fixed with 4% glutaraldehyde (Wako Pure Chemical Industries) for 12 h at 4°C. After further fixation with osmium tetroxide (PGM CHEMICALS (PTV) LTD., NEW Germany, USA) for 30 min at room temperature, samples were dried with t-butylalcohol (Wako Pure Chemical Industries) using a VFD-20 drying apparatus (Hitachi, Ltd., Tokyo, Japan) and plasma coated with osmium tetroxide using an osmium plasma coater (Nihon Lazor Denshi, Ichinomiya, Japan). The SEM images were obtained using S-800 electron microscope (Hitachi, Ltd.).

3.3. Results

3.3.1. Comparing cell preference of amino acids in cardiovascular tissues

We compared three types of normal human cells (ECs, SMCs, and FBs) that contribute to cardiovascular tissues to investigate the cell-selective preference of particular amino acids, which may determine the effect of ECM on selective cells (**Fig. 1**). In evaluating cell adhesion (with one

hour incubation), an amino acid repeat number more than five provided a relative cell-selective preference (**Fig. 2A**, detailed data in **Fig. S1**, **Table S1**).

In particular, longer repeats of hydrophobic amino acids (isoleucine, valine, leucine, and phenylalanine) were found to contribute to enhance EC adhesion compared to the other two cell types, especially peptides with 7-repeated steps of elongation. Isoleucine, valine, and leucine contributed proportionally to promote adhesion of ECs, indicating a stronger effect with shorter repeats. In contrast, two positively charged amino acids (arginine and lysine), which are conventionally considered to have cell adhesion properties, were found to be too universal to control selective cellular organization. But the positively charged amino acid histidine demonstrated no preference between these three cell types. And two negatively charged amino acids (asparatic acid, glutamic acid), which are considered not to have cell adhesion properties, were found to be non-adhesion properties.

Fig. 2B indicates the proliferation rates (after three-day incubation) on the different amino acids (detailed data in **Fig. S2**, **Table S1**). This result also shows that the residues, such as charged residues, previously shown to have cell adhesion properties indicate no preference for cell type but that isoleucine has a preference for enhancing ECs and valine has a preference for enhancing FBs. In spite of the wide inhibitory preferences of SMCs, such as hydrophobic amino acids, enhancive preference of SMCs was not clear. These results suggest that the amino acid preference for SMCs is largely different than that of ECs and FBs. Throughout the experiment, preference data from peptides synthesized by less than 5-repeated elongation were found to have larger standard error (ECs on 3-repeated elongation: 21.5% of average, SMCs on 3-repeated elongation: 20.2% of average, FBs on 3-repeated elongation: 59.1% of average) (**Fig. S1** and **Fig. S2,** and 3-mer data not shown). However, a similar tendency was also clearly observed in the short proliferation assay (1

day) (data not shown), therefore such amino acid preference effect could be firm with longer peptides. In this aspect, we focused the comparison between 1-mer and longer peptides.

3.3.2. SEM analysis of cell morphology on preferred amino acids

To investigate the detailed effect on the cells of particular amino acids, cell morphology was monitored by SEM (**Fig. 3**). The hepta-Ile (array spot with 7-repeated steps of elongation with Ile) was chosen as the best EC-selective peptide. On hepta-Ile, relatively high numbers of adherent ECs were observed compared to other cells (**Fig. 3A-C**). Filopodias and fibers of extracellular matrix from ECs were found on hepta-Ile (arrows indicated) than on both of the negative controls (other cell types on the same peptide disk), indicating that ECs prefer the peptide-coated surface for adhesion (**Fig. 3A**). This result supports that the biological effect is triggered by cell-selective preference on such preference amino acids.

3.3.3. Involvement of serum-derived ECM proteins in cellular adhesion preferences

Each of the PIASPAC assays described above was carried out in serum- or serum-related supplement-containing medium to mimic the natural cellular *in vivo* conditions. However, in these assays, the cellular preference for amino acids could be explained by a dominant effect of the amino acid itself, of the serum-derived proteins that accumulate on amino acids, or both. Therefore, we examined the accumulation rate of fibronectin (FN) and vitronectin (VN), two of the major ECM proteins that affect cell adhesion and proliferation, on amino acid repeated sequences on the peptide arrays. FN was found to accumulate on tyrosine (**Fig. 4A**, detailed data in **Fig. S3**, **Fig. S5A**), residues that contain aromatic side chains. VN was found to accumulate on lysine and arginine, positively charged residues (**Fig. 4B**, detailed data in **Fig. S4**, **Fig. S5B**). These three

amino acids were the universal cell-attracting residues (i.e., no cellular preference) (**Fig. 2**). Although our hybridization scheme can not deny the probability to detect false-positive signal from the non-selective accumulation of primary antibody to high density peptides, the found cell-selective amino acids (such as Ile, Val) did not show ECM protein accumulation. Therefore, we concluded that any dominant effect of serum-derived proteins on the cell preference of identified amino acids is unlikely.

3.3.4. Confirmation of controlling cell adhesion and proliferation by designed cell-selective peptides

To further confirm the possibility of cell-selective organization controlled by amino acid preferences, we newly designed peptides consisting of selected amino acids that indicated cellular selectivity (**Fig. 5**, detailed data in **Fig. S6**). To design 30 peptides, 9 amino acids were selected to represent three categories; (Category 1) inhibitory peptides without cell-selectivity (aspartic acid and glutamic acid), (Category 2) enhancive peptides without cell-selectivity (lysine, arginine, and tyrosine), and (Category 3) enhancive peptides with EC-selectivity (phenylalanine, isoleucine, and leucine). In each category, amino acids were randomly selected to build 7-mer peptides. Interestingly, EC-selectivity could be designed by the combination of any type of EC-selective amino acids. With non-selective amino acids, clear change in the cell-selective effect was not observed by combinations. Such results indicates that such simple physicochemical property of amino acids have potential to control the cellular organization.

3.4. Discussion

In this study, we reported for the first time the cell-selective preferences of particular amino acids in adhesion and proliferation by comparing three types of typical cardiovascular cells. We examined the cell preferences of simple repeats of amino acids to investigate our hypothesis that the ECM functions to control cellular self-organization *in vivo* and that this process would be controlled not only by ligand-specific rare domains (such as RGD) but also by the physicochemical properties of the surface environment provided by the ECM proteins. To assay these cell-selective preferences in peptide interactions in a combinatorial manner, we utilized our PIASPAC method, the application of SPOT array to directly assay cell adhesion and proliferation.

From the cell preference assay for adhesion and proliferation, we found that there are largely two types of cell preference in cardiovascular cells; ECs and FBs prefer repeats of hydrophobic residues, and SMCs have less of a preference for adhesion but prefer repeats of aromatic residues for proliferation (**Fig. 2**). It was also found that the amino acids that contributed to cell-selective adhesion also contributed to proliferation. Because no single amino acid was preferred by particular cell, we concluded that domain-like physicochemical properties are more important for cell preference than the exact residue. Such amino acid preference was also confirmed with an assay of other random sequence peptides, which consisted of EC-selective amino acids (**Fig. 5**). We also confirmed that the non-selective preference of aromatic side chains amino acids and (tyrosine) positively charged amino acids (lysine and arginine) are probably due to the attracted serum-derived proteins (FN and VN) on these peptides (**Fig. 4**). These observations support our hypothesis that the control of cell-selective organization can be maintained by physicochemical-based affinities that accept broad candidate molecules that form domain-like property on the surface of extracellular matrix, rather than sequence-based affinities, such as ligand-receptor interactions.

We also found several simple amino-acid effects that control cellular organization: longer elongation of isoleucine attracted ECs and eliminates SMCs and FBs (**Fig. 3**). The introduction of isoleucine also contributed to provide EC-selective effect on random sequence peptides (**Fig. 5**). Because these amino acid preferences were assayed using serum-containing medium, peptides containing these amino acids could be promising practical candidates to enhance proper cell organization on medical devices and products. However, it should be noted that the more the elongation step increases, the more the impurity of peptide spot would appear in some amino acids by insufficient synthesis. In this aspect, our 7-mer peptide spots may include fewer percentages of perfect 7-mer repeats with some types of amino acids. Combining the facts that our spots consist of single amino acid (produce no mismatch sequences) and our data has high reproducibility (**Fig. S1** and **Fig. S2**), we consider that there are accumulative effects of amino acids on determining cell-selective preferences.

If physicochemical-based affinity can control the cell-selective organization, a rule based on amino acid indices should support the design of artificial molecules or polymers for medical device coatings. To extract the physicochemical rule to design cell-selective peptides, we analyzed the total data (20 peptides of repeated amino acids and 30 peptides of randomly selected amino acids) by classification and regression tree (CART) (Supplementary information (SI), **Table S1**). CART analysis automatically calculates the combination of physiochemical variables, as opposed to manually interpreted by a researcher, to obtain the final classification model. In other words, the selected variable from such analysis reflect the exhaustive consideration of all possible combinations of candidate physicochemical properties for the best classification. For the classification, we divided our data in three categories (**Table S1**); (1) enhancive peptides without cell selectivity (ALL_Enh), (2) inhibitory peptides without cell selectivity (ALL_Inh), and (3)

enhancive peptides with EC-selectivity (EC_SL). To classify the three categories of peptides, thirteen amino acid indices (**Table S2**) [26-36] from AAindex1 (http://www.genome.ad.jp/dbget-bin/www_bfind?aaindex) [37] were examined by CART for best parameter combination. By this objective analysis, we found that the isoelectric point (threshold = -4.418) is the primary property that classifies "adhesive peptides" and "non-adhesive peptides". The result also indicated that the combination of isoelectric point (>-4.418) and the hydropathy (>+3.241) was found to be a defining characteristic of EC preferred structures (**Fig. S7**). Although such analysis is still limited in our achieved data, such interpreted rule would characterize the surface physicochemical property to control the cell-selective organization on medical devices. The concept of using a medical device coating material to enhance proper cell organization could be important for overcoming the contradictory effects of endothelialization and stenosis.

Whether the minimum functional molecule for providing physicochemical-based affinities for cell self-organization is "domain consists of amino acids" or "domain consist of peptides" is still not clear. Therefore, further investigation is needed to understand the mechanism of controlling cellular organization for next-generation medical device coating.

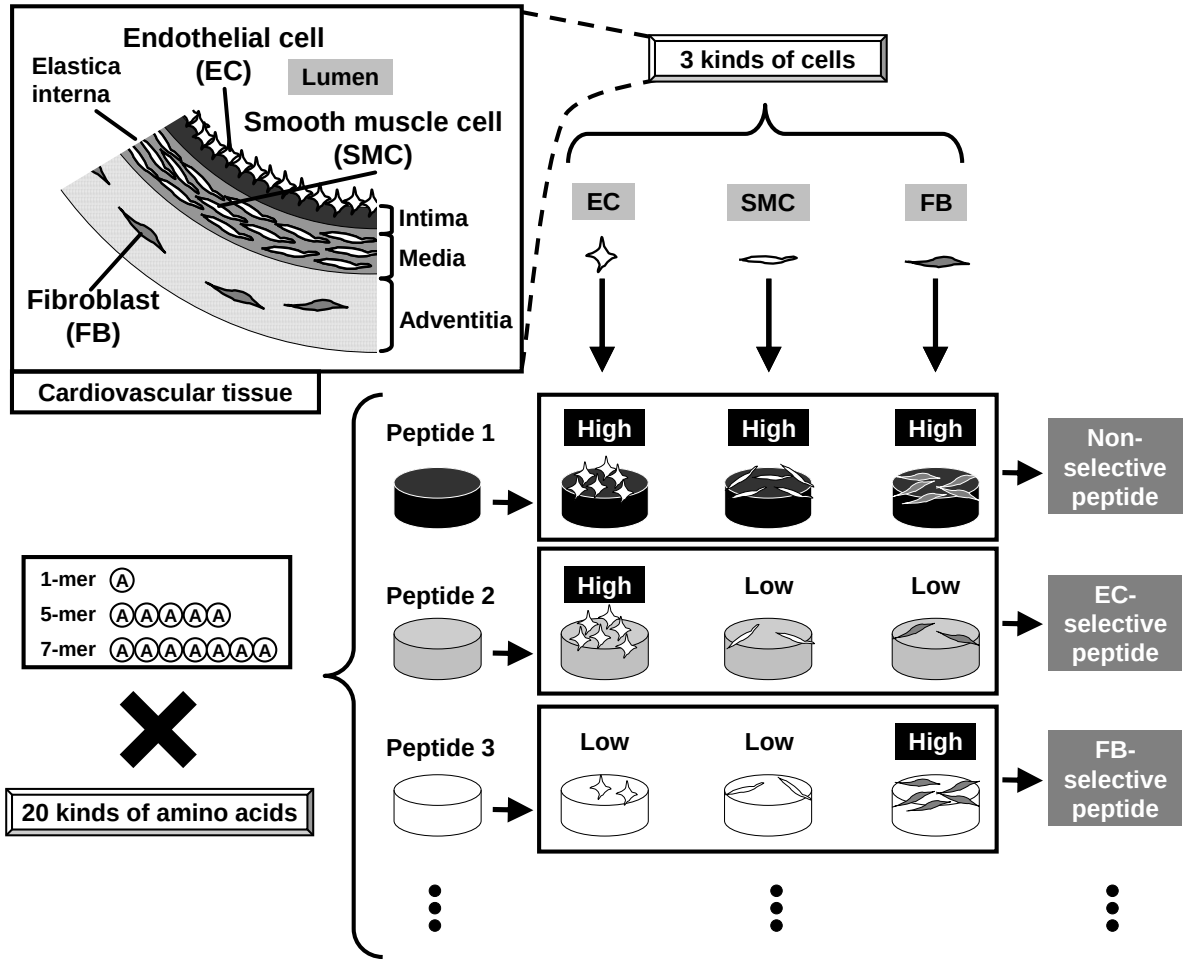

Figure 1. A schematic illustration of this study. Three kinds of cells that comprise cardiovascular tissues were chosen for determining the cell selectivity. Twenty kinds of amino acids were chosen to design tandem repeat peptides for investigating the cell adhesion and proliferation. Cells were seeded to each peptide sequence on the peptide array spot and evaluated as the relative cell adhesion or proliferation rate for each cell type.

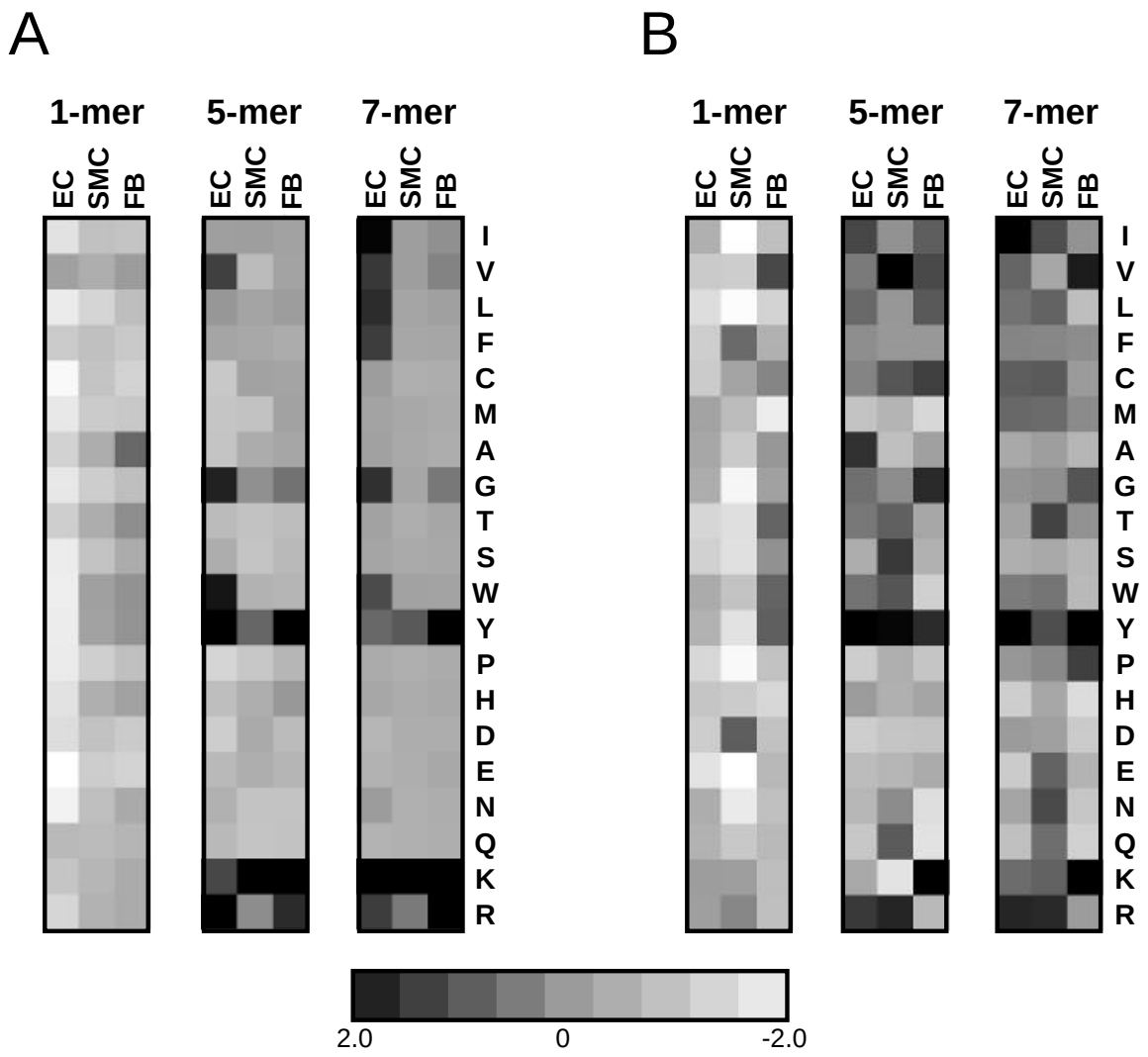

Figure 2. The heatmap of cell adhesion and proliferation on simple repeats of 20 kind of amino acids. The intensity of cell adhesion (A) and proliferation (B) were determined for each cell and each peptide and indicated as gradation of colors. (A) Each cell was seeded on the each peptide array spot and incubated for one hour. Arrays were then washed three times and stained with calcein AM for fluorescent detection. Signal was measured by a fluorescent plate reader at Ex485/Em538. (B) Seeded cells were incubated for three days and stained by calcein AM. Samples were then washed and measured in the same way as for the adhesion assay. The values were normalized in each cell type. Black color indicates high adhesion (+2.0), and white color indicates low adhesion (-2.0).

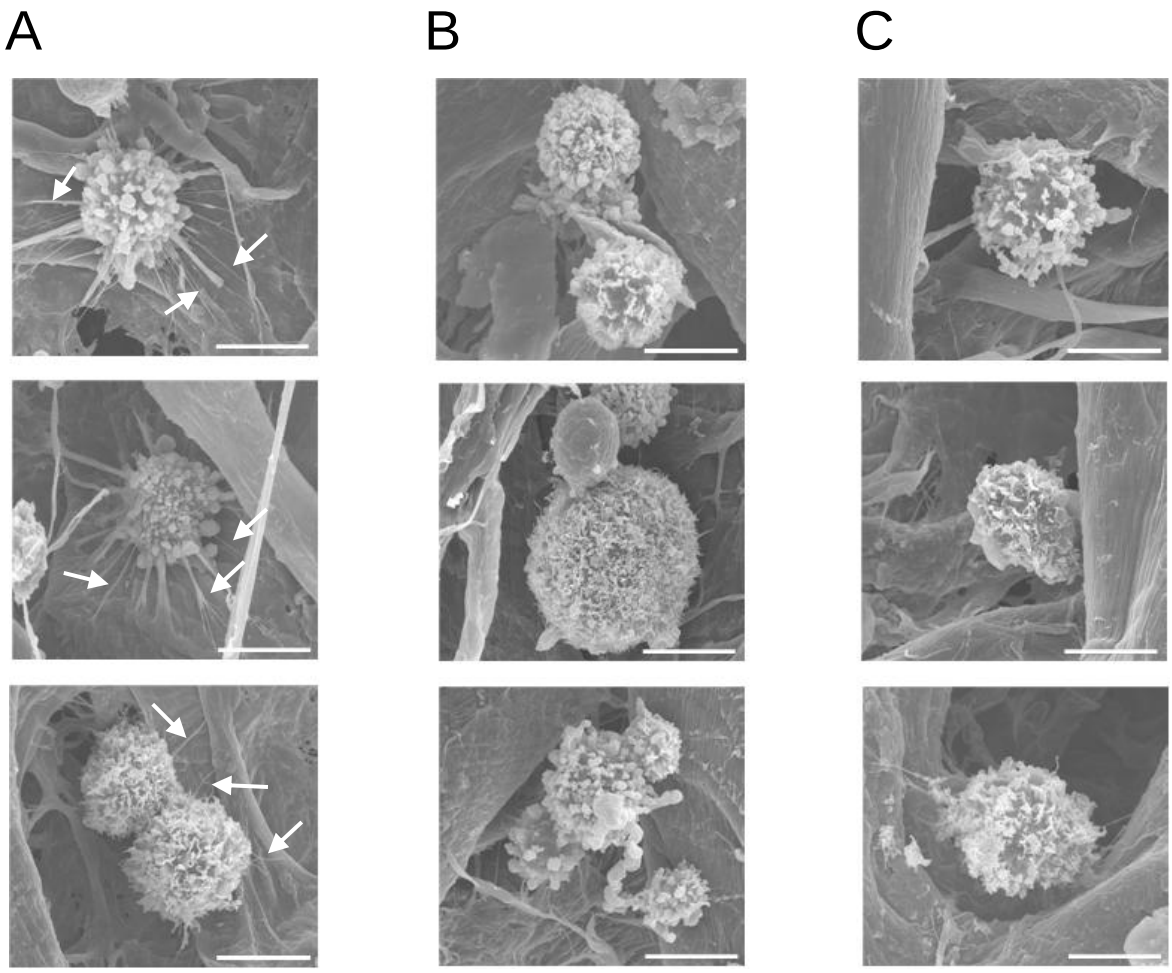

Figure 3. SEM image of cells on EC-selective peptide (Hepta-Ile). SEM images (three fields of views) of morphology after one hour of cell adhesion are shown. (A) ECs, (B) SMCs, and (C) FBs. All images are in the same magnification (scale bar is 10 μm). The large fibrous three dimensional background is due to the cellulose support of SPOT array. Arrows indicate filopodias or ECM fibers from cells.

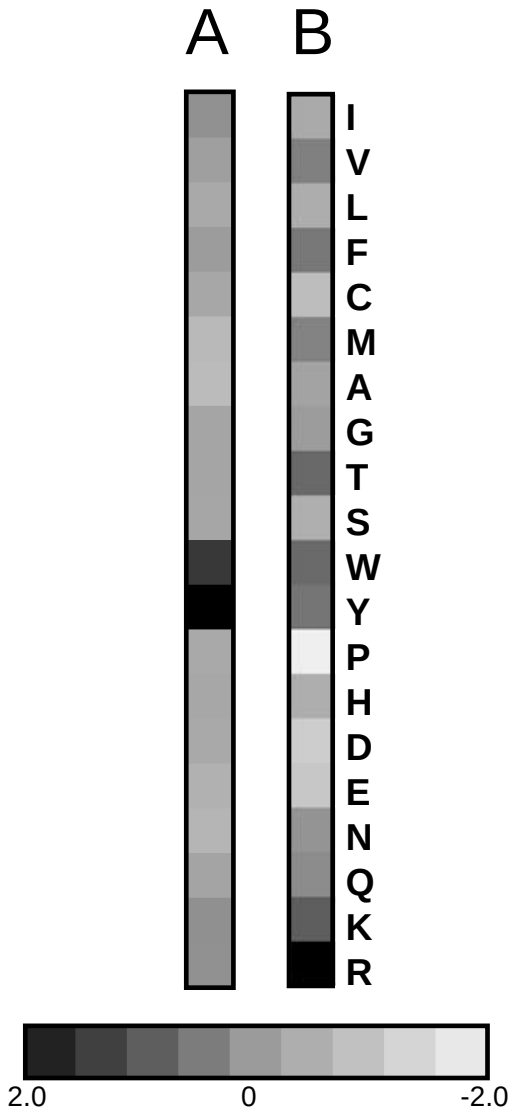

Figure 4. Heatmap of ECM molecule binding to 20 kinds of amino acids (7-mer). Interaction with (A) fibronectin and (B) vitronectin. The peptide array was incubated with the medium containing 10% serum for one hour. Arrays were then hybridized by anti-rabbit human fibronectin IgG or anti-rabbit human vitronectin IgG for two hours then hybridized with anti-rabbit IgG-conjugated Alexa 488 for one hour. Arrays were scanned by FLA-7000 (Ex473/Em520). The fluorescent intensity values were firstly subtracted from the array results with ECM protein and second antibody (without first antibody), and normalized for each ECM protein and illustrated as Figure 2.

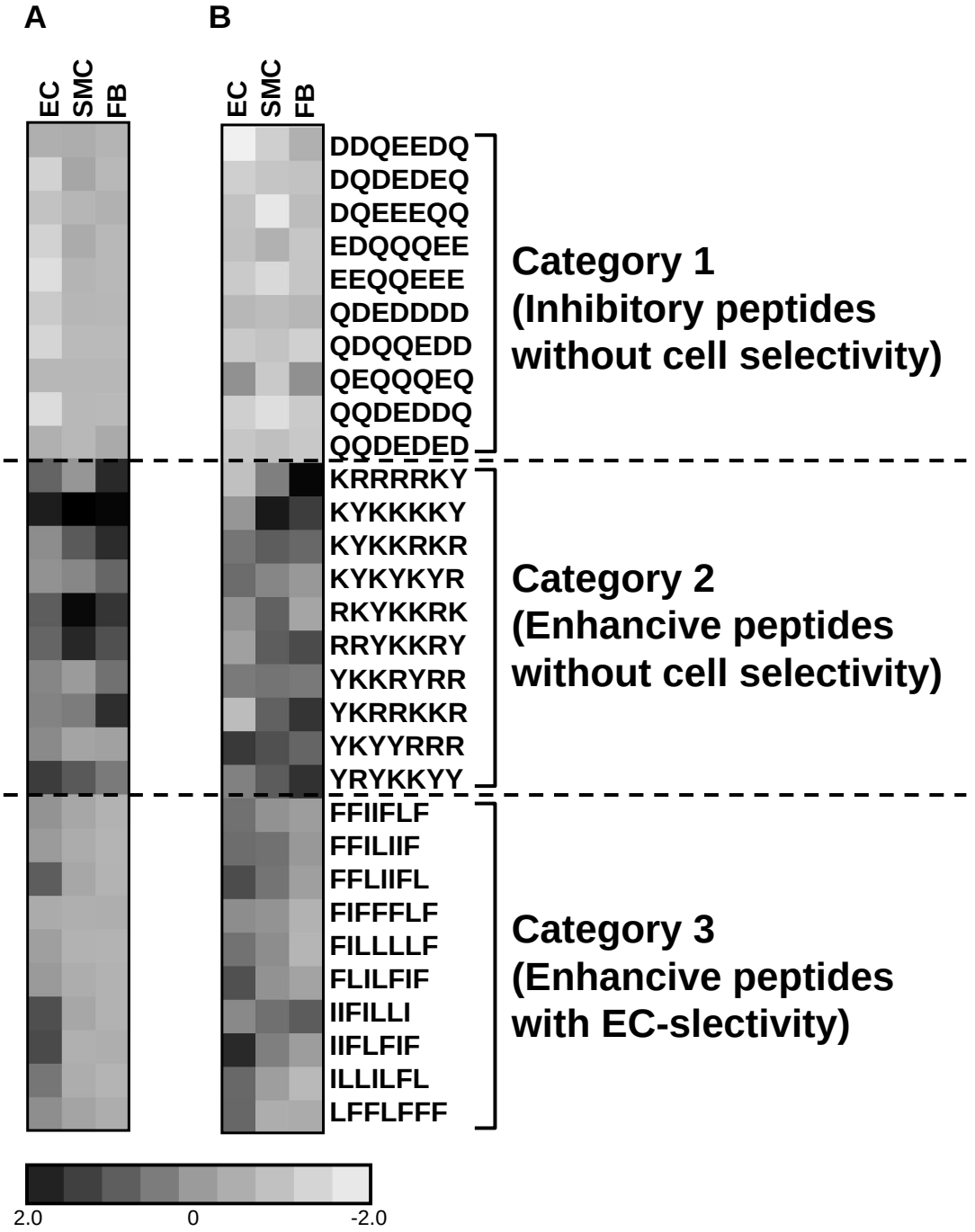

Figure 5. Heatmap of cell adhesion and proliferation on random 7-mer sequences consist of selected amino acids. Nine amino acids were selected to represent three categories; (1) inhibitory peptides without cell selectivity (Asp, Glu and Gln), (2) enhancive peptides without cell selectivity (Lys, Arg, and Tyr), and (3) enhancive peptides with EC- selectivity (Phe, Ile, and Leu). The intensity of cell adhesion and proliferation were determined and illustrated as Figure 2.

3.5. Supplementary Information

3.5.1 Classification and regression tree (CART) analysis

To interpret the physicochemical feature that controls the cell-selective preference of amino acids to design cell-selective molecules, we analyzed the physicochemical properties (amino acid indices) of residues with cell preferences by decision tree analysis. The data was processed as material and methods:

3.5.2 Data labeling and normalization

For the decision tree analysis, (1) cell adhesion rate and (2) cell proliferation rate of each 7-mer peptide (50 peptides; 20 tandem amino acid repeats, 30 selected amino acid random combinations) was obtained by the PIASPAC method with the same protocol described in the material and methods section (**Table S2**). All ratio values were compared with the negative control (no peptide spot) as 1.0. A new index to summarize both cell adhesion rate and cell proliferation rate was introduced as: (3) comprehensive value of adhesion and proliferation (CVAP= (1) x (2)) (**Table S2**). CVAP was then standardized to average=0, SD=1 as (4) sCVAP (**Table S2**). Peptides that were top 30% sCVAP in the normal distribution of sCVAP (> 0.525) were selected and flagged as 1 (positive peptide), and the rest of the peptide were labeled as 0 ((5) in **Table S2**). Peptides that had worst 30% sCVAP (> 0.525) were selected and flagged as 1 (negative peptide), and the rest of the peptide were labeled as 0 ((6) in **Table S2**). SUM indicates the sum of flags through three types of cells. From the total flags, each peptide was labeled with one of four categories (ALL_Enh, ALL_Inh, EC_SL, and NON) ((7) in **Table S2**). Peptides with three enhancive flags were labeled as ALL_Enh. Peptides with three inhibitory flags were labeled as ALL_Inh. Peptides with enhancive flags for EC only were labeled as EC_SL. All the remaining peptides were labeled as NON.

3.5.3 Data conversion to amino acid indices

Peptides were then converted into 13 amino acid indices [26-36] (**Table S3**) from AAindex1 (http://www.genome.ad.jp/dbget-bin/www_bfind?aaindex) [37] with its positional information. The 13 amino acid indices were chosen as the representative most individual indices from the total amino acid indices database. All the existing amino acid indices were standardized and analyzed by hierarchical clustering using Cluster 3.0 (http://bonsai.ims.u-tokyo.ac.jp/~mdehoon/software/cluster/software.htm) with average linkage option to obtain representative few indices. A total of 544 amino acid indices registered in the database (version 9.1, as of January 2008) were found to consist of 21 clusters that have high correlation. Clusters with members found to be too divergent or with inadequate information for peptide interactions were eliminated and the remaining 13 indices were selected as 13 independent indices representing 13 clusters. The selected 13 amino acid indices were: (1) Isoelectric point, (2) Normalized van der Waals volume, (3) Alpha-helix indices for beta-proteins, (4) Beta-strand indices for beta-proteins, (5) Side-chain contribution to protein stability, (6) The stability scale from the knowledge-based atom-atom potential, (7) Hydropathy index, (8) Normalized frequency of turn, (9) Free energy in beta-strand region, (10) Free energy in alpha-helical region, (11) Polarity, (12) Side chain interaction parameter, and (13) Amino acid distribution, listed in **Table S4**. For each peptide, a total for each of the 13 indices were calculated as the physicochemical property of the peptide (**Table S4**). For example, the score of isoelectric point of AAAAAAA was calculated as -0.01498(index value of alanine) x7 = -0.10485.

3.5.4 CART analysis

Decision tree analysis was processed by SPSS (SPSS Japan Inc., an IBM company, Tokyo,

Japan) using 3 categorical labels (ALL_Enh; 6 samples, ALL_Inh; 7 samples, and EC_SL; 10 samples) as output variables and a summary of physicochemical values of peptides as input variables.

The decision tree automatically calculated the combination of physiochemical variables, as opposed to manually interpreted by a researcher, to maximize classification accuracy. In other words, the selected combination reflects the exhaustive consideration of all possible combinations of 13 physicochemical properties for the best classification. **Fig. S2** displays the classification results using a two-dimensional plot (not illustrated in decision tree form for feasible understanding). The numbers and their order (first: isoelectric point, and second: hydrophathy) has significant meaning, and it indicates that other physicochemical properties could not provide better classification results. From the analysis, we found that the isoelectric point is the primary property that classifies “adhesive peptides” and “non-adhesive peptides” at the threshold -4.418 at the first branch (**Fig. S1**). These findings may reflect the known property of cell preference for positively charged surfaces, such as polylysine. However, the EC-selective peptides were found to be more neutral than the universally effective peptides. The combination of isoelectric point (>-4.418) and the hydropathy (>+3.241) was found to be a defining characteristic of EC preferred structures. In the CART analysis shown in **Fig. S1**, the category NON (27 samples) was eliminated from the analysis since it was found to consist of several sub-classes (data not shown). However, when all the 50 samples, including the fourth category (NON) in **Table S2**, were used for the CART analysis, the same classification was found by using isoelectric point and hydropathy (data not shown). From our limited data, we were unable to define a clear physicochemical rule to clearly classify the three groups (EC-selective peptides, SMC-selective peptides, and FB-selective peptides). However, these data provide evidence of the possibility of relatively EC-selective growth control.

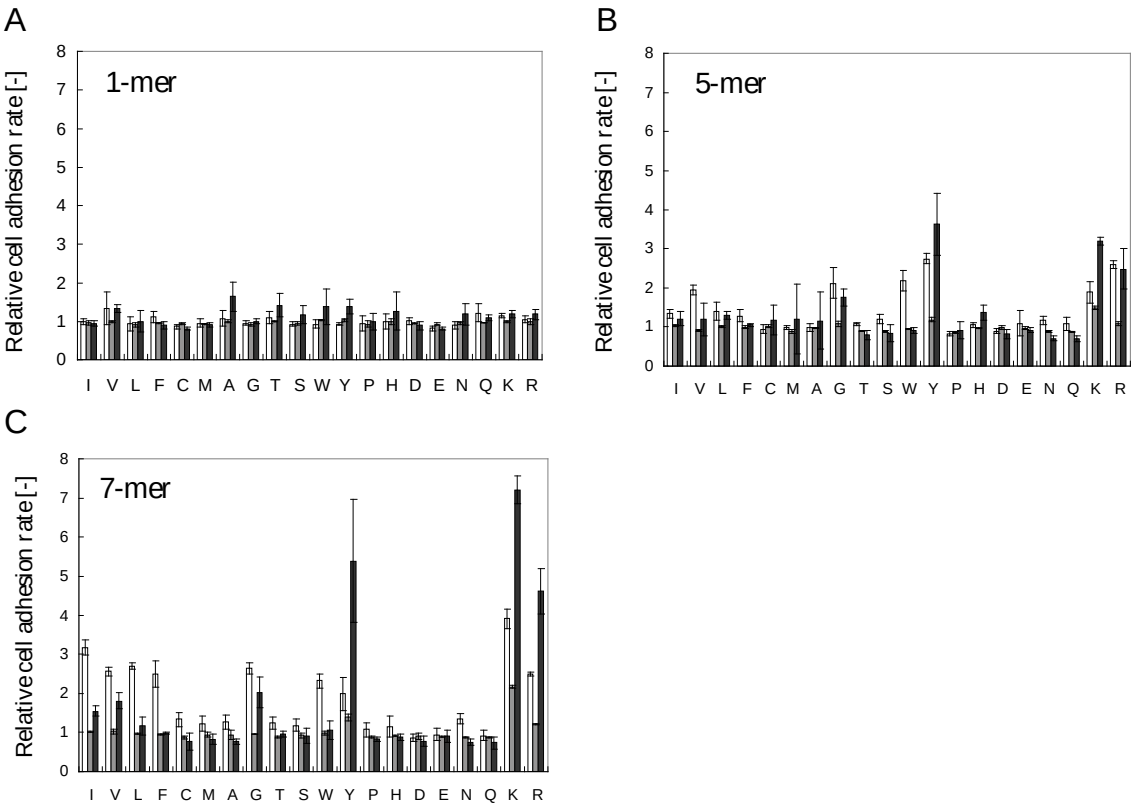

Figure S1. The results of cell adhesion on simple repeats of 20 kind of amino acids (1-mer, 5-mer, and 7-mer). The relative intensity of cell adhesion ratio was determined for each cell and each peptide and indicated as bars (N=3). All ratio values were compared with the negative control (no peptide spot) as 1.0. White bar indicates EC adhesion, gray bar indicates SMC adhesion and black bar indicates FB adhesion. (A) 1-mer, (B) 5-mer and (C) 7-mer.

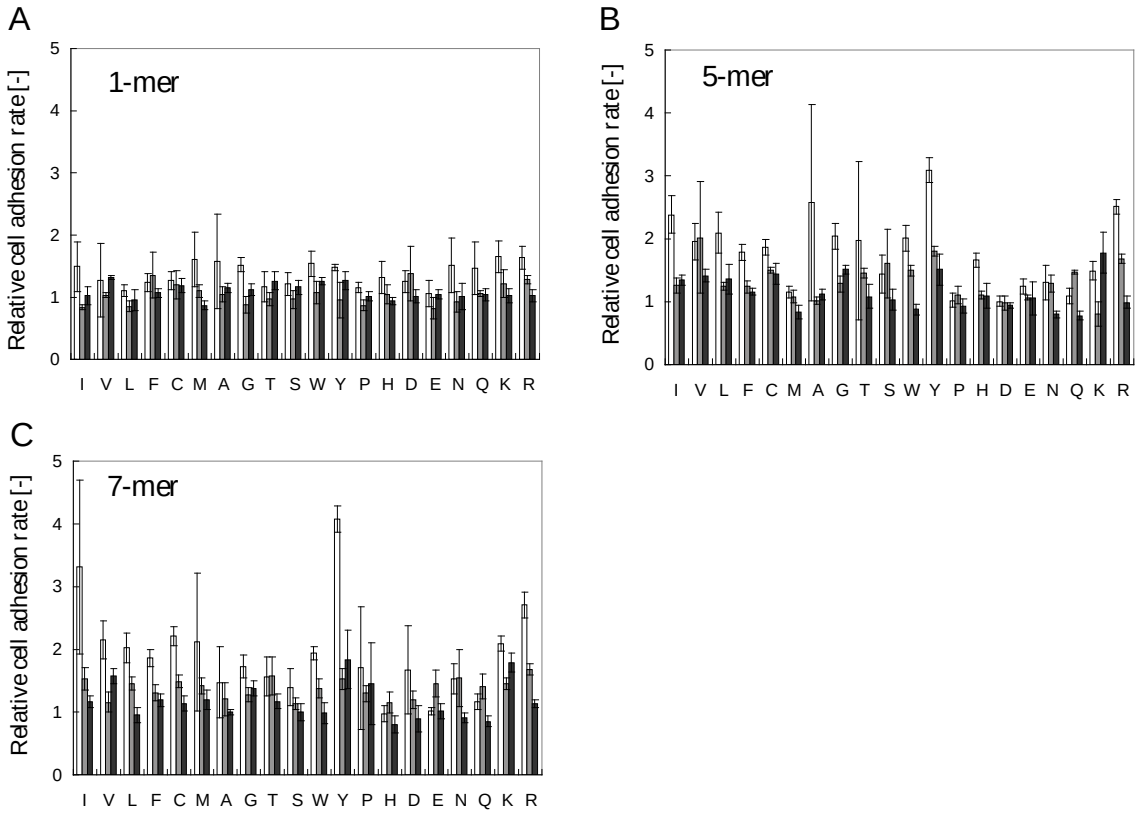

Figure S2. The results of cell proliferation on simple repeats of 20 kind of amino acids (1-mer, 5-mer, and 7-mer). The relative intensity of cell proliferation ratio was determined for each cell and each peptide and indicated as bars (N=3). All ratio values were compared with the negative control (no peptide spot) as 1.0. White bar indicates EC proliferation, gray bar indicates SMC proliferation and black bar indicates FB proliferation. (A) 1-mer, (B) 5-mer and (C) 7-mer.

A

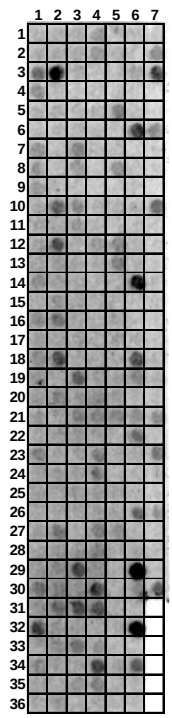

	1	2	3	4	5	6	7
1	Q	AAA	QQQQ Q	RRR	A	T	R
2	No peptide	HHHHHH H	III	WWW	W	D	KKKK K
3	RRRRRR R	YYYYYY Y	MMM	AAAAAA A	SSS	MMMMMM M	KKKKKK K
4	FFFF F	No peptide	EEE	P	III	DDD	EEEEEE E
5	W	R	QQQ	K	KKKK K	No peptide	G
6	TTT	PPPP P	H	HHHH H	NNNN N	KKKKKK K	WWWWWW W
7	LLL	AAAAAA A	LLLL L	Q	SSSS S	DDDDDD D	No peptide
8	VVVVVV V	TTTT T	FFF	NNNN N	RRRR R	AAAA A	No peptide
9	MMM	NNNNNN N	AAA	D	DDD	VVVV V	DDD
10	I	FFFFFF F	WWW	HHH	VVVV V	GGG	LLLLLL L
11	VVV	SSSSSS S	RRR	HHHH H	TTTTTT T	PPP	PPPP P
12	QQQQ Q	LLLLLL L	E	MMMMMM M	LLLL L	GGGG G	No peptide
13	E	GGG	H	PPPPPP P	WWWW W	W	EEEE E
14	MMMM M	F	Q	AAA	AAAAAA A	KKKKKK K	Y
15	VVV	WWW	NNN	SSSS S	EEEEEE E	A	HHHH H
16	VVVVVV V	LLLL L	N	TTTTTT T	HHHHHH H	E	PPPPPP P
17	No peptide	QQQQQQ Q	F	SSS	QQQ	PPP	V
18	MMMM M	YYYY Y	TTTT T	SSSSSS S	TTT	WWWWWW W	HHHHHH H
19	A	TTTTTT T	RRRRRR R	QQQQQQ Q	No peptide	FFFF F	HHH
20	M	IIIII	No peptide	MMMM M	No peptide	QQQQQQ Q	S
21	GGGGGG G	G	IIIII	LLL	MMMMMM M	YYY	WWWW W
22	T	EEE	PPPPPP P	V	DDDD D	FFFFFF F	NNNNNN N
23	FFF	NNN	PPPP P	RRRR R	K	GGGGGG G	IIIIIII
24	SSS	L	M	WWWW W	V	L	III
25	AAAA A	No peptide	M	GGGG G	F	S	PPP
26	TTTT T	QQQ	Y	L	No peptide	RRRRRR R	RRRR R
27	No peptide	YYY	No peptide	KKK	IIIII	EEEEEE E	I
28	T	No peptide	HHH	FFF	NNNNNN N	R	AAAA A
29	N	No peptide	IIIIIII	GGGGGG G	D	YYYYYY Y	S
30	YYY	K	G	WWWWWW W	EEEE E	VVVVVV V	KKKK K
31	Y	FFFF F	IIIIIII	YYYY Y	NNN	SSSS S	
32	YYYY Y	VVVV V	I	H	No peptide	YYYYYY Y	
33	DDDDDD D	GGG	KKK	RRR	VVV	DDDD D	
34	LLL	NNNN N	P	LLLLLL L	GGGG G	FFFFFF F	
35	P	DDDD D	MMM	KKK	N	EEE	
36	QQQQ Q	No peptide	DDDDDD D	SSSSSS S	EEEE E	TTT	

B

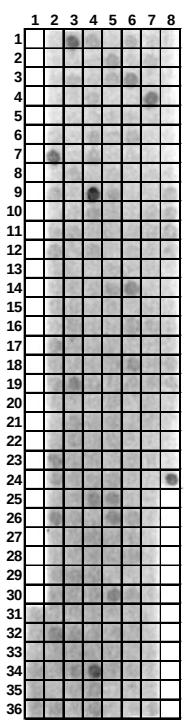

	1	2	3	4	5	6	7	8
1		TTTT T	LLLLLL L	IIIII	SSSS S	IIIII	PPPP P	M
2		W	GGGG G	Q	LLLL L	No peptide	KKK	T
3		WWWWWW W	YYY	VVVV V	YYYY Y	FFFFFF F	NNN	T
4		PPP	EEE	LLL	EEEEEE E	SSSSSS S	LLLLLL L	A
5		N	HHH	PPPPPP P	QQQQ Q	WWWWWW W	HHHH H	No peptide
6		MMM	I	KKK	GGG	IIIII	AAAAAA A	S
7		KKKKKK K	W	KKK	QQQQQQ Q	WWWWWW W	TTT	AAAA A
8		TTTTTT T	FFF	No peptide	F	TTTTTT T	WWWW W	No peptide
9		FFFF F	EEE	KKKKKK K	RRRR R	V	WWW	LLLL L
10		DDD	No peptide	YYYY Y	R	N	RRR	KKKK K
11		VVVVVV V	MMMM M	PPPP P	SSSS S	QQQQQQ Q	QQQQ Q	LLLL L
12		YYYYYY Y	Y	FFF	TTTT T	G	AAA	RRRR R
13		PPPP P	A	TTT	M	H	EEEEEE E	No peptide
14		WWWW W	A	G	RRRR R	FFFFFF F	DDDDDD D	D
15		VVVV V	HHHHHH H	Q	No peptide	D	V	HHHHHH H
16		HHHHHH H	GGGG G	WWW	H	MMMMMM M	No peptide	R
17		LLL	SSS	GGGGGG G	DDDD D	NNNN N	TTTTTT T	SSSS S
18		K	EEEEEE E	GGGGGG G	PPP	RRRRRR R	VVV	YYYY Y
19		YYY	FFFFFF F	MMMM M	S	QQQ	PPPPPP P	RRRRRR R
20		L	V	T	P	DDDDDD D	SSSSSS S	Y
21		S	LLL	SSS	QQQ	NNN	No peptide	E
22		No peptide	RRR	TTT	F	I	No peptide	TTTT T
23		KKKK K	HHH	AAA	NNNNNN N	L	HHH	III
24		RRRRRR R	QQQ	VVVV V	MMMM M	PPP	NNNNNN N	KKKKKK K
25		No peptide	G	YYYYYY Y	KKKK K	AAA	AAAA A	
26		IIIIIII	K	E	IIIIIII	FFFF F	P	
27		H	D	GGGG G	QQQQ Q	R	DDD	
28		DDD	NNN	Q	No peptide	VVVVVV V	NNNN N	
29		WWW	FFF	GGG	DDDDDD D	N	WWWW W	
30		III	E	M	IIIIIII	YYY	MMM	
31	SSS	AAAAAA A	EEE	I	NNNNNN N	No peptide	AAAA A	
32	EEEE E	YYYYYY Y	MMMMMM M	No peptide	III	GGGGGG G	P	
33	DDDD D	AAAAAA A	VVV	SSSSSS S	No peptide	EEEE E	VVV	
34	No peptide	HHHH H	RRR	LLLLLL L	GGG	K	PPPPPP P	
35	EEEE E	DDDD D	No peptide	MMMMMM M	NNNN N	F	W	
36	Y	VVVVVV V	L	FFFF F	HHHH H	QQQQQQ Q	MMM	

Figure S3. The image of fibronectin attraction assay on peptide array. (A) the image of the assay with first antibody (anti-human fibronectin antibody) (B) without first antibody. Left, actual spot image; right, the peptide sequence on the spot.

A

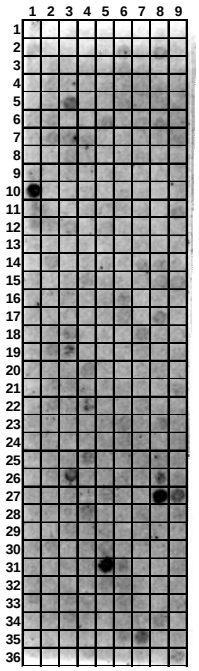

	1	2	3	4	5	6	7	8	9
1	No peptide	EEE	No peptide	G	GGG	PPPPPPP	L	YYY	CCCCCC C
2	YYYYY	NNNN N	F	No peptide	PPPPPPP	YYYYY	No peptide	KKKK K	No peptide
3	K	No peptide	TTT	EEEEEE E	V	FFFFFF F	No peptide	AAAA A	No peptide
4	QQQ	GGG	No peptide	IIIIIII	No peptide	QQQ	AAAAAA A	No peptide	TTT
5	PPP	HHHHHH H	YYYYYYY	AAAA A	Q	KKK	HHH	No peptide	No peptide
6	No peptide	No peptide	T	AAA	RRRR R	W	No peptide	WWWW W	TTTTTT T
7	No peptide	No peptide	FFFFFF F	No peptide	PPPPPPP	SSS	E	NNNN N	SSSSS
8	AAA	I	FFFFFF F	No peptide	D	No peptide	KKK	CCC	V
9	No peptide	CCCCCC C	No peptide	P	WWW	HHH	GGG	M	P
10	KKKKKK K	Q	SSS	No peptide	H	RRR	EEEE E	PPPPP	DDD
11	D	PPP	FFF	No peptide	No peptide	K	KKK	P	LLLLLL L
12	No peptide	LLLL L	LLLLLL L	EEEEEE E	GGGG G	E	EEEEEE E	DDDD D	SSSSSS S
13	IIIIII	DDDDDD D	QQQQQQ Q	TTTTT	CCC	A	FFF	No peptide	HHHH H
14	HHHHHH H	MMMM M	C	No peptide	LLL	M	No peptide	RRRR R	IIIII
15	No peptide	V	EEEEE	WWWWWW W	No peptide	No peptide	GGGG G	FFFF F	MMMMMM M
16	QQQQ Q	W	No peptide	IIIII	No peptide	WWWW W	DDDDDD D	No peptide	VVV
17	VVVVVV V	QQQQQQ Q	No peptide	CCCCCC C	No peptide	GGGG G	AAAAAA A	KKKK K	D
18	L	No peptide	MMMM M	N	NNNN N	I	No peptide	No peptide	GGGGGG G
19	VVVVV	LLLL L	RRRRRR R	Y	I	SSSSSS S	No peptide	TTTTTT T	No peptide
20	No peptide	No peptide	No peptide	FFFF F	L	HHHH H	M	No peptide	DDD
21	T	No peptide	S	No peptide	VVVVVV V	No peptide	No peptide	CCCC C	WWWW W
22	PPPP P	LLLL L	EEEE E	RRRRRR R	AAAAAA A	HHHH H	MMM	N	NNNNNN N
23	No peptide	N	QQQQ Q	C	III	FFFF F	WWW	No peptide	TTTTT
24	Y	CCCC C	EEE	AAAA A	No peptide	YYY	VVVVVV V	S	VVVV
25	H	Q	W	YYYY Y	EEE	CCCC C	No peptide	No peptide	No peptide
26	DDDD D	VVVV	KKKK K	No peptide	No peptide	WWW	E	RRRRRR R	LLL
27	GGGGGG G	NNN	G	Y	MMMM M	NNNNNN N	TTTTTT T	KKKKKK K	YYYYYY Y
28	No peptide	No peptide	G	MMMMMM M	R	No peptide	No peptide	AAA	RRR
29	TTT	SSSSSS S	MMM	No peptide	IIIIIII	T	No peptide	QQQQQQ Q	A
30	No peptide	YYY	QQQQ Q	No peptide	MMMMMM M	No peptide	No peptide	CCC	No peptide
31	No peptide	PPP	IIIII	SSSSS	KKKKKK K	WWWWWW W	VVV	H	No peptide
32	SSS	No peptide	NNNNNN N	HHH	No peptide	LLL	TTTTT	F	QQQ
33	MMM	III	K	No peptide	R	No peptide	NNN	NNN	SSSSS
34	HHHHHH H	GGGGGG G	No peptide	No peptide	DDD	No peptide	C	LLLLLL L	A
35	F	III	PPPPP	S	No peptide	RRRR R	YYYYYY Y	DDDD D	RRR
36	VVV	No peptide	R	FFF	No peptide	No peptide	No peptide	DDDDDD D	WWWWWW W

B

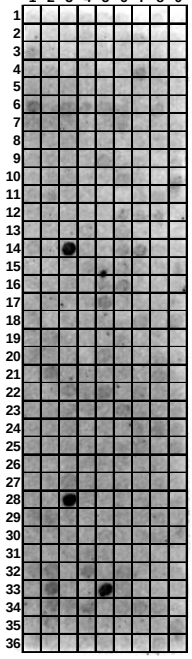

	1	2	3	4	5	6	7	8	9
1	HHHH H	VVVV	VVVVVV	LLLL L	GGGG G	No peptide	CCCCCC C	MMM	EEEE E
2	DDD	HHHHHH H	G	No peptide	SSSSS	No peptide	RRRRRR R	QQQ	SSS
3	WWWW W	EEEEEE E	No peptide	IIIIIII	E	W	NNN	Q	CCCC C
4	HHHHHH H	IIIII	QQQQQQ Q	DDDDDD D	No peptide	K	YYYY Y	No peptide	RRR
5	CCC	NNNNNN N	N	EEE	S	TTTTTT T	No peptide	L	FFF
6	YYYYYY Y	I	GGG	WWWW W	GGGG G	W	No peptide	LLLLLL L	A
7	GGG	CCCCCC C	No peptide	NNN	No peptide	RRRR R	V	AAA	LLL
8	TTT	K	No peptide	No peptide	No peptide	PPPP P	W	FFF	No peptide
9	No peptide	HHHH H	PPPPP	CCC	FFFF F	No peptide	No peptide	H	WWWWWW W
10	F	KKK	EEEEE	D	Y	FFFFFF F	No peptide	SSS	YYYY Y
11	No peptide	WWWWWW W	G	No peptide	No peptide	P	No peptide	YYY	No peptide
12	SSSSS	AAAA A	M	S	I	RRRRRR R	RRRR R	RRRRRR R	TTTTTT T
13	P	R	D	EEEEE	P	GGGG G	QQQQQQ Q	I	CCC
14	No peptide	QQQQQQ Q	KKKKKK K	No peptide	N	RRRR R	KKKK K	No peptide	III
15	TTTTT	TTTTT	Y	RRR	No peptide	No peptide	GGGGGG G	SSSSS	No peptide
16	M	VVV	No peptide	K	WWWWWW W	KKKK K	L	AAAAAA A	No peptide
17	No peptide	GGGGGG G	No peptide	EEE	YYYYYY Y	No peptide	AAA	No peptide	No peptide
18	No peptide	H	No peptide	IIIIIII	No peptide	DDDD D	FFFF F	V	MMMMMM M
19	VVVVVV V	No peptide	KKK	VVVVV	T	QQQQ Q	No peptide	NNNNNN N	Y
20	No peptide	QQQQ Q	QQQ	NNN	MMM	TTT	A	LLL	No peptide
21	E	No peptide	NNNN N	SSSSSSS	F	No peptide	III	LLLLLL L	QQQQ Q
22	No peptide	No peptide	FFFF F	G	LLLLLL L	A	MMM	No peptide	WWW
23	C	EEE	YYY	No peptide	HHH	LLLL L	No peptide	No peptide	WWWW W
24	S	CCCC C	No peptide	AAAAAA A	No peptide	EEEEEE E	No peptide	MMMM M	No peptide
25	IIIII	HHH	WWW	No peptide	HHH	WWW	No peptide	C	FFFFFF F
26	HHHHHH H	AAAA A	VVV	VVVVVV V	DDD	No peptide	CCCC C	SSS	T
27	E	III	MMMM M	No peptide	R	LLL	AAAAAA A	HHHH H	PPPPPP P
28	DDDDDD D	No peptide	KKKKKK K	No peptide	T	No peptide	DDDD D	No peptide	M
29	YYY	KKK	No peptide	C	No peptide	EEEEEE E	GGG	No peptide	AAAA A
30	F	PPPPPP P	Q	TTT	IIIII	NNNNNN N	No peptide	No peptide	No peptide
31	PPP	CCCCCC C	No peptide	No peptide	No peptide	TTTTT	No peptide	AAA	PPPPPP P
32	FFF	MMMMMM M	N	No peptide	DDDD D	No peptide	No peptide	VVV	No peptide
33	V	YYYYYY Y	PPP	TTTTTT T	KKKKKK K	VVVVV	PPP	DDDDDD D	No peptide
34	Q	YYYY Y	No peptide	KKKK K	NNNN N	IIIIIII	LLLL L	No peptide	SSSSSS S
35	L	MMMMMM M	No peptide	No peptide	R	SSSSSS S	PPPP P	NNNN N	MMMM M
36	RRR	GGGGGG G	H	D	No peptide	No peptide	DDD	FFFFFF F	QQQ

Figure S4. The image of vitronectin attraction assay on peptide array. (A) the image of the assay with first antibody (anti-human vitronectin antibody) (B) without first antibody (vitronectin antibody). Left, actual spot image; right, the peptide sequence on the spot.

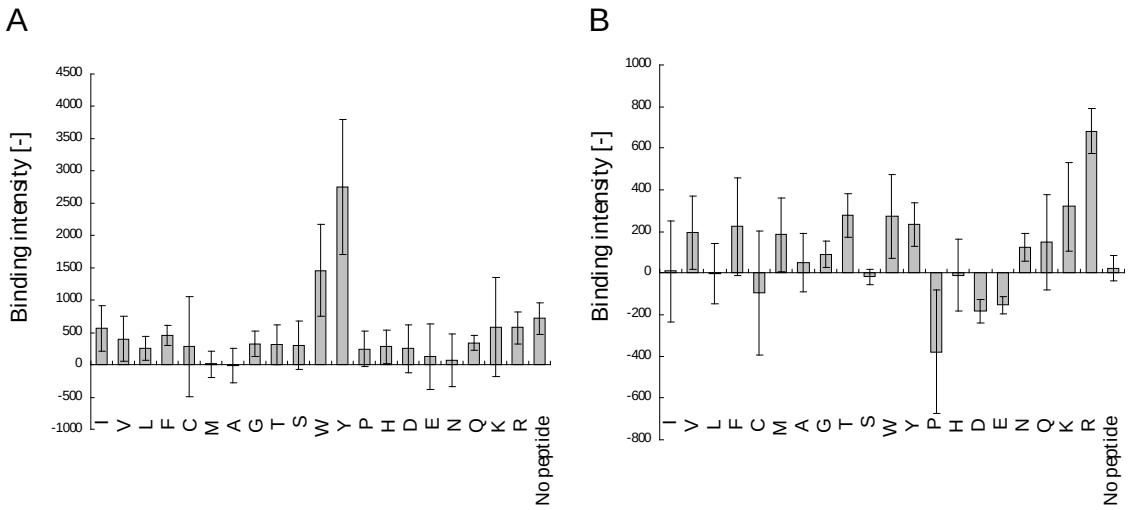

Figure S5. The numerically converted array results of ECM protein binding on 7-mer amino acids. (A) fibronectin (B) vitronectin. The binding intensity was obtained by subtracting two assay results: (fluorescent intensity of hybridization result with first antibody)-(fluorescent intensity of hybridization result with without first antibody) (N=3).

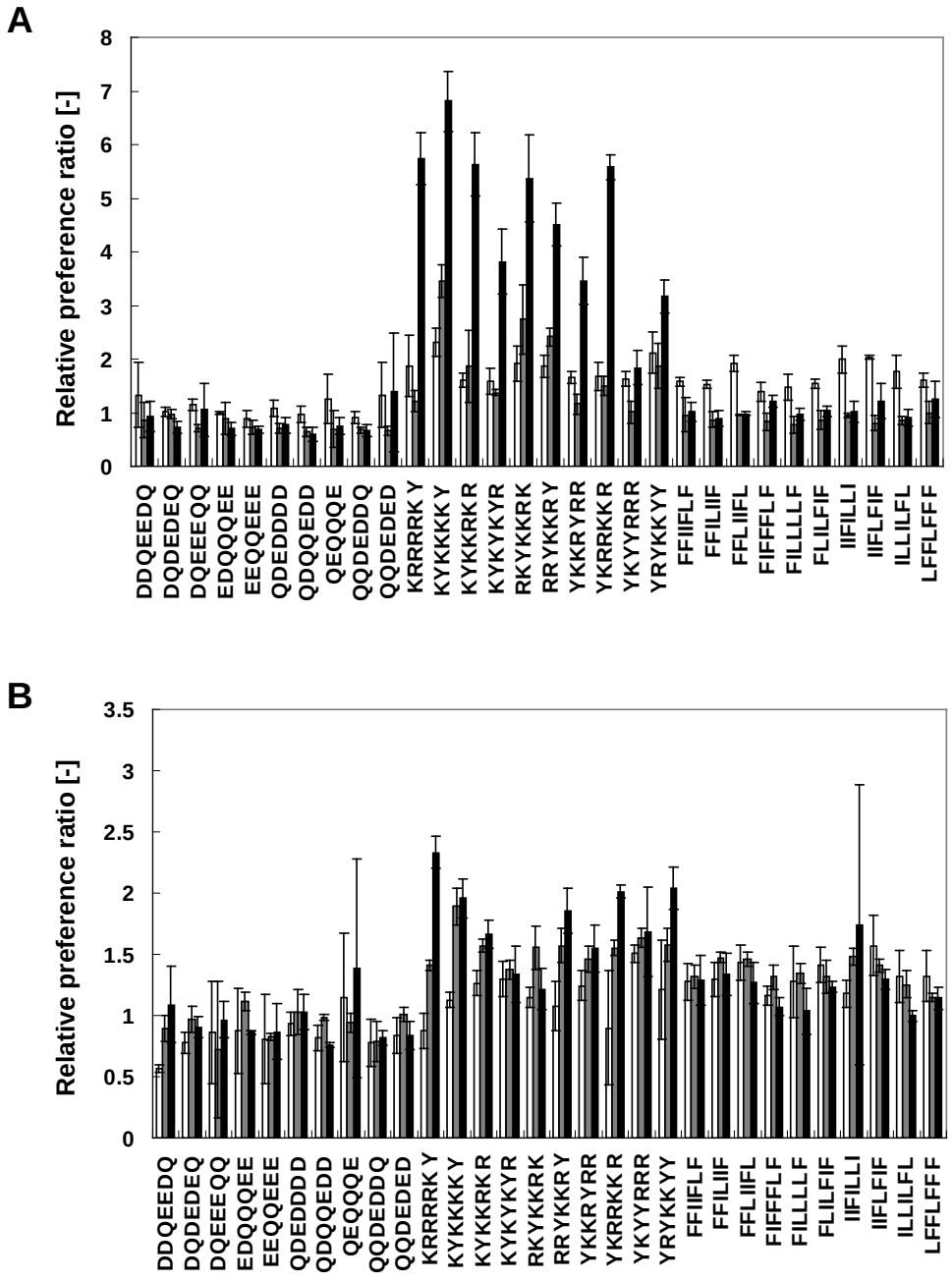

Figure S6. The numerical results of cell adhesion and proliferation on random 7-mer sequences consist of selected amino acids. The relative intensity of cell adhesion and proliferation ratio were determined for each cell and each peptide and indicated as bars (N=3). All ratio values were compared with the negative control (no peptide spot) as 1.0. White bar indicates EC, gray bar indicates SMC and black bar indicates FB.

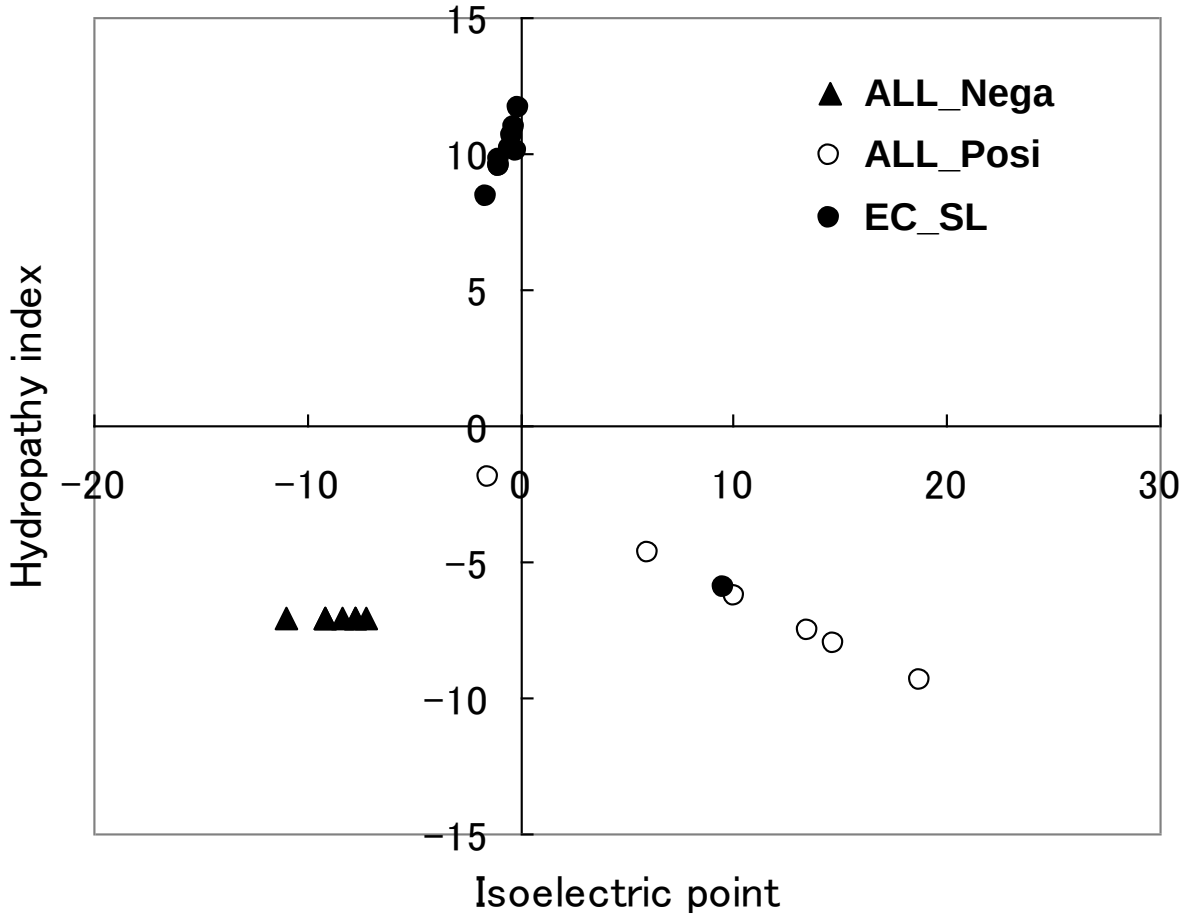

Figure S7. Peptide classification with physicochemical property by CART analysis. The CART was performed to classify three peptide categories with total property numbered according to 13 amino acid indices (**Table S3**). Each symbol indicates the physicochemical property of each peptide (23 samples). ALL_Enh; peptide that enhances both cell adhesion and proliferation with no cell selectivity. ALL_Inh; peptide that inhibits both cell adhesion and proliferation with no cell selectivity. EC_SL; peptide that enhances both cell adhesion and proliferation with EC- selectivity.

Table S1. Cell adhesion and proliferation data from PIASPAC assay

Amino acid	Adhesion									Proliferation								
	1-mer			5-mer			7-mer			1-mer			5-mer			7-mer		
	EC	SMC	FB	EC	SMC	FB	EC	SMC	FB	EC	SMC	FB	EC	SMC	FB	EC	SMC	FB
I	0.99	0.96	0.95	1.34	1.03	1.21	3.18	1.02	1.54	1.49	0.84	1.02	2.39	1.26	1.34	3.31	1.53	1.17
V	1.34	1.00	1.32	1.93	0.92	1.19	2.56	1.02	1.81	1.28	1.04	1.32	1.95	2.02	1.41	2.15	1.16	1.57
L	0.94	0.91	1.01	1.40	1.01	1.30	2.70	0.96	1.17	1.11	0.85	0.96	2.10	1.25	1.36	2.03	1.45	0.96
F	1.11	0.96	0.90	1.28	1.00	1.05	2.49	0.95	0.99	1.24	1.35	1.07	1.78	1.24	1.15	1.86	1.31	1.19
M	0.95	0.93	0.91	0.98	0.89	1.21	1.23	0.94	0.82	1.60	1.10	0.87	1.15	1.08	0.83	2.12	1.42	1.19
A	1.08	1.01	1.64	0.99	0.98	1.16	1.26	0.94	0.77	1.58	1.05	1.15	2.58	1.01	1.12	1.48	1.21	1.00
G	0.95	0.93	1.00	2.12	1.08	1.75	2.64	0.96	2.03	1.52	0.88	1.12	2.04	1.28	1.51	1.72	1.28	1.38
T	1.10	1.01	1.41	1.07	0.89	0.79	1.24	0.90	0.96	1.17	0.97	1.26	1.97	1.45	1.08	1.56	1.58	1.17
S	0.93	0.95	1.17	1.20	0.88	0.85	1.19	0.93	0.91	1.21	0.96	1.16	1.44	1.60	1.03	1.40	1.14	0.99
W	0.92	1.04	1.38	2.19	0.95	0.92	2.33	0.99	1.06	1.54	1.07	1.26	2.01	1.50	0.87	1.94	1.38	0.98
Y	0.93	1.03	1.37	2.74	1.19	3.62	1.98	1.39	5.39	1.48	0.96	1.27	3.09	1.80	1.51	4.08	1.53	1.84
P	0.94	0.92	0.99	0.83	0.87	0.90	1.08	0.89	0.83	1.16	0.87	1.01	1.02	1.11	0.93	1.71	1.30	1.45
H	0.99	1.00	1.27	1.05	0.97	1.37	1.15	0.91	0.88	1.32	1.04	0.94	1.66	1.11	1.09	0.98	1.15	0.80
D	1.02	0.96	0.89	0.90	0.99	0.81	0.87	0.90	0.77	1.25	1.38	1.01	1.00	0.98	0.94	1.67	1.20	0.89
E	0.81	0.93	0.81	1.09	0.97	0.92	0.95	0.89	0.91	1.06	0.82	1.05	1.24	1.07	1.06	1.02	1.45	1.01
N	0.90	0.96	1.19	1.17	0.89	0.70	1.35	0.88	0.76	1.52	0.93	1.02	1.31	1.29	0.80	1.53	1.55	0.91
Q	1.21	0.97	1.09	1.09	0.88	0.70	0.92	0.88	0.73	1.48	1.06	1.04	1.09	1.47	0.78	1.17	1.41	0.86
K	1.15	0.98	1.18	1.89	1.49	3.20	3.91	2.17	7.21	1.65	1.22	1.02	1.49	0.80	1.78	2.09	1.46	1.79
R	1.05	0.99	1.19	2.60	1.08	2.48	2.50	1.22	4.62	1.64	1.28	1.02	2.51	1.68	0.99	2.71	1.68	1.14

Table S2. Peptide list for CART analysis

Sequence	Library type	(1)			(2)			(3)			(4)			(5)				(6)				(7)
		HUVEC	SMC	NHDF	HUVEC	SMC	NHDF	HUVEC	SMC	NHDF	HUVEC	SMC	NHDF	HUVEC	SMC	NHDF	SUM	HUVEC	SMC	NHDF	SUM	
1 AAAAAAA	Tandem repeats	1.28	0.89	0.92	1.50	1.21	1.13	1.92	1.08	1.04	-0.73	-0.61	-0.50	0	0	0	0	1	1	0	2	NON
2 DDDDDDD	Tandem repeats	0.88	0.86	0.93	1.69	1.20	1.01	1.49	1.03	0.94	-0.88	-0.72	-0.52	0	0	0	0	1	1	0	2	NON
3 EEEEEEE	Tandem repeats	0.96	0.85	1.09	1.03	1.45	1.15	0.99	1.23	1.25	-1.05	-0.28	-0.45	0	0	0	0	1	0	0	1	NON
4 FFFFFFF	Tandem repeats	2.53	0.90	1.19	1.89	1.31	1.35	4.78	1.18	1.60	0.27	-0.39	-0.38	0	0	0	0	0	0	0	0	NON
5 GGGGGGG	Tandem repeats	2.68	0.91	2.43	1.75	1.28	1.56	4.69	1.16	3.80	0.24	-0.44	0.12	0	0	0	0	0	0	0	0	NON
6 HHHHHHH	Tandem repeats	1.17	0.87	1.06	0.99	1.15	0.90	1.16	1.00	0.96	-0.99	-0.77	-0.52	0	0	0	0	1	1	0	2	NON
7 IIIIIII	Tandem repeats	3.22	0.97	1.84	3.36	1.53	1.33	10.82	1.49	2.44	2.38	0.26	-0.19	1	0	0	1	0	0	0	0	EC_SL
8 KKKKKKK	Tandem repeats	3.97	2.06	8.64	2.12	1.46	2.03	8.40	3.00	17.52	1.53	3.47	3.18	1	1	1	3	0	0	0	0	ALL_Enh
9 LLLLLLL	Tandem repeats	2.74	0.91	1.40	2.06	1.45	1.08	5.64	1.33	1.51	0.57	-0.08	-0.40	1	0	0	1	0	0	0	0	EC_SL
10 MMMMMMM	Tandem repeats	1.25	0.90	0.98	2.15	1.42	1.36	2.68	1.28	1.33	-0.46	-0.19	-0.44	0	0	0	0	0	0	0	0	NON
11 NNNNNNN	Tandem repeats	1.37	0.84	0.91	1.55	1.55	1.03	2.13	1.30	0.94	-0.65	-0.15	-0.52	0	0	0	0	1	0	0	1	NON
12 PPPPPPP	Tandem repeats	1.09	0.84	1.00	1.73	1.30	1.65	1.89	1.10	1.65	-0.74	-0.57	-0.37	0	0	0	0	1	1	0	2	NON
13 QQQQQQQ	Tandem repeats	0.94	0.84	0.88	1.19	1.41	0.97	1.11	1.18	0.85	-1.01	-0.41	-0.54	0	0	0	0	1	0	1	2	NON
14 RRRRRRR	Tandem repeats	2.53	1.16	5.53	2.74	1.68	1.29	6.95	1.95	7.13	1.03	1.23	0.86	1	1	1	3	0	0	0	0	ALL_Enh
15 SSSSSSS	Tandem repeats	1.21	0.88	1.09	1.42	1.14	1.13	1.71	1.01	1.23	-0.80	-0.77	-0.46	0	0	0	0	1	1	0	2	NON
16 TTTTTTT	Tandem repeats	1.26	0.85	1.15	1.58	1.58	1.33	1.99	1.34	1.54	-0.70	-0.05	-0.39	0	0	0	0	1	0	0	1	NON
17 VVVVVVV	Tandem repeats	2.60	0.97	2.17	2.18	1.16	1.79	5.65	1.12	3.88	0.58	-0.52	0.13	1	0	0	1	0	0	0	0	EC_SL
18 WWWWWWW	Tandem repeats	2.37	0.94	1.26	1.97	1.38	1.12	4.66	1.30	1.41	0.23	-0.14	-0.42	0	0	0	0	0	0	0	0	NON
19 YYYYYYY	Tandem repeats	2.01	1.32	6.45	4.13	1.54	2.09	8.33	2.02	13.46	1.51	1.39	2.27	1	1	1	3	0	0	0	0	ALL_Enh
20 DDQEEDQ	Random sequence	1.33	0.85	0.92	0.57	0.89	1.09	0.76	0.76	1.00	-1.43	-0.65	-0.61	0	0	0	0	1	1	1	3	ALL_Inh
21 DQDEDEQ	Random sequence	1.00	0.97	0.73	0.78	0.97	0.90	0.78	0.94	0.65	-1.39	-0.52	-0.70	0	0	0	0	1	0	1	2	NON
22 DQEEEQQ	Random sequence	1.15	0.71	1.05	0.86	0.72	0.96	0.99	0.51	1.01	-1.09	-0.84	-0.61	0	0	0	0	1	1	1	3	ALL_Inh
23 EDQQQEE	Random sequence	1.00	0.88	0.69	0.88	1.11	0.86	0.87	0.98	0.60	-1.26	-0.48	-0.71	0	0	0	0	1	0	1	2	NON
24 EEQQEEE	Random sequence	0.88	0.73	0.69	0.81	0.82	0.87	0.72	0.60	0.60	-1.49	-0.77	-0.71	0	0	0	0	1	1	1	3	ALL_Inh
25 QDEDDDD	Random sequence	1.07	0.70	0.76	0.93	1.03	1.03	1.00	0.73	0.78	-1.09	-0.68	-0.66	0	0	0	0	1	1	1	3	ALL_Inh
26 QDQQEDD	Random sequence	0.97	0.63	0.59	0.81	0.98	0.76	0.79	0.62	0.45	-1.39	-0.76	-0.75	0	0	0	0	1	1	1	3	ALL_Inh
27 QEQQQEQ	Random sequence	1.26	0.69	0.74	1.15	0.94	1.39	1.45	0.65	1.03	-0.44	-0.74	-0.60	0	0	0	0	0	1	1	2	NON
28 QQDEDDQ	Random sequence	0.90	0.67	0.66	0.78	0.79	0.82	0.70	0.53	0.54	-1.51	-0.83	-0.72	0	0	0	0	1	1	1	3	ALL_Inh
29 QQDEDED	Random sequence	1.33	0.66	1.38	0.84	1.01	0.84	1.11	0.67	1.16	-0.92	-0.72	-0.57	0	0	0	0	1	1	1	3	ALL_Inh
30 FFIIFLF	Random sequence	1.58	0.95	1.00	1.28	1.32	1.29	2.01	1.25	1.29	0.37	-0.28	-0.54	0	0	0	0	0	0	1	1	NON
31 FFILIIF	Random sequence	1.52	0.86	0.89	1.29	1.48	1.34	1.97	1.27	1.19	0.31	-0.26	-0.56	0	0	0	0	0	0	1	1	NON
32 FFLIIFL	Random sequence	1.91	0.96	0.97	1.43	1.46	1.27	2.74	1.41	1.23	1.41	-0.16	-0.55	1	0	0	1	0	0	1	1	EC_SL
33 FIFFFLF	Random sequence	1.38	0.83	1.21	1.16	1.31	1.07	1.60	1.08	1.29	-0.22	-0.41	-0.54	0	0	0	0	0	0	1	1	NON
34 FILLLLF	Random sequence	1.48	0.77	0.97	1.27	1.34	1.03	1.89	1.03	1.00	0.19	-0.45	-0.61	0	0	0	0	0	0	1	1	NON
35 FLILFIF	Random sequence	1.53	0.86	1.03	1.41	1.32	1.23	2.16	1.13	1.27	0.59	-0.37	-0.54	1	0	0	1	0	0	1	1	EC_SL
36 IIFILLI	Random sequence	2.00	0.95	1.02	1.18	1.48	1.74	2.36	1.40	1.77	0.86	-0.17	-0.42	1	0	0	1	0	0	0	0	EC_SL
37 IIFLFIF	Random sequence	2.03	0.80	1.21	1.57	1.41	1.30	3.19	1.12	1.57	2.06	-0.38	-0.47	1	0	0	1	0	0	0	0	EC_SL
38 ILLILFL	Random sequence	1.75	0.85	0.90	1.32	1.25	1.00	2.31	1.07	0.90	0.79	-0.42	-0.64	1	0	0	1	0	0	1	1	EC_SL
39 LFFLFFF	Random sequence	1.61	1.00	1.25	1.32	1.15	1.14	2.12	1.14	1.42	0.53	-0.36	-0.51	1	0	0	1	0	0	0	0	EC_SL
40 KRRRRKY	Random sequence	1.87	1.21	5.74	0.87	1.41	2.33	1.63	1.71	13.38	-0.17	0.07	2.50	0	0	1	1	0	0	0	0	NON
41 KYKKKKY	Random sequence	2.30	3.45	6.81	1.13	1.89	1.96	2.60	6.53	13.34	1.21	3.72	2.49	1	1	1	3	0	0	0	0	ALL_Enh
42 KYKKRKR	Random sequence	1.61	1.86	5.62	1.26	1.57	1.66	2.04	2.92	9.35	0.41	0.99	1.49	0	1	1	2	0	0	0	0	NON
43 KYKYKYR	Random sequence	1.58	1.37	3.81	1.30	1.38	1.33	2.06	1.89	5.08	0.44	0.20	0.41	0	0	0	0	0	0	0	0	NON
44 RKYKKRK	Random sequence	1.91	2.74	5.36	1.15	1.55	1.21	2.19	4.26	6.50	0.63	2.00	0.77	1	1	1	3	0	0	0	0	ALL_Enh
45 RRYKKRY	Random sequence	1.86	2.41	4.51	1.07	1.57	1.86	1.99	3.79	8.38	0.34	1.64	1.24	0	1	1	2	0	0	0	0	NON
46 YKKRYRR	Random sequence	1.65	1.15	3.45	1.24	1.46	1.55	2.06	1.69	5.35	0.43	0.05	0.48	0	0	0	0	0	0	0	0	NON
47 YKRRKKR	Random sequence	1.67	1.49	5.58	0.90	1.55	2.01	1.50	2.32	11.23	-0.36	0.53	1.96	0	1	1	2	0	0	0	0	NON
48 YKYYRRR	Random sequence	1.63	1.01	1.83	1.51	1.63	1.68	2.46	1.65	3.08	1.01	0.02	-0.09	1	0	0	1	0	0	0	0	EC_SL
49 YRYKKYY	Random sequence	2.11	1.87	3.16	1.21	1.58	2.04	2.56	2.95	6.44	1.16	1.01	0.76	1	1	1	3	0	0	0	0	ALL_Enh

Table S3. List of names of 13 amino acid indices

Index number	Index name	Reference
1	Isoelectric point	26
2	Normalized van der Waals volume	27
3	Alpha-helix indices for beta-proteins	28
4	Beta-strand indices for beta-proteins	28
5	Side-chain contribution to protein stability	29
6	The stability scale from the knowledge-based atom-atom potel	30
7	Hydropathy index	31
8	Normalized frequency of turn	32
9	Free energy in beta-strand region	33
10	Free energy in alpha-helical region	33
11	Polarity	34
12	Side chain interaction parameter	35
13	Amino acid distribution	36

Table S4. List of values of 13 amino acid indices

Amino acid	Amino acid index number												
	1	2	3	4	5	6	7	8	9	10	11	12	13
A	-0.01	-1.42	1.00	-0.51	-0.09	-0.61	0.77	-1.32	0.24	-1.28	-0.62	-0.25	1.71
D	-1.84	-0.51	1.00	-1.24	-0.78	-0.89	-1.01	0.73	0.37	-0.09	1.65	0.69	0.42
E	-1.59	0.01	1.24	-2.29	-0.85	-0.80	-1.01	-1.19	0.21	-1.07	1.66	0.76	0.19
F	-0.31	1.10	-1.38	1.24	1.77	1.82	1.10	0.12	-0.60	0.05	-0.60	-1.20	-0.57
G	-0.03	-1.94	-0.99	-0.51	-1.47	-1.27	0.03	1.17	1.15	1.55	-0.62	0.72	1.33
H	0.88	0.46	0.29	0.25	0.21	-0.39	-0.91	-0.20	-0.30	0.30	1.73	0.48	-1.25
I	0.00	0.12	0.42	0.62	0.96	0.91	1.67	-1.10	-0.78	-0.30	-0.61	-1.35	0.04
K	2.10	0.52	0.27	0.03	0.01	-0.65	-1.14	0.28	-0.05	-0.65	1.64	1.72	0.80
L	-0.03	0.12	0.37	1.02	0.93	1.05	1.44	-1.00	-0.21	-0.82	-0.61	-0.46	1.25
M	-0.16	0.34	0.62	0.54	0.21	0.34	0.80	-1.10	-0.29	-0.84	-0.56	-1.28	-1.48
N	-0.35	-0.42	0.27	-1.46	-0.96	-0.82	-1.01	1.30	0.11	0.51	-0.47	0.80	-0.04
P	0.15	-0.54	-1.78	-1.42	0.65	-0.67	-0.37	1.46	3.74	3.15	-0.55	1.32	-0.42
Q	-0.21	0.10	0.13	0.40	-1.13	-0.62	-1.01	-0.30	0.00	-0.71	-0.46	0.74	-0.49
R	2.68	1.22	-1.80	0.54	-0.44	-0.26	-1.34	-0.71	-0.17	-0.77	1.75	0.97	-0.34
S	-0.20	-1.12	-0.12	-0.33	-1.10	-0.95	-0.10	0.79	-0.17	0.05	-0.54	0.33	1.10
T	-0.21	-0.60	-1.07	0.51	-0.49	-0.61	-0.07	0.12	-0.63	0.37	-0.54	0.21	0.49
V	-0.04	-0.39	-0.89	1.13	0.69	0.43	1.57	-1.70	-0.90	-0.06	-0.61	-0.80	0.87
W	-0.08	2.23	1.64	0.47	1.94	2.20	-0.14	0.69	-0.42	-0.17	-0.52	-1.09	-1.71
Y	-0.21	1.40	0.02	1.34	0.96	1.25	-0.27	1.08	-0.65	0.21	-0.55	-0.65	-0.57

Values are all normalized as average = 0, SD = 1.0.

Table S5. List of peptides for CART analysis with averaged amino acid indices

	Sequence	Library type	Amino acid index number												
			1	2	3	4	5	6	7	8	9	10	11	12	13
1	AAAAAAA	Tandem repeats	-0.10	-9.97	6.97	-3.58	-0.60	-4.25	5.37	-9.24	1.69	-8.98	-4.34	-1.74	11.97
2	DDDDDDD	Tandem repeats	-12.88	-3.55	6.97	-8.67	-5.43	-6.22	-7.05	5.08	2.59	-0.62	11.53	4.84	2.93
3	EEEEEEE	Tandem repeats	-11.10	0.06	8.71	-16.06	-5.92	-5.58	-7.05	-8.35	1.45	-7.49	11.60	5.34	1.33
4	FFFFFFF	Tandem repeats	-2.16	7.68	-9.69	8.65	12.42	12.72	7.71	0.83	-4.20	0.34	-4.23	-8.37	-3.99
5	GGGGGGG	Tandem repeats	-0.22	-13.58	-6.94	-3.58	-10.26	-8.88	0.21	8.21	8.08	10.84	-4.34	5.03	9.31
6	HHHHHHH	Tandem repeats	6.19	3.24	2.04	1.77	1.47	-2.73	-6.35	-1.41	-2.12	2.11	12.14	3.39	-8.78
7	IIIIIII	Tandem repeats	-0.03	0.86	2.91	4.32	6.70	6.39	11.69	-7.68	-5.44	-2.12	-4.30	-9.44	0.27
8	KKKKKKK	Tandem repeats	14.69	3.64	1.90	0.24	0.09	-4.52	-7.99	1.95	-0.36	-4.57	11.47	12.04	5.59
9	LLLLLLL	Tandem repeats	-0.18	0.86	2.62	7.12	6.50	7.36	10.05	-7.00	-1.49	-5.75	-4.30	-3.24	8.78
10	MMMMMMM	Tandem repeats	-1.13	2.41	4.36	3.81	1.47	2.40	5.60	-7.68	-2.04	-5.86	-3.89	-8.95	-10.38
11	NNNNNNN	Tandem repeats	-2.44	-2.93	1.90	-10.20	-6.71	-5.76	-7.05	9.11	0.74	3.57	-3.26	5.61	-0.27
12	PPPPPPP	Tandem repeats	1.08	-3.76	-12.44	-9.95	4.53	-4.66	-2.60	10.23	26.16	22.03	-3.84	9.25	-2.93
13	QQQQQQQ	Tandem repeats	-1.49	0.68	0.88	2.79	-7.89	-4.34	-7.05	-2.08	-0.03	-4.95	-3.21	5.19	-3.46
14	RRRRRRR	Tandem repeats	18.73	8.55	-12.59	3.81	-3.06	-1.82	-9.40	-4.99	-1.22	-5.40	12.27	6.80	-2.39
15	SSSSSSS	Tandem repeats	-1.37	-7.81	-0.85	-2.31	-7.70	-6.63	-0.73	5.53	-1.22	0.37	-3.81	2.28	7.72
16	TTTTTTT	Tandem repeats	-1.45	-4.20	-7.52	3.55	-3.46	-4.25	-0.49	0.83	-4.44	2.61	-3.81	1.47	3.46
17	VVVVVVV	Tandem repeats	-0.26	-2.75	-6.21	7.88	4.83	3.04	10.99	-11.93	-6.31	-0.43	-4.30	-5.61	6.12
18	WWWWWWW	Tandem repeats	-0.54	15.59	11.46	3.30	13.60	15.38	-0.96	4.86	-2.91	-1.21	-3.67	-7.64	-11.97
19	YYYYYYY	Tandem repeats	-1.45	9.78	0.16	9.41	6.70	8.73	-1.90	7.54	-4.57	1.44	-3.83	-4.58	-3.99
20	DDQEEDQ	Random sequenc	-9.12	-1.31	5.73	-7.51	-6.27	-5.50	-7.05	-0.80	1.51	-3.82	7.34	5.08	0.65
21	DQDEDEQ	Random sequenc	-9.12	-1.31	5.73	-7.51	-6.27	-5.50	-7.05	-0.80	1.51	-3.82	7.34	5.08	0.65
22	DQEEEQQ	Random sequenc	-7.24	-0.19	5.11	-6.93	-6.70	-5.14	-7.05	-3.74	0.97	-5.42	5.24	5.20	-0.49
23	EDQQQEE	Random sequenc	-7.24	-0.19	5.11	-6.93	-6.70	-5.14	-7.05	-3.74	0.97	-5.42	5.24	5.20	-0.49
24	EEQQEEE	Random sequenc	-8.36	0.24	6.47	-10.68	-6.49	-5.22	-7.05	-6.56	1.02	-6.76	7.37	5.30	-0.04
25	QDEDDDD	Random sequenc	-11.00	-2.43	6.35	-8.09	-5.85	-5.86	-7.05	2.14	2.05	-2.22	9.44	4.96	1.79
26	QDQQEDD	Random sequenc	-7.75	-1.22	4.61	-4.82	-6.56	-5.32	-7.05	0.09	1.30	-3.46	5.22	5.06	-0.04
27	QEQQQEQ	Random sequenc	-4.24	0.50	3.12	-2.60	-7.33	-4.69	-7.05	-3.87	0.39	-5.67	1.02	5.23	-2.09
28	QQDEDDQ	Random sequenc	-7.75	-1.22	4.61	-4.82	-6.56	-5.32	-7.05	0.09	1.30	-3.46	5.22	5.06	-0.04
29	QQDEDED	Random sequenc	-9.12	-1.31	5.73	-7.51	-6.27	-5.50	-7.05	-0.80	1.51	-3.82	7.34	5.08	0.65
30	FFIIFLF	Random sequenc	-1.27	4.76	-4.33	7.19	9.94	10.15	9.18	-2.72	-4.16	-1.23	-4.26	-7.94	-0.95
31	FFILIIF	Random sequenc	-0.96	3.78	-2.53	6.57	9.12	9.24	9.75	-3.94	-4.34	-1.58	-4.27	-8.10	-0.34
32	FFLIIFL	Random sequenc	-0.99	3.78	-2.57	6.97	9.10	9.38	9.52	-3.84	-3.78	-2.10	-4.27	-7.21	0.87
33	FIFFFLF	Random sequenc	-1.57	5.73	-6.13	7.81	10.76	11.05	8.61	-1.51	-3.99	-0.88	-4.25	-7.79	-1.56
34	FILLLLF	Random sequenc	-0.73	2.81	-0.85	7.16	8.22	8.75	9.62	-4.86	-2.83	-3.49	-4.28	-5.59	3.92
35	FLILFIF	Random sequenc	-0.99	3.78	-2.57	6.97	9.10	9.38	9.52	-3.84	-3.78	-2.10	-4.27	-7.21	0.87
36	IIFILLI	Random sequenc	-0.38	1.83	1.03	5.74	7.46	7.57	10.66	-6.27	-4.13	-2.80	-4.29	-7.52	2.09
37	IIFLFIF	Random sequenc	-0.96	3.78	-2.53	6.57	9.12	9.24	9.75	-3.94	-4.34	-1.58	-4.27	-8.10	-0.34
38	ILLILFL	Random sequenc	-0.42	1.83	0.95	6.54	7.41	7.85	10.19	-6.08	-3.00	-3.84	-4.29	-5.74	4.52
39	LFFLFFF	Random sequenc	-1.60	5.73	-6.17	8.21	10.73	11.19	8.38	-1.41	-3.42	-1.40	-4.25	-6.90	-0.34
40	KRRRRKY	Random sequenc	14.69	7.32	-6.63	3.59	-0.77	-1.08	-7.92	-1.22	-1.45	-4.19	9.74	6.67	-0.34
41	KYKKKKY	Random sequenc	10.08	5.39	1.40	2.86	1.98	-0.73	-6.25	3.55	-1.57	-2.86	7.10	7.29	2.85
42	KYKKRKR	Random sequenc	13.54	5.92	-2.49	2.57	0.14	-1.86	-7.52	0.76	-1.21	-3.95	9.51	8.17	1.94
43	KYKYKYR	Random sequenc	8.35	6.97	-0.92	4.68	2.47	1.54	-5.58	3.35	-2.29	-2.12	5.03	4.17	0.34
44	RKYKKRK	Random sequenc	13.54	5.92	-2.49	2.57	0.14	-1.86	-7.52	0.76	-1.21	-3.95	9.51	8.17	1.94
45	RRYKKRY	Random sequenc	11.81	7.50	-4.81	4.39	0.63	0.42	-6.85	0.57	-1.93	-3.21	7.44	5.05	-0.57
46	YKKRYRR	Random sequenc	11.81	7.50	-4.81	4.39	0.63	0.42	-6.85	0.57	-1.93	-3.21	7.44	5.05	-0.57
47	YKRRKKR	Random sequenc	14.12	6.62	-4.56	3.08	-0.31	-1.47	-7.72	-0.23	-1.33	-4.07	9.63	7.42	0.80
48	YKYYRRR	Random sequenc	9.50	8.38	-5.06	5.70	1.57	2.32	-5.98	1.37	-2.53	-2.35	5.26	2.67	-1.94
49	YRYKKYY	Random sequenc	6.04	7.85	-1.17	5.99	3.42	3.44	-4.71	4.15	-2.89	-1.26	2.84	1.80	-1.03

Values from amino acid indices are all normalized as average = 0, SD = 1.0. Total amino acid indices were averaged within the single peptide by each index.

3.6. Summary

Effective surface modification with biocompatible molecules is known to be effective in reducing the life-threatening risks related to artificial cardiovascular implants. In recent strategies in regenerative medicine, the enhancement and support of natural repair systems at the site of injury by designed biocompatible molecules has succeeded in rapid and effective injury repair. Therefore, such a strategy could be also effective for rapid endothelialization of cardiovascular implants to lower the risk of thrombosis and stenosis. To achieve this enhancement of the natural repair system, a biomimetic molecule that mimics proper cellular organization at the implant location is required. In spite of the fact that many reported peptides have cell-attracting properties on material surfaces, there have been few peptides that could control cell-selective adhesion. For the advanced cardiovascular implants, peptides that can mimic the natural mechanism that controls cell-selective organization have been strongly anticipated. To obtain such peptides, we hypothesized the cellular bias towards certain varieties of amino acids and examined the cell preference (in terms of adhesion, proliferation, and protein attraction) of varieties and of repeat length on SPOT peptide arrays. To investigate the role of selective peptides in controlling the organization of various cardiovascular-related cells, we compared endothelial cells (ECs), smooth muscle cells (SMCs), and fibroblasts (FBs). A clear, cell-selective preference was found for amino acids (longer than 5-mer) using three types of cells, and the combinational effect of the physicochemical properties of the residues was analyzed to interpret the mechanism.

3.7. Acknowledgements

The authors deeply thank Dr. Yoshikazu Fujita, Nagoya University School of Medicine, for help in obtaining SEM images.

3.8. References

[1] Bourassa MG. Fate of venous grafts: the past, the present and the future. J Am Coll Cardiol. 1991;17:1081-3.

[2] Sumpio BE, Riley JT, Dardik A. Cells in focus: endothelial cell. Int J Biochem Cell Biol. 2002;34:1508-12.

[3] LoGerfo FW, Quist WC, Cantelmo NL, Haudenschild CC. Integrity of vein grafts as a function of initial intimal and medial preservation. Circulation. 1983;68:II117-24.

[4] Kraitzer A, Kloog Y, Zilberman M. Approaches for prevention of restenosis. J Biomed Mater Res B Appl Biomater. 2008;85:583-603.

[5] Camenzind E, Steg PG, Wijns W. Stent thrombosis late after implantation of first-generation drug-eluting stents: a cause for concern. Circulation. 2007;115:1440-55; discussion 55.

[6] Rafat M, Matsuura T, Li F, Griffith M. Surface modification of collagen-based artificial cornea for reduced endothelialization. J Biomed Mater Res A. 2009;88:755-68.

[7] Yu Y, Gao Y, Wang H, Huang L, Qin J, Guo R, et al. The matrix protein CCN1 (CYR61) promotes proliferation, migration and tube formation of endothelial progenitor cells. Exp Cell Res. 2008;314:3198-208.

[8] Bu X, Yan Y, Zhang Z, Gu X, Wang M, Gong A, et al. Properties of Extracellular Matrix-Like Scaffolds for the Growth and Differentiation of Endothelial Progenitor Cells. J Surg Res. 2009;164:50-7.

[9] Cardinal KO, Williams SK. Assessment of the intimal response to a protein-modified stent in a tissue-engineered blood vessel mimic. Tissue Eng Part A. 2009;15:3869-76.

[10] Letourneur D, Machy D, Pelle A, Marcon-Bachari E, D'Angelo G, Vogel M, et al. Heparin and non-heparin-like dextrans differentially modulate endothelial cell proliferation: *in vitro*

evaluation with soluble and crosslinked polysaccharide matrices. J Biomed Mater Res. 2002;60:94-100.

[11] Stellos K, Langer H, Daub K, Schoenberger T, Gauss A, Geisler T, et al. Platelet-derived stromal cell-derived factor-1 regulates adhesion and promotes differentiation of human CD34+ cells to endothelial progenitor cells. Circulation. 2008;117:206-15.

[12] Rodenberg EJ, Pavalko FM. Peptides derived from fibronectin type III connecting segments promote endothelial cell adhesion but not platelet adhesion: implications in tissue-engineered vascular grafts. Tissue Eng. 2007;13:2653-66.

[13] Larsen CC, Kligman F, Tang C, Kottke-Marchant K, Marchant RE. A biomimetic peptide fluorosurfactant polymer for endothelialization of ePTFE with limited platelet adhesion. Biomaterials. 2007;28:3537-48.

[14] Blindt R, Vogt F, Astafieva I, Fach C, Hristov M, Krott N, et al. A novel drug-eluting stent coated with an integrin-binding cyclic Arg-Gly-Asp peptide inhibits neointimal hyperplasia by recruiting endothelial progenitor cells. J Am Coll Cardiol. 2006;47:1786-95.

[15] Yin M, Yuan Y, Liu C, Wang J. Development of mussel adhesive polypeptide mimics coating for in-situ inducing re-endothelialization of intravascular stent devices. Biomaterials. 2009;30:2764-73.

[16] von der Mark K, Park J, Bauer S, Schmuki P. Nanoscale engineering of biomimetic surfaces: cues from the extracellular matrix. Cell Tissue Res. 2010;339:131-53.

[17] Aoki J, Serruys PW, van Beusekom H, Ong AT, McFadden EP, Sianos G, et al. Endothelial progenitor cell capture by stents coated with antibody against CD34: the HEALING-FIM (Healthy Endothelial Accelerated Lining Inhibits Neointimal Growth-First In Man) Registry. J Am Coll Cardiol. 2005;45:1574-9.

[18] Pfisterer M, Brunner-La Rocca HP, Buser PT, Rickenbacher P, Hunziker P, Mueller C, et al.

Late clinical events after clopidogrel discontinuation may limit the benefit of drug-eluting stents: an observational study of drug-eluting versus bare-metal stents. J Am Coll Cardiol. 2006;48:2584-91.

[19] Komoriya A, Green LJ, Mervic M, Yamada SS, Yamada KM, Humphries MJ. The minimal essential sequence for a major cell type-specific adhesion site (CS1) within the alternatively spliced type III connecting segment domain of fibronectin is leucine-aspartic acid-valine. J Biol Chem. 1991;266:15075-9.

[20] Graf J, Ogle RC, Robey FA, Sasaki M, Martin GR, Yamada Y, et al. A pentapeptide from the laminin B1 chain mediates cell adhesion and binds the 67,000 laminin receptor. Biochemistry. 1987;26:6896-900.

[21] Pytela R, Pierschbacher MD, Ruoslahti E. Identification and isolation of a 140 kd cell surface glycoprotein with properties expected of a fibronectin receptor. Cell. 1985;40:191-8.

[22] Kato R, Kaga C, Kunimatsu M, Kobayashi T, Honda H. Peptide array-based interaction assay of solid-bound peptides and anchorage-dependant cells and its effectiveness in cell-adhesive peptide design. J Biosci Bioeng. 2006;101:485-95.

[23] Kaga C, Okochi M, Tomita Y, Kato R, Honda H. Computationally assisted screening and design of cell-interactive peptides by a cell-based assay using peptide arrays and a fuzzy neural network algorithm. Biotechniques. 2008;44:393-402.

[24] Okochi M, Nomura S, Kaga C, Honda H. Peptide array-based screening of human mesenchymal stem cell-adhesive peptides derived from fibronectin type III domain. Biochem Biophys Res Commun. 2008;371:85-9.

[25] Frank R. SPOT-Synthesis: An easy technique for the positionally addressable, parallel chemical synthesis on a membrane support. Tetrahedron. 1992;48:9917-32.

[26] Fauchere JL, Charton M, Kier LB, Verloop A, Pliska V. Amino acid side chain parameters for

correlation studies in biology and pharmacology. Int J Pept Protein Res. 1988;32:269-78.

[27] Kyte J, Doolittle RF. A simple method for displaying the hydropathic character of a protein. J Mol Biol. 1982;157:105-32.

[28] Zimmerman JM, Eliezer N, Simha R. The characterization of amino acid sequences in proteins by statistical methods. J Theor Biol. 1968;21:170-201.

[29] Roberts MJGFDB. Amino acid preferences for secondary structure vary with protein class. Int J Biol Macromol. 1980;2:387-9.

[30] Takano K, Yutani K. A new scale for side-chain contribution to protein stability based on the empirical stability analysis of mutant proteins. Protein Eng. 2001;14:525-8.

[31] Zhou H, Zhou Y. Quantifying the effect of burial of amino acid residues on protein stability. Proteins. 2004;54:315-22.

[32] Crawford JL, Lipscomb WN, Schellman CG. The reverse turn as a polypeptide conformation in globular proteins. Proc Natl Acad Sci U S A. 1973;70:538-42.

[33] Munoz V, Serrano L. Intrinsic secondary structure propensities of the amino acids, using statistical phi-psi matrices: comparison with experimental scales. Proteins. 1994;20:301-11.

[34] Grantham R. Amino acid difference formula to help explain protein evolution. Science. 1974;185:862-4.

[35] Krigbaum WR, Komoriya A. Local interactions as a structure determinant for protein molecules: II. Biochim Biophys Acta. 1979;576:204-48.

[36] Jukes TH, Holmquist R, Moise H. Amino acid composition of proteins: Selection against the genetic code. Science. 1975;189:50-1.

[37] Kawashima S, Pokarowski P, Pokarowska M, Kolinski A, Katayama T, Kanehisa M. AAindex: amino acid index database, progress report 2008. Nucleic Acids Res. 2008;36:D202-5.

Chapter 4

Specific tripeptides that contribute to the cell-selectivity of extracellular matrixes

4.1. Introduction

There is a potential for life-threatening complications with long-term implantation of medical devices for cardiovascular diseases. The most common risk associated with vascular implants is post operative restenosis, commonly triggered by thrombosis and neointimal hyperplasia [1-5]. Thrombosis is caused by the atypical attraction of serum proteins, platelets and circulating blood cells to damaged inner-surfaces lacking endothelium [6-10]. Neointimal hyperplasia, caused by excessive smooth muscle cell growth, is also another risk related to endothelial damage together with expansion pressure from stent-like implants [11, 12]. In blood vessels, there are naturally organized layers of cells; (1) the intima, which consists of endothelial cells that inhibit the accumulation of thrombosis-related proteins and cells, and (2) the media, mainly consisting of smooth muscle cells, which sustain the strength and flexibility of the vessel. These well-organized cellular environments are easily disturbed by the implantation of a medical device. This disturbance of cellular organization combined with the exposure of artificial materials is believed to be the

fundamental trigger of the inflammatory response that leads to restenosis.

To reduce the risks associated with vascular implants, there are two essential but counter-opposed conditions that must be satisfied. The first condition needed is accelerating the rate of re-endothelialization. It is known that re-endothelialization is the most comprehensive natural recovery process that can best mitigate risk of stenosis. Proper establishment of the endothelial layer assures not only the reduction of platelet adhesion, but also many other factors contributing to stenosis. Another essential condition, neglected by many implant designs, is the inhibition of growth and invasion of smooth muscle cells from the media into the intima. The unregulated growth and invasion of smooth muscle cells to the luminal side of the vasculature narrows the luminal space and leads to restenosis. Drug eluting stents have clinically demonstrated that growth-inhibition of surrounding cells is effective in reducing the risks of restenosis. It has been challenging to achieve preferential EC adhesion and SMC inhibition on the implant surface due to the paradoxical nature of simultaneously engaging the two cellular processes.

We know that endothelial enhancement and SMC inhibition is a natural wound healing mechanism in blood vessels. The biology of this mechanism suggests that the key to unlock the paradox lies in the extracellular matrixes (ECMs) [13]. Some ECM-derived short peptides have been reported as partially functioning ECMs [14-19]. Peptides that have cell-selective characteristics were also reported. For example, the REDV peptide from fibronectin preferentially adheres to endothelial cells, as compared to other types of cells [20]. By comparison, smooth muscle cells preferentially bind VAPG derived from elastin as compared to other types of cells [21]. The precise mechanisms of how various ECMs regulate complex cellular organization are poorly understood. Although the reported peptides may be sufficient to exhibit cell-selectivity, they are not sufficient for determining overall cellular preferences unique to an individual ECM type. For example, elastin functions as an effective scaffold for endothelial cell growth and maturation,

however the endothelial-selective REDV sequence does not exist in this protein. In addition, previous work with fibronectin identified several cell-adhesion peptides comparable with the conventional RGD ligand [22]. Amino acid substitution revealed that certain flexibility in peptide sequence is possible, but was confined to certain physiochemical parameters [23]. These fibronectin-derived peptides had lower cellular affinity than RGD, suggesting that the novel peptides may work together with RGD-like ligands to recruit and anchor specific cell types respectively. We propose that the cell-selectivity of certain ECM types is supported not only by cell receptor ligands but also by peptides that are uniquely enriched in the given ECM type. The focus of the present work is to determine which sequences govern the cellular preferences that are unique to a particular ECM type.

To obtain functional peptide material that performs similar to a given ECM type, we started by eliminating tripeptide sequences shared across ECM types *in silico*. The remaining candidate tripeptides were termed “unique ECM-specific peptides” (uECM-peptides) (**Fig. 1A**). Collagen type IV was chosen for this study and the candidate peptides were given the separate designation "uCOL4-peptides". Collagen type IV is a major ECM component of the basement membrane, which is exposed to both the EC and SMC layers in blood vessels. The collagen type IV rich basement membrane also functions as the boundary to maintain the distinct organization of two cell types. Each of these characteristics of collagen IV makes it a good example of cell-selectivity.

The resultant uCOL4-peptides were assayed for cellular preference using peptide array [22-25]. Specifically, differential adhesion of ECs and SMCs was examined. We aimed to characterize tripeptides with one of two distinct properties: (1) EC-selective function, which we consider to be the function of simultaneously attracting ECs and limiting invasion of SMCs, or (2) SMC-selective function, which is the function that simultaneously attracts SMCs and inhibits EC adhesion.

Finally, we demonstrated the practical application of the novel ECM-specific cell-selective

peptide, CAG. Poly-ε-caprolactone was functionalized with CAG by mixing and forming a fine-fiber mesh. Selective adhesion of ECs and SMCs to the functionalized mesh was evaluated. Here we report evidence of ECM-specific tripeptides that contribute to the cellular preference of ECM and recapitulate the cellular preferences on a functionalized biomaterial matrix.

4.2. Materials and Methods

4.2.1. Cells and cell culture

Human aortic endothelial cells (Cell Applications, Inc., San Diego, USA) were maintained in HuMedia-EG2 (Kurabo Industries Ltd., Osaka, Japan) and designated as ECs. Human umbilical artery smooth muscle cells (Cell Applications, Inc.) were maintained in smooth muscle growth medium (Cell Applications) and designated as SMCs. Penicillin and streptomycin (Life Technologies Corporation, Carlsbad, CA, USA) were used as antibiotics in the medium. Cells were maintained at 37°C, 5% CO_2, and used within 4 to 6 passages for assays.

4.2.2. *In silico* analysis of tripeptides from extracellular matrixes

The protein sequence data of the following human collagens was obtained from UniProt (http://www.uniprot.org/): collagen type I (COL1A1: P02452, COL1A2: P08123), collagen type II (COL2A1: P02458), collagen type III (COL3A1: P02461), collagen type IV (COL4A1: P02462, COL4A2: P08572, COL4A3: Q01955, COL4A4: P53420, COL4A5: P29400, COL4A6: Q14031), and collagen type V (COL5A1: P20908, COL5A2: P05997, COL5A3: P25940). All possible tripeptide sequences from each of the ECMs were identified, counted, and summarized by the original C source code program (detailed data in **Table S1**). A diagram of the uECM-peptide identification process is illustrated in **Fig. 1A**. First tripeptides were identified from all ECMs.

Second, the redundant tripeptides within each collagen type were counted, and the overlapping peptides were excluded. Third, the non-redundant tripeptides in each collagen type were listed. Fourth, redundancies across the different collagen types were counted and non-redundant peptides were listed. Finally, the tripeptides that were unique to individual collagen types were listed as uECM-peptides. From the uECM-peptides, tripeptides only found in collagen type IV were designated as uCOL4-peptides. Since our objective was to find sequences that are specific and broadly represented within the ECM primary structure, the 114 uCOL4-peptides that most frequently repeated in collagen type IV were selected as candidate peptides for peptide array synthesis.

4.2.3. Peptide array synthesis

Peptide arrays for the cellular assay were synthesized as previously described [22, 25]. Briefly, standard Fmoc synthesis using 0.25 M activated amino acid was spotted with a peptide auto-spotter (ASP222; Intavis Bioanalytical Instruments AG, Köln, Germany) in accordance with the manufacturer's instructions with some modifications. The synthesized array membrane was then thoroughly washed three times for 2 hours with diethyl ether (Wako Pure Chemical Industries, Osaka, Japan) and methanol (Wako Pure Chemical Industries), respectively. The array was then washed for 6 hours with Dulbecco's phosphate buffered saline (PBS) (pH 7.2) (Nissui Pharmaceutical Co., Ltd., Tokyo, Japan). Finally, the array was soaked in methanol (Wako Pure Chemical Industries) and air dried on a clean bench. Each array was designed as a 96-well array of 7-mm-diameter spots. In this synthesis protocol, the approximate peptide density on a peptide spot was 3 nmol/mm^2. In the array for the cellular assay, each of the peptide sequences was synthesized in triplicate for each array.

4.2.4. PIASPAC (peptide array-based interaction assay of solid-bound peptides and anchorage-dependent cells) for cell-selectivity adhesion assay

The previously described PIASPAC protocol was applied to assay the relative cell adhesion of ECs and SMCs with some modifications [22, 25]. Briefly, 1.5×10^4 cells/well were directly seeded onto disks that were punched out from the peptide array, and incubated for 1 hour for the cell adhesion measurements. After three washes with PBS to remove cells that were unattached, the viable attached cells were stained by calcein AM (Life Technologies Corporation) for 30 min, and fluorescence intensity was measured by Fluoroskan Ascent (type 374; Labsystems, Helsinki, Finland). Results collected from the triplicate spots were averaged. The average fluorescence intensity of each cell type was divided by the average of the negative control (without peptide, N=3) to normalize the fluorescence intensities and obtain the relative ratio of cell adhesion (rRATIO). The "cell-selective rates" are expressed as the difference between the rRATIO of ECs minus the rRATIO of SMCs. (Detailed data that describes each rRATIO and standard deviations are listed in **Table S2**). In this instance, peptides that indicated a positive cell-selective rate were considered to be EC-selective. Peptides that indicated a negative cell-selective rate were considered to be SMC-selective.

4.2.5. Preparation of fine-fiber sheets containing EC-selective peptide

CAG was introduced to the poly-ε-caprolactone (PCL) (Wako) fine-fiber sheet fabricated by the electrospinning technique described previously [26]. Some modifications to the method were made. Briefly, synthesized CAG peptides (70.07% purity) were dissolved in 1,1,1,3,3,3-hexafluoro-2-propanol (HFIP) (Wako) with to a final concentration of 1 wt%, and mixed together with PCL. The mixed solution was loaded into a 5 ml syringe equipped with a blunt-ended 18-gauge needle and clamped to the positive electrode as the material source.

Electrospinning was performed with a voltage range of 10–15 kV with Electrospinning unit (MECC Co., Ltd., Fukuoka, Japan) to form a non-woven fine-fiber sheet.

4.2.6. Composition analysis of fine-fiber sheet containing EC-selective peptide

Fine-fiber sheet elemental composition was measured by CHN coder MT-5 (Yanaco, Kyoto, Japan) to measure the total nitrogen content originating from the introduced CAG peptide, confirming its presence in the fine-fiber sheet. The fine-fiber sheet was decomposed in the combustion tube using mixed carrier gas (7.5% pure O_2 in pure He, flow speed: He, 200 mL min^{-1}; O_2, 15 mL min^{-1}) at 949°C. The decomposition products were then converted to CO_2, NO_X, and H_2O at 848°C. Decomposition products were collected by absorption to the oxidation tube and detected at 99°C by three thermal conductivity detectors. The concentration of each component was calculated by the differential thermal conductivity method using antipyrine (N%: 14.88%) as the standard reagent. Individual measurements were performed by averaging five replicate samples. The average and standard deviation of percent nitrogen concentration for the standard reagent was 14.88% and 0.03%, respectively. Other operational parameters were set as follows: reductive tube temperature; 498°C, pump temperature; 54°C, bridge current; H = 85 mA, C = 65 mA, N = 120 mA.

4.2.7. Surface characterization of fine-fiber sheets containing EC-selective peptides

The surface chemical composition of the fine-fiber sheets were measured by X-ray photoelectron spectroscopy (XPS) (ESCAlab220i-XL MKαII, Thermo Fisher Scientific, Inc., Waltham, MA, USA). The instrument was equipped with Mg anode. The binding energy drift was corrected by normalizing the measured binding energy to the C 1s core level, 285.0 eV [27].

4.2.8. Morphological evaluation of cells on fine-fiber sheets containing EC-selective peptides

ECs and SMCs were seeded onto fine-fiber sheets containing EC-selective peptides with 1.5 × 10^4 of each cell type/well. Cell adhesion was induced with the same operation protocol as the PIASPAC method described above. Cells were fixed to the sheet using 2% glutaraldehyde (Wako Pure Chemical Industries) for 12 h at 4°C. After further fixation with osmium tetroxide (PGM chemicals (PTV) Ltd., New Germany, USA) for 30 min at room temperature, samples were dried with t-butylalcohol (Wako Pure Chemical Industries) using a VFD-20 drying apparatus (Hitachi, Ltd., Tokyo, Japan) and plasma coated with osmium tetroxide using an osmium plasma coater (Nihon Lazor Denshi, Ichinomiya, Japan). To evaluate the cellular adhesion and morphological changes in detail, cells were observed by scanning electron microscopy with an S-800 electron microscope (Hitachi, Ltd.).

4.3. Results

4.3.1. ECM-specific peptide listing from human collagens *in silico*

To identify uECM-peptides for investigating cell-selectivity characteristics representative of ECM function, tripeptides from particular ECMs were screened and compared *in silico* (**Fig. 1A**). Tripeptides were generated from five human collagen types (type I: 2,826, type II: 1,485, type III: 1,464, type IV: 10,105, type V: 5,076) presently registered in the UniProt database. Non-redundant tripeptides from each collagen type were listed as: type I (940), type II (642), type III (647), type IV (1,986), and type V (1,802). The detailed sequences are listed in the supplementary data (**Table S1**). Since our hypothesis was that uECM-peptides should be uniquely found in a single target ECM and not found in other ECMs, we compared the redundancy across ECMs. The number of unique tripeptides in each collagen type was found to be: type I (163), type

II (72), type III (86), type IV (907), and type V (674). Among the five types of collagens, we designated the uECM-peptides in collagen type IV as "uCOL4-peptides"and focused on collagen type IV since it is known to interact with both ECs and SMCs by its localization in basement membrane tissue that divides both types of cells (**Fig. 1B**). Among the 907 uCOL4-peptides, there were several peptides that frequently repeated (>10 times) within type IV. Since higher frequency repeat uCOL4-peptides were considered to have a greater chance to interact and control surrounding cells, we selected the most frequent 114 uCOL4-peptides to test their cell selectivity.

4.3.2. Screening of cell-selective peptides from uCOL4-peptides on peptide arrays

We compared the cellular selective adhesion of ECs and SMCs on uCOL4-peptides using a peptide array (**Table 1**, **Table S2**). From the screening, we found novel EC-selective tripeptides (12 peptides (cell-selective rate > +1.0)) and SMC-selective tripeptides (9 peptides (cell-selective rate < -1.0)) (**Fig. 2**).

The RGD peptide, known as a strong integrin binder, was found to have a slight bias for EC adhesion enhancement, although consequently showed non-specific cell adhesion to both ECs and SMCs. Compared to the RGD peptide, the screened EC-selective peptides indicated higher EC biased adhesion compared to SMCs. Interestingly, most of EC-selective peptides indicated a higher cell-selectivity rate because of the "inhibitory effect on SMC adhesion" compared to RGD peptide.

SMC-selective peptides appeared less frequently than EC-selective peptides among uCOL4-peptides. However, since SMCs are important in various types of tissues (such as ureter, intestinal tracts, etc.), the SMC-selective peptides that were discovered are considered to be rare and significant peptide material, useful for SMC cultures.

The total cell number in the adhesion assay revealed that the adhesion potential of SMCs (compared by raw fluorescent intensity data) was about 36% lower than ECs in all our assayed

peptides, even in the optimized medium for SMCs. Therefore, it is possible SMCs have weaker anchorage than ECs, which is one reason why we did not perform a competitive assay of two cell types. We believe that the two cell types are best compared under conditions optimized for each cell type. This allows for the best performance of each cell type.

4.3.3. Design of fine-fiber sheet containing the EC-selective peptide CAG

From uCOL4-peptides, we selected the tripeptide CAG (Cys-Ala-Gly), one of the top EC-selective peptides, as a model peptide to further examine the applicability of our proposed uECM-peptides in enhancing the performance of medical devices. Since the target device in this study was the vascular graft, CAG was expected to enhance the rapid endothelialization together with inhibiting overgrowth of SMCs for better and longer therapeutic effects. An electro-spun PCL fine-fiber sheet was selected to represent a vascular graft (previously reported to have *in vitro* [28, 29] and *in vivo* [30] utility as a scaffold for small caliber vascular grafts). We mixed the soluble CAG peptide with PCL as the fiber source for electro-spinning fabrication.

The fine-fiber sheet containing CAG was analyzed for its basic chemical characteristics prior to the assay. As shown in **Fig. 3**, the fiber morphology of the fabricated fine-fibers was relatively similar with or without peptide introduction. From the image analysis of SEM images, peptide introduction was found to cause no significant difference to the fiber physical properties: fiber diameter (control: 1.46 ± 0.02 μm, CAG: 1.26 ± 0.12 μm ($p > 0.1$, n=3)), thin fiber diameter (control: 0.283 ± 0.007 μm, CAG: 0.351 ± 0.026 μm ($p > 0.05$, n=3)), and porosity (control: 28.1 ± 5.5%, CAG: 27.2 ± 5.4 (n=3)) From the CHN coder element analysis shown in **Table 2**, the nitrogen ratio of the CAG containing sheet was calculated to be 0.14% (weight percent) of the PCL, which approximately matched to the prepared molecular ratio of the electro-spun solution (0.18%). Estimation of the peptide concentration per area in the fine-fiber sheet from its weight percentage

was <1.0 nmol/mm^2, which was much less than 3-fold the estimated peptide concentration of our peptide array spot (approximate 3.0 nmol/mm^2). From the XPS surface analysis, the N1s peak could be observed at 395 eV in the CAG containing sheet, indicating the evidence of existence of introduced CAG peptide on the material surface (**Fig. 4A and B**).

4.3.4. Effect of EC-selective peptide to control cell-selectivity on fine-fiber PCL sheets

We examined cellular adhesion to the CAG-containing fine-fiber sheet *in vitro* by comparing the relative adhesion of ECs and SMCs. As shown in **Fig. 5**, the rRATIO of ECs and SMCs were 1.9 and 0.8 respectively, indicating that CAG significantly modified the cell-selectivity of PCL fine-fiber sheets to favor EC-selectivity.

Cell morphology was also evaluated (**Fig. 6** and **Fig. 7**). On the CAG-containing fine-fiber sheet, ECs were found to spread widely and covered an apparently larger field area (**Fig. 6B** and **Fig. 6D**) compared to cells on the control sheet (**Fig. 6A** and **Fig. 6C**). In contrast, SMCs appeared shrunken and rounded on the CAG-containing fine-fiber (**Fig. 7B** and **Fig. 7D**), whereas SMCs cultured on the CAG-free control sheet grew as normal (**Fig. 7A** and **Fig. 7C**). Therefore, it was clear that incorporating CAG onto PCL formed a surface that attracts ECs, which at the same time rejects SMCs. It is notable that the cell selectivity observed with the CAG-modified fine-fiber sheet was reproduced using the cellulose membrane of the peptide array (C-terminal linked). Reproduction of cell-selectivity was possible even though the peptide density and the directional uniformity were highly variable from dissolving the peptides in the PCL support. In sum, the effect of the CAG peptide was strong considering its low surface display rate. This effect could be reproduced by various types of surface functionalization methods without strict consideration of the direction of peptide display.

4.4. Discussion

In this study, we hypothesized that uECM-peptides serve as important functional peptide motifs that govern ECM-specific cell-selectivity and regulate surrounding cellular organization. If the rules that dictate the cell-selective properties of ECM could be interpreted, artificial biomaterials could be effectively designed to enhance proper cellular organization on medical device surfaces.

To validate our hypothesis, we compiled the unique tripeptides found only in human collagen type IV by comparing five types of human collagen protein sequences *in silico* (uCOL4-peptides), and investigated their cellular preferences in peptide array experiments. From 114 uCOL-peptides, 21 tripeptides (18%) indicated cell-selective adhesion; 12 EC-selectivity and 9 SMC-selectivity. As shown in Table 1, EC-selective peptides were found to have some sequence flexibility, but maintain certain physiochemical rules. This sequence flexibility can be described as a C-X-G motif, where X is either A, N, S or D. Together with previous observations from fibronectin-derived cell adhesion peptides [23], this discovery also supports the concept of two peptide types that contribute to cell-selective adhesion in ECMs. One class of peptides shows strict ligand-receptor relationships, such as REDV and VAPG. Their function is also fully dependent on amino acid sequence, and infrequently appears in the primary structure. The second class of peptides is characterized by their flexible sequence, which function more like motifs dependent on their physiochemical properties. We propose that such sequence flexibility allows ECM molecules to form a larger cellular recruitment surface capable of "funneling" cells toward anchoring sites in a selective manner. The milder, more flexible environment is likely what allows more frequent cell-matrix interactions to occur, with the receptor-ligand interactions creating the later and stronger cellular adhesion events.

One of the best performing uCOL4-peptides, CAG, was found to provide EC-selectivity not only on the surface of the peptide screening array but also on the surface of PCL fine-fiber sheets, the

same material used in some vascular grafts. Since simple peptide mixing fabrication succeeded to form a cellular selective surface, it is expected that our proposed uECM-peptides may function regardless of presentation direction, similar to a native protein structure. However, to maximize peptide function, linker molecule and peptide conjugation technologies are under investigation.

To better understand the native function of the resulting ECM-specific peptides, we mapped the top 20 EC/SMC-selective peptides to analyze the positional localization from the original protein sequences (**Table S3**, **Fig. S1**). SMC-selective peptides were localized in the C-terminus side of native collagen type IV, while EC-selective peptides were widely distributed. We interpreted these observations as a possible reason to conclude that collagen type IV may promote endothelialization more through generally distributed EC-selective peptides rather than SMC rejection. Although further investigation of the role of localized SMC-selective peptides is needed, such localization may indicate some insight to the fibrous organization of collagen IV in ECM.

In this report, we have shown data resulting from screens for ECM-specific peptides defined as "peptides uniquely found in a target type of ECM (uECM-peptides)". However, it is also possible that common peptide sequences, which may be abundantly represented in various ECMs, may regulate similar functions through frequency of sequence repeats within the ECM protein. We defined these ECM-specific peptides as "frequent ECM-specific peptides (fECM-peptides)" (Schematic concept in **Fig. S2**), and listed fCOL4-peptides (fECM-peptides that were more frequently found in collagen type IV) for the same type of investigation (data not shown, detailed in supplementary information, **Fig. S2**, **Fig. S3**, **Table S4**). From this fCOL4-peptide screening, 30% of screened peptides from 87 peptides indicated cell-selectivity; 20 EC-selective peptides (cell-selectivity rate > +1.0), and 6 SMC-selective peptides (cell-selectivity rate < -1.0). Therefore, the concept of screening for ECM-specific peptides was reconfirmed to effectively provide more cell-selective peptides.

Our data verifies the existence of numerous short peptides that provide a cell-selective function confirmed by screening for "ECM-specific peptides". The successful application of the CAG peptide is only one example demonstrating the practical use of PCL fine-fibers. Although the detailed interaction mechanism of ECM-specific peptides with cells is still unclear, it was predicted that a new type of moderately binding peptide would exist. This novel peptide type contributes to the cell-selective function of ECMs, and is distinct from the ligand-type peptides. If cell-selective interactions are governed by strict sequences, it would be unlikely that alternative sequences would be readily discovered. Instead, our data allows for the possibility of designing new cell-selective biomaterials by mimicking the less prominent aspects of the ECM environment. With the combined list of uECM- and fECM peptides, further investigation of combinatorial or synergetic effects of peptides is now under investigation.

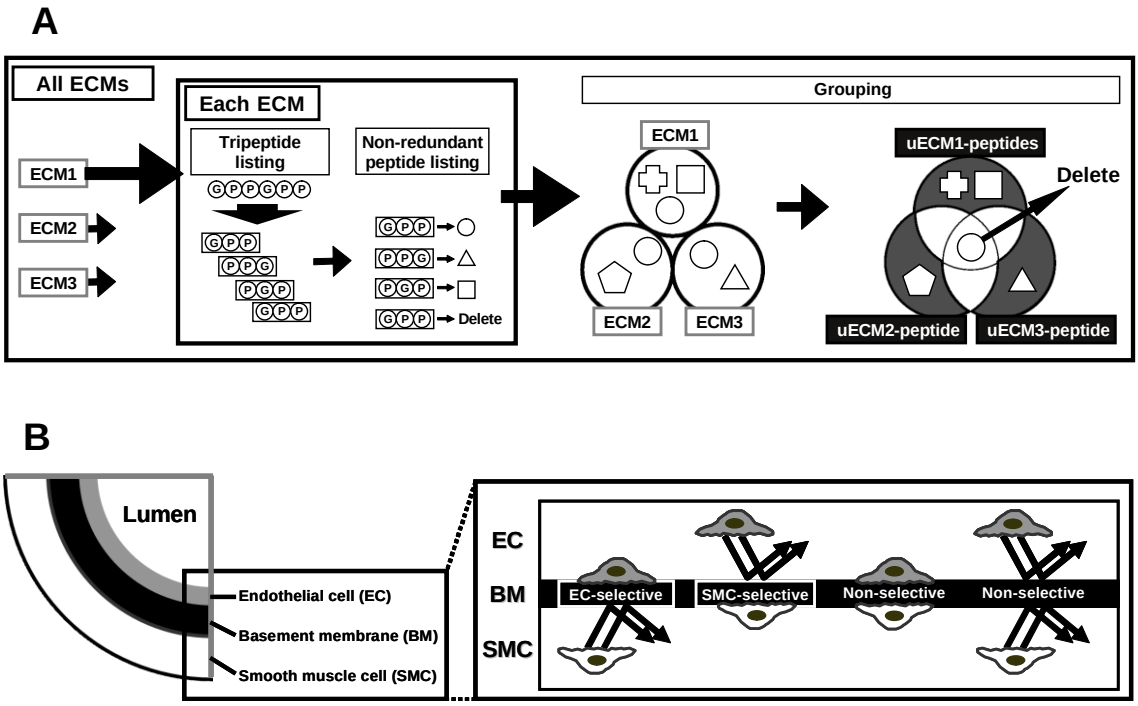

Figure 1. A schematic concept of uECM-peptides. (A) Flow of *in silico* analysis to obtain uECM-peptides. First, with each target ECM, a non-redundant tripeptide list within each ECM is listed. Second, within all target ECMs, non-redundant unique tripeptides are listed as uECM-peptides. (B) Model of expected function of uCOL4-peptides. EC-selective: image of peptide that attracts ECs while rejecting SMCs. SMC-selective: model of a peptide that attracts SMCs while rejecting ECs. Non-selective: model of a peptide that either attracts both types of cells or rejects both types of cells.

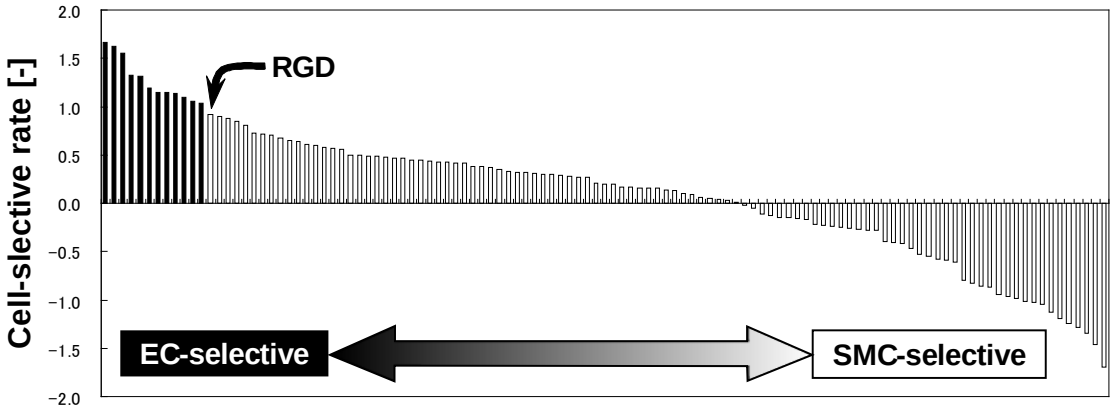

Figure 2. Cell-selective peptide screening result. Positive value expresses the EC-selective function, attracts ECs and rejects SMCs. Negative value expresses SMC-selective function, attracts SMCs and rejects ECs. The RGD peptide is used as a reference. Black bars, peptides with significant cell selection (> +1.0 or < -1.0).

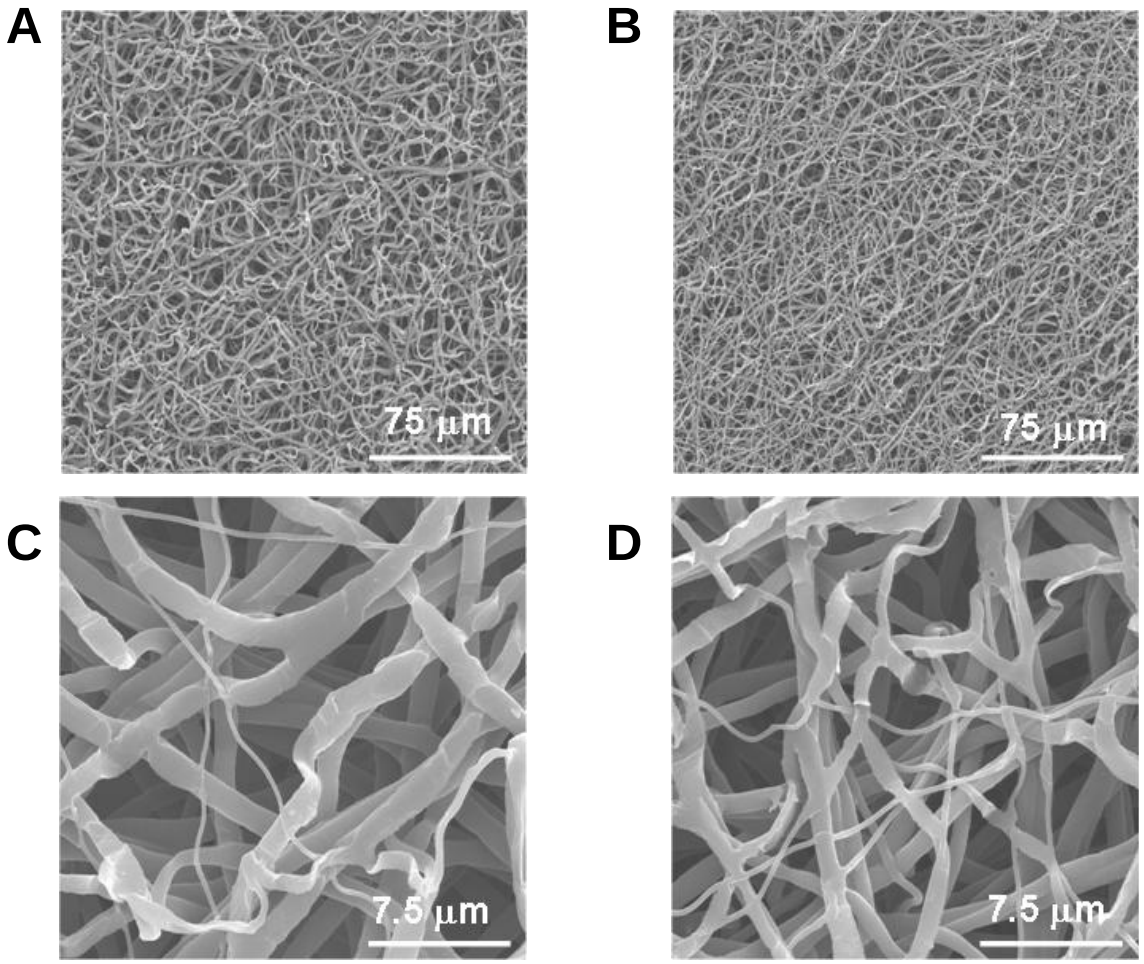

Figure 3. SEM image of PCL fine-fiber sheet fabricated with electrospinning. (A), (C), control sheet without peptide; (B), (D), sheet containing CAG peptide.

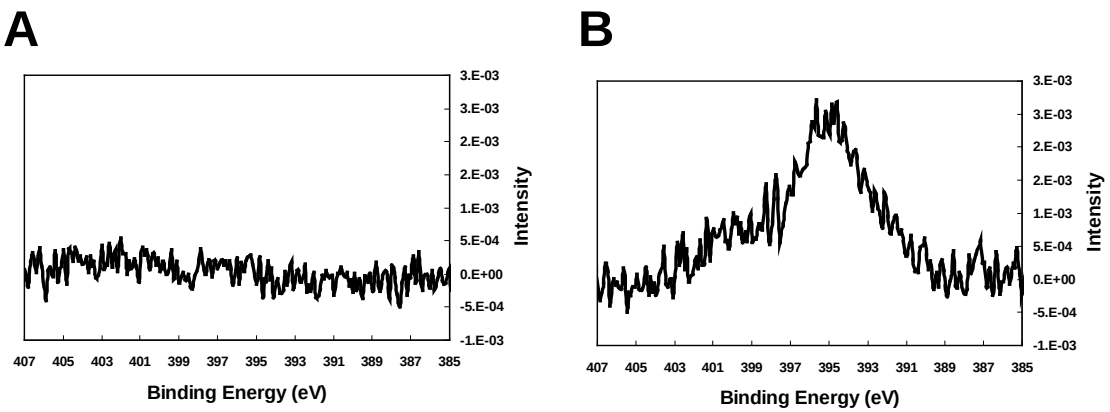

Figure 4. The result of XPS analysis. (A), (B), N1s spectra. (A) control sheet without peptide; (B) sheet contain CAG peptide.

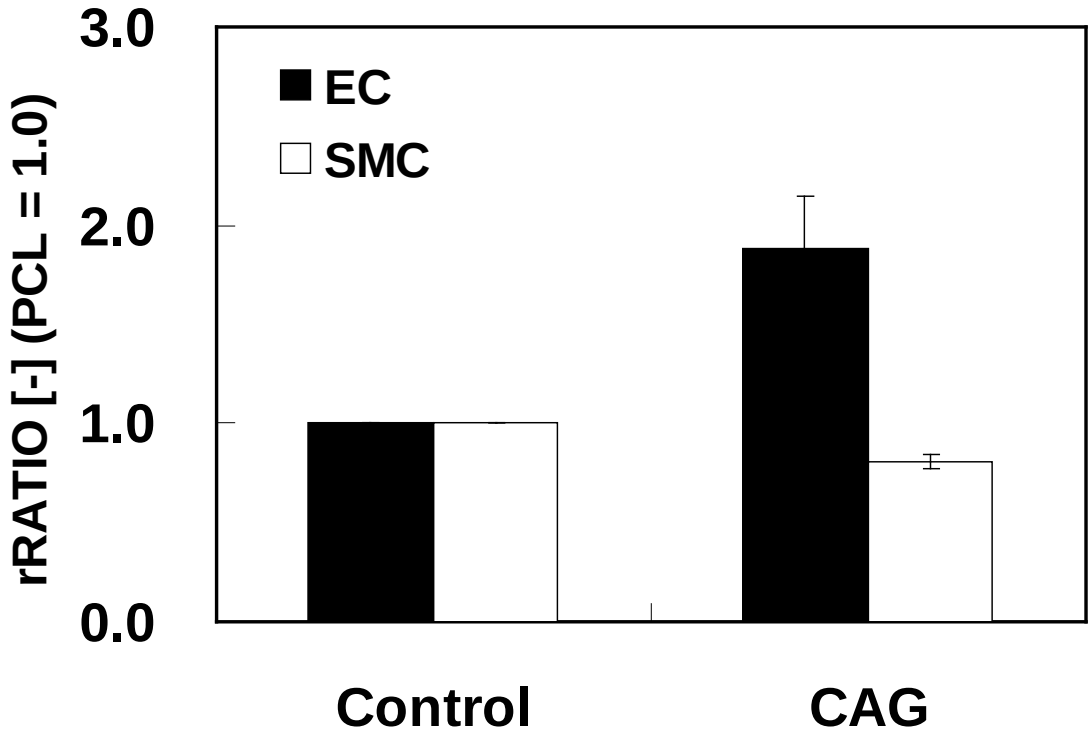

Figure 5. Relative cell adhesion ratio of PCL fine-fiber sheet containing the CAG peptide. Black bars, cell adhesion of ECs (N=3); white bars, cell adhesion of SMCs (N=3). Control; control sheet without peptide. CAG; sheet containing CAG peptide.

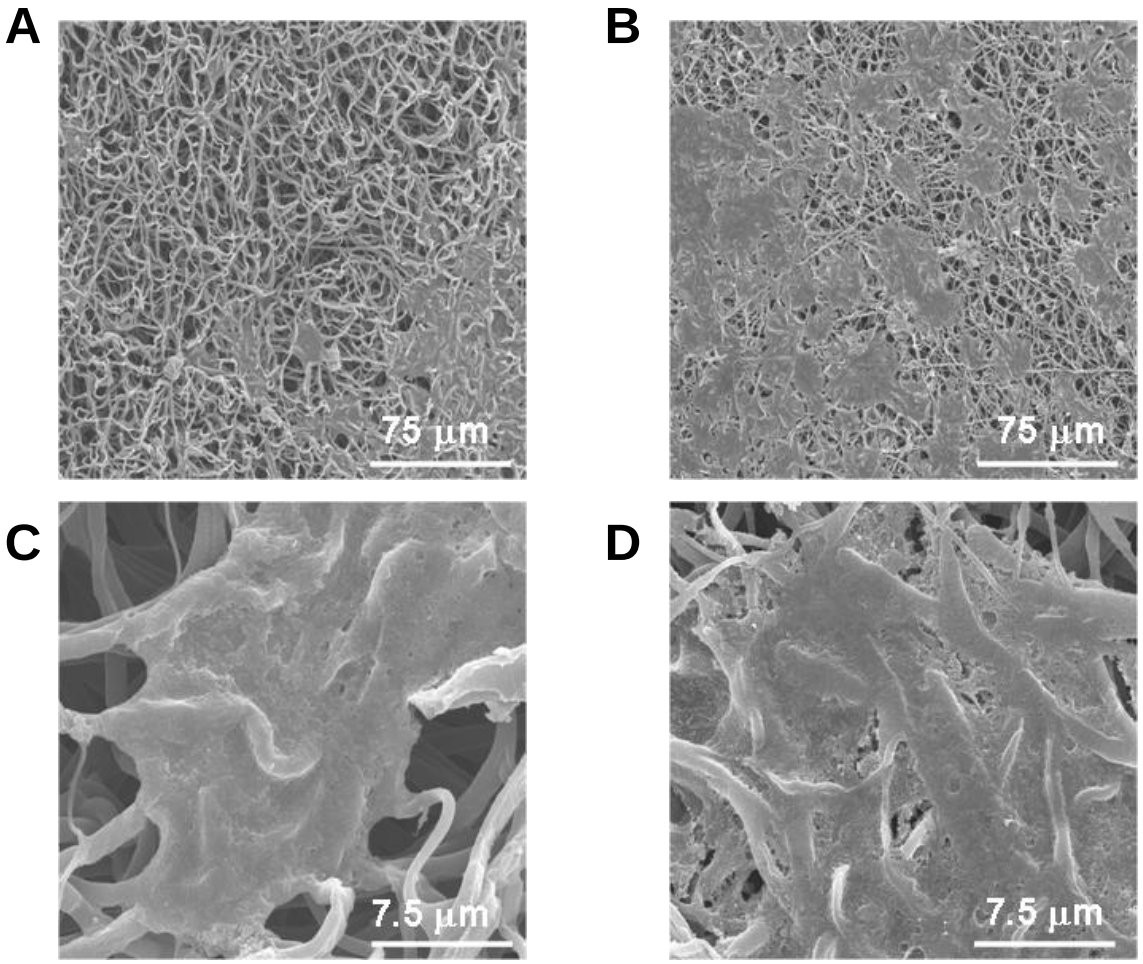

Figure 6. SEM image of ECs on CAG peptide containing PCL fine-fiber sheet. (A), (C), control sheet without peptide; (B), (D), sheet containing CAG peptide.

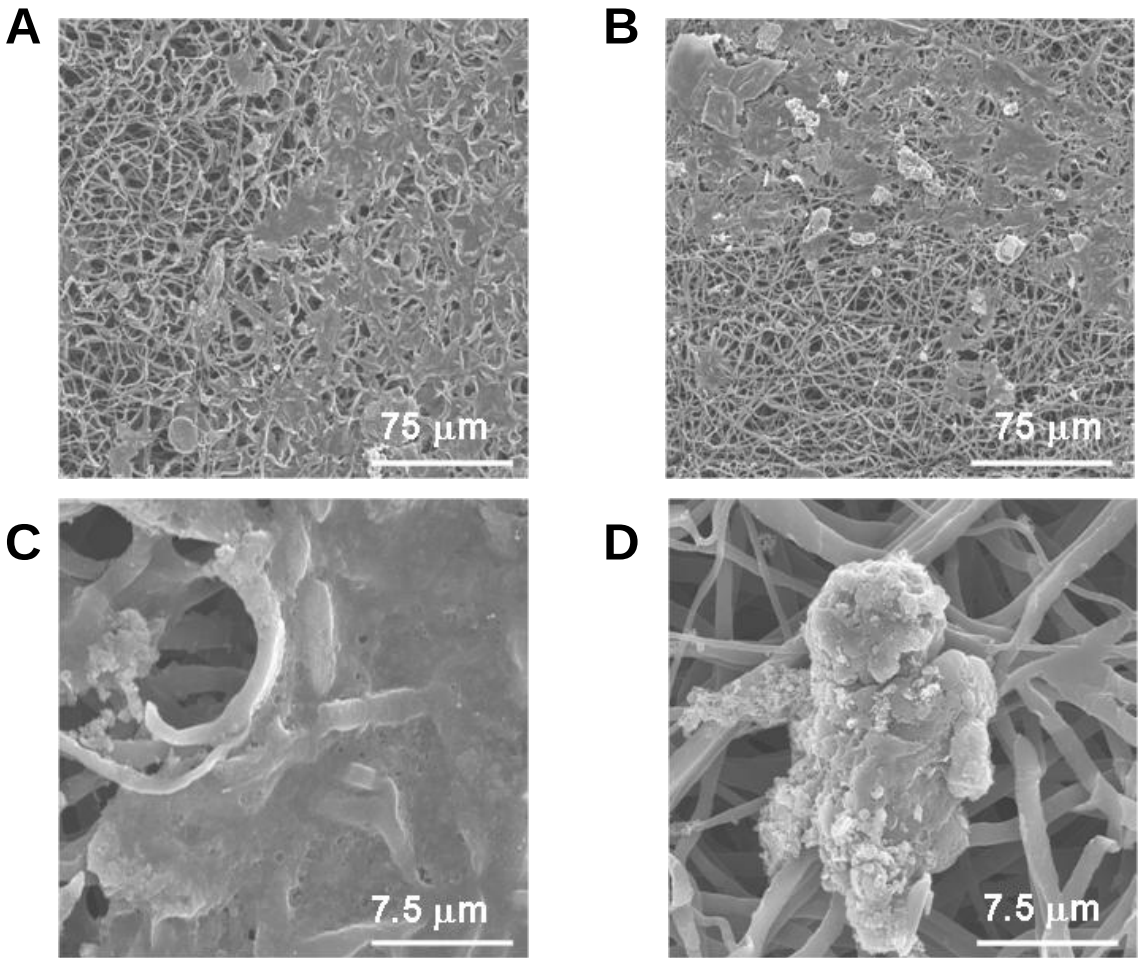

Figure 7. SEM image of SMCs on CAG peptide containing PCL fine-fiber sheet. (A), (C), control sheet without peptide; (B), (D), sheet containing CAG peptide.

Table 1. List of cell-selective tripeptides

Cell selectivity	Number	Sequence	rRATIO [-]		Cell-selective rate [-] ((rRATIO of EC) - (rRATIO of SMC))
			EC	SMC	
EC	1	CAG	2.85	1.18	1.67
	2	CNG	2.68	1.05	1.63
	3	CSG	2.43	0.88	1.55
	4	GYL	2.57	1.24	1.32
	5	CNY	2.25	0.94	1.31
	6	PCG	2.56	1.37	1.19
	7	CDG	2.31	1.16	1.15
	8	AVA	2.19	1.05	1.15
	9	FLM	2.03	0.90	1.14
	10	GPY	2.38	1.28	1.10
SMC	1	GSC	2.26	3.59	-1.33
	2	PGQ	1.20	2.49	-1.30
	3	HSQ	1.06	2.34	-1.28
	4	PGD	1.33	2.55	-1.22
	5	GDQ	2.31	3.42	-1.10
	6	KGE	1.62	2.68	-1.06
		RGD	3.20	2.29	0.91

Table 2. The element composition of elecrtospun fine-fiber sheet

Sample	Elements		
	H [% ± SD]	C [% ± SD]	N [% ± SD]
Control	8.70 ± 0.08	62.24 ± 0.28	0.03 ± 0.04
CAG	8.74 ± 0.01	62.25 ± 0.05	0.14 ± 0.01

4.5. Supplementary Information

In this research, extracellular matrix (ECM)-specific peptides, comparing collagen type IV and other collagens (collagen type I, II, III, and V) were screened for their cellular selection using aortic endothelial cells (ECs) and smooth muscle cells (SMCs). In this supplementary data, the complete dataset from the cellular selection assay is supplied. This data describes not only the concept of uECM-peptides (**Table S1**, **Table S2**, **Fig. 1** and **Fig.2**), but also the fECM-peptides (**Table S4**, **Fig. S1** and **S2**). The two distinct concepts for peptide definition are as follows: (1) uECM-peptides; tripeptides that are only found in target ECM (collagen type IV) and not found in other comparable ECMs (designated as uCOL4-peptide), and (2) fECM-peptides; tripeptides that may exist across ECMs, but more frequently exist in a specific ECM (e.g., collagen type IV) and are not usually found in other comparative ECMs (designated as fCOL4-peptide).

The method to obtain uCOL4-peptides is described in the material and methods section in the main manuscript. The method to obtain fCOL4-peptide is illustrated in **Fig. S1**. First, the redundancies of each tripeptide in one collagen type were counted by a custom C source program, and a non-redundant peptide list with the redundancy percentage was produced. Second, with non-redundant peptides from all evaluated ECMs, all redundancy percentages were compared against all target ECMs. When the peptide had a higher redundancy percentage against its own sequence compared to any other type of collagen, the peptide was nominated as fCOL4-peptide. The cell-selective adhesion assay performed on a peptide array (PIASPAC method) was carried out using the same protocol described in the materials and methods section in the main manuscript.

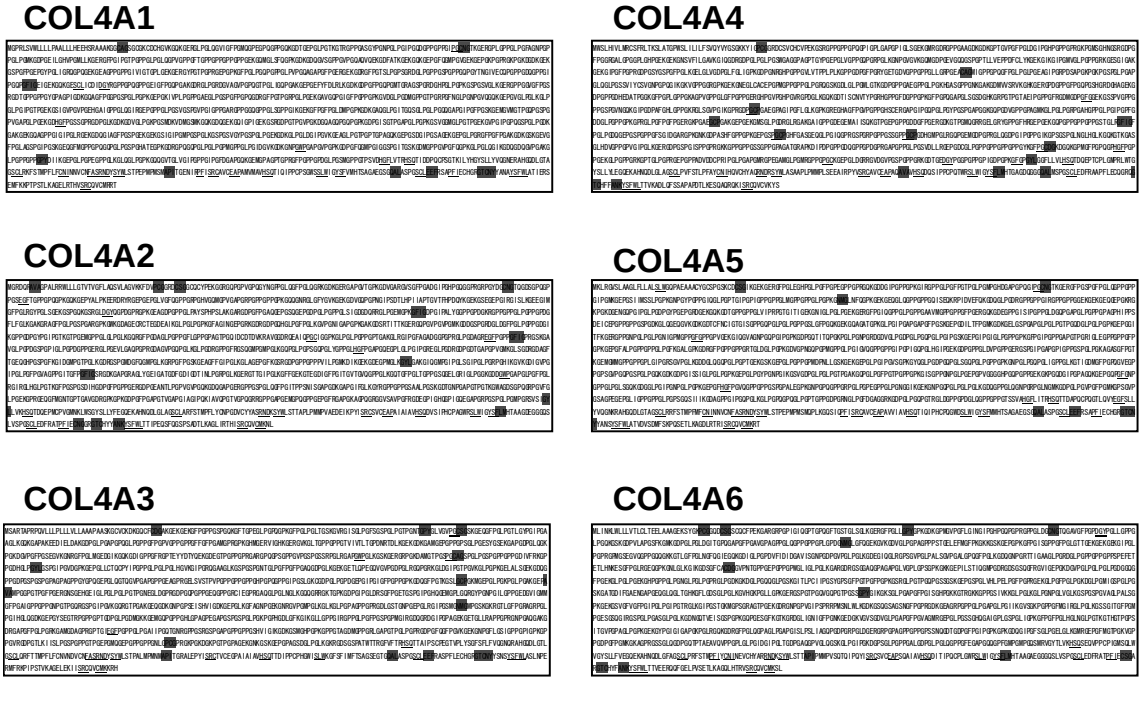

Figure S1. Positional areas of uCOL4-peptides in human collagen type IV. Positional areas containing the top 20 EC-selective peptides are indicated with black boxes. Positional areas containing the top 20 SMC-selective peptides are indicated with underlines.

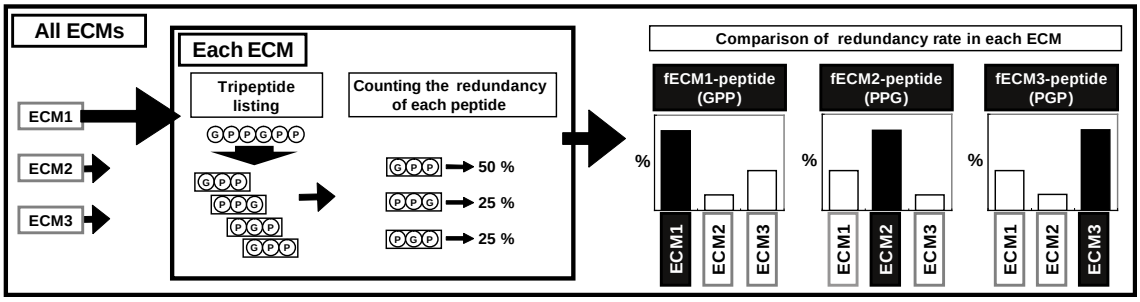

Figure S2. A schematic flow of *in silico* analysis to obtain fECM-peptides.

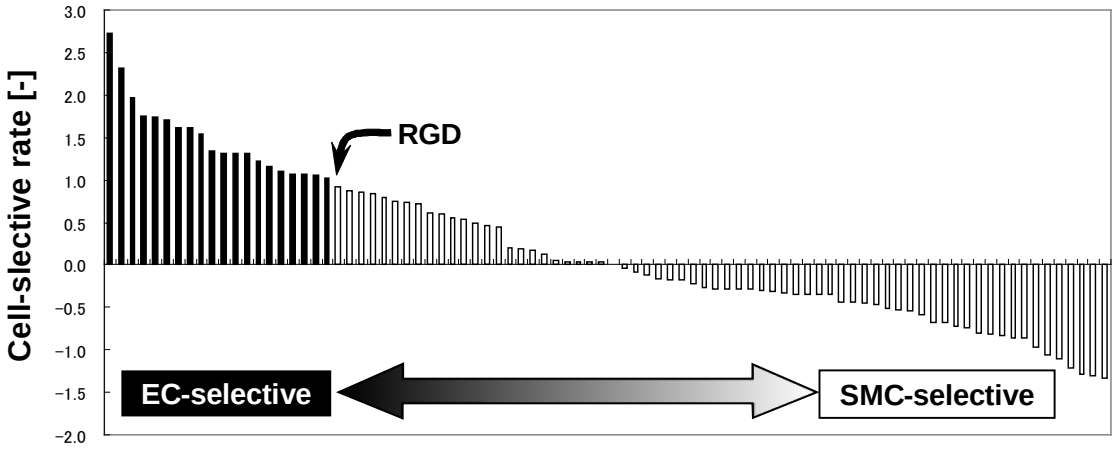

Figure S3. Cell-selective peptide screening result. Positive value expresses the EC-selective function, attracts ECs and rejects SMCs. Negative value expresses SMC-selective function, attracts SMCs and rejects ECs. The RGD peptide is indicated as a reference. Black bars, peptides with significant cell selection (> +1.0 or < -1.0).

Table S1. The tripeptide profiles in *in silico* analysis

Collagen type	Collagen isoform	Uniprot accession number	Length (AA)	Number of tripeptides (with redundancy)	Number of tripeptides in each type (with redundancy)	Number of non-redundant tripeptides in each type	Number of uECM-peptides (relative precentage)
Type I	COL1A1	P02452	1464	1462	2826	940	163 (17.3%)
	COL1A2	P08123	1366	1364			
Type II	COL2A1	P02458	1487	1485	1485	642	72 (11.2%)
Type III	COL3A1	P02461	1466	1464	1464	647	86 (13.3%)
Type IV	COL4A1	P02462	1669	1667	10105	1986	907 (45.7%)
	COL4A2	P08572	1712	1710			
	COL4A3	Q01955	1670	1668			
	COL4A4	P53420	1690	1688			
	COL4A5	P29400	1685	1683			
	COL4A6	Q14031	1691	1689			
Type V	COL5A1	P20908	1838	1836	5076	1802	674 (37.4%)
	COL5A2	P05997	1499	1497			
	COL5A3	P25940	1745	1743			

Table S2. Cell adhesion results of uCOL4-peptides

Number	Sequence	EC				SMC				Cell-selectivity rate [-]
		Average of fluorescent intensity [-]	S.D. of fluorescent intensity	rRATIO [-]	S.D. of rRATIO	Average of fluorescent intensity [-]	S.D. of fluorescent intensity	rRATIO [-]	S.D. of rRATIO	
1	CAG	40.29	3.33	2.85	0.24	11.70	0.11	1.18	0.01	1.67
2	CNG	37.84	2.83	2.68	0.20	10.39	1.42	1.05	0.14	1.63
3	CSG	34.40	5.86	2.43	0.41	8.73	1.03	0.88	0.10	1.55
4	GYL	36.30	4.01	2.57	0.28	12.29	2.56	1.24	0.26	1.32
5	CNY	31.73	5.88	2.25	0.42	9.26	0.78	0.94	0.08	1.31
6	PCG	36.20	9.87	2.56	0.70	13.55	0.26	1.37	0.03	1.19
7	CDG	32.60	5.71	2.31	0.40	11.44	1.50	1.16	0.15	1.15
8	AVA	31.00	9.70	2.19	0.69	10.36	1.08	1.05	0.11	1.15
9	FLM	28.75	6.51	2.03	0.46	8.85	0.33	0.90	0.03	1.14
10	GPY	33.63	2.32	2.38	0.16	12.67	3.13	1.28	0.32	1.10
11	GCP	43.36	10.38	3.07	0.73	19.87	1.20	2.01	0.12	1.06
12	QAL	27.86	3.79	1.97	0.27	9.26	0.69	0.94	0.07	1.03
13	FIG	44.11	2.03	3.12	0.14	21.98	1.37	2.22	0.14	0.90
14	GTC	41.87	2.74	2.96	0.19	20.63	2.07	2.09	0.21	0.87
15	EEF	23.55	1.13	1.67	0.08	8.07	0.47	0.82	0.05	0.85
16	GFI	43.50	5.05	3.08	0.36	22.46	2.65	2.27	0.27	0.81
17	ANK	36.14	14.00	2.56	0.99	18.05	1.98	1.83	0.20	0.73
18	ALA	22.75	2.93	1.61	0.21	8.78	1.29	0.89	0.13	0.72
19	API	22.26	2.47	1.58	0.17	8.62	1.26	0.87	0.13	0.70
20	NMG	25.85	4.59	1.83	0.32	11.43	2.85	1.16	0.29	0.67
21	MHT	20.67	3.06	1.46	0.22	8.05	1.29	0.81	0.13	0.65
22	FIE	24.77	1.64	1.75	0.12	11.07	1.13	1.12	0.11	0.63
23	DCS	19.46	3.37	1.38	0.24	7.57	1.95	0.77	0.20	0.61
24	QTI	21.22	0.54	1.50	0.04	8.97	2.76	0.91	0.28	0.59
25	KYS	26.19	6.42	1.85	0.45	12.59	2.43	1.27	0.25	0.58
26	APF	23.20	3.86	1.64	0.27	10.62	2.27	1.07	0.23	0.57
27	QVC	20.86	4.03	1.48	0.29	9.04	1.30	0.91	0.13	0.56
28	ATP	18.47	3.18	1.31	0.23	7.95	0.71	0.80	0.07	0.50
29	PPC	24.72	7.11	1.75	0.50	12.41	2.82	1.26	0.29	0.49
30	VSR	26.71	4.06	1.89	0.29	13.83	4.03	1.40	0.41	0.49
31	NKY	32.25	3.47	2.28	0.25	17.74	3.45	1.80	0.35	0.49
32	NIN	18.33	1.55	1.30	0.11	8.05	2.95	0.82	0.30	0.48
33	LYG	20.47	2.12	1.45	0.15	9.70	1.84	0.98	0.19	0.47
34	DTL	19.15	6.20	1.36	0.44	8.81	1.34	0.89	0.14	0.46
35	CHY	24.22	3.11	1.71	0.22	12.51	1.38	1.27	0.14	0.45
36	KGF	23.80	6.46	1.68	0.46	12.24	1.56	1.24	0.16	0.45
37	AHN	24.84	5.29	1.76	0.37	13.01	3.38	1.32	0.34	0.44
38	LPA	17.75	1.66	1.26	0.12	8.20	0.99	0.83	0.10	0.43
39	PCP	23.23	7.74	1.64	0.55	12.06	1.74	1.22	0.18	0.42
40	QGT	25.67	4.01	1.82	0.28	13.81	4.46	1.40	0.45	0.42
41	YYA	23.09	3.44	1.63	0.24	12.00	2.34	1.22	0.24	0.42
42	WLA	26.16	2.24	1.85	0.16	14.51	3.94	1.47	0.40	0.38
43	MGD	18.51	1.28	1.31	0.09	9.22	1.23	0.93	0.12	0.38
44	GFM	30.60	5.76	2.17	0.41	17.74	9.40	1.80	0.95	0.37
45	LWI	22.22	4.66	1.57	0.33	12.11	3.17	1.23	0.32	0.35
46	CQV	15.44	2.27	1.09	0.16	7.56	2.24	0.76	0.23	0.33
47	AGM	21.75	3.48	1.54	0.25	12.09	2.37	1.22	0.24	0.32
48	MPM	17.30	2.02	1.22	0.14	8.99	0.24	0.91	0.02	0.31
49	FLF	23.57	1.30	1.67	0.09	13.45	10.28	1.36	1.04	0.31
50	FFG	26.71	2.85	1.89	0.20	15.71	2.21	1.59	0.22	0.30
51	YWL	21.66	5.67	1.53	0.40	12.19	1.86	1.23	0.19	0.30
52	YSL	21.45	2.09	1.52	0.15	12.19	2.06	1.23	0.21	0.28
53	GNM	26.74	4.24	1.89	0.30	15.92	1.73	1.61	0.18	0.28
54	VCM	23.04	3.80	1.63	0.27	13.42	1.01	1.36	0.10	0.27
55	ALP	14.58	1.06	1.03	0.08	7.52	0.85	0.76	0.09	0.27
56	CHG	26.50	2.20	1.88	0.16	16.47	1.22	1.67	0.12	0.21
57	CSV	21.69	2.81	1.54	0.20	13.18	2.01	1.33	0.20	0.20
58	QCP	21.85	3.42	1.55	0.24	13.30	2.70	1.35	0.27	0.20
59	MGT	16.06	1.81	1.14	0.13	9.58	0.28	0.97	0.03	0.17
60	SLP	20.37	1.67	1.44	0.12	12.60	5.36	1.28	0.54	0.17
61	CLE	13.36	2.79	0.95	0.20	7.74	1.68	0.78	0.17	0.16
62	EAI	14.82	1.55	1.05	0.11	8.78	0.44	0.89	0.04	0.16
63	STP	17.45	1.31	1.24	0.09	10.65	2.14	1.08	0.22	0.16
64	WIG	21.38	5.84	1.51	0.41	13.53	1.96	1.37	0.20	0.14
65	YGP	16.43	2.49	1.16	0.18	10.24	1.00	1.04	0.10	0.13
66	ASP	15.44	4.98	1.09	0.35	9.79	1.60	0.99	0.16	0.10
67	WLS	19.28	1.70	1.36	0.12	12.60	0.34	1.28	0.03	0.09
68	LVT	13.32	1.04	0.94	0.07	8.75	2.47	0.89	0.25	0.06
69	TRG	17.74	1.30	1.26	0.09	11.87	0.88	1.20	0.09	0.05
70	SRN	19.37	2.26	1.37	0.16	13.13	2.13	1.33	0.22	0.04
71	IPS	17.28	1.57	1.22	0.11	11.75	2.10	1.19	0.21	0.03
72	IPQ	13.05	0.55	0.92	0.04	9.02	1.76	0.91	0.18	0.01
73	EFR	18.22	4.88	1.29	0.35	12.93	1.21	1.31	0.12	-0.02
74	ISL	19.16	1.97	1.36	0.14	13.90	3.64	1.41	0.37	-0.05
75	HNQ	12.66	0.45	0.90	0.03	9.90	2.15	1.00	0.22	-0.11
76	IIS	13.63	0.63	0.96	0.04	10.79	3.23	1.09	0.33	-0.13
77	NDY	21.26	7.43	1.50	0.53	16.32	1.01	1.65	0.10	-0.15
78	IGV	15.83	1.38	1.12	0.10	12.53	1.79	1.27	0.18	-0.15
79	IIK	18.95	1.93	1.34	0.14	14.82	3.17	1.50	0.32	-0.16
80	IAV	21.35	2.69	1.51	0.19	16.56	5.53	1.68	0.56	-0.17
81	PEK	13.53	1.32	0.96	0.09	11.62	4.23	1.18	0.43	-0.22
82	LMH	22.64	4.98	1.60	0.35	18.10	4.34	1.83	0.44	-0.23
83	SFW	24.65	4.71	1.74	0.33	19.62	1.25	1.99	0.13	-0.24
84	TMP	16.01	2.02	1.13	0.14	13.68	4.32	1.38	0.44	-0.25
85	AVH	22.61	4.38	1.60	0.31	18.36	2.24	1.86	0.23	-0.26
86	LLY	23.48	2.03	1.66	0.14	19.10	18.63	1.93	1.89	-0.27
87	VHS	21.24	2.68	1.50	0.19	17.58	2.99	1.78	0.30	-0.28
88	GYS	33.84	6.52	2.39	0.46	26.40	1.21	2.67	0.12	-0.28
89	GMQ	12.96	2.46	0.92	0.17	13.02	4.54	1.32	0.46	-0.40
90	GMS	13.25	0.61	0.94	0.04	13.32	2.22	1.35	0.22	-0.41
91	ECH	16.87	2.53	1.19	0.18	15.92	2.11	1.61	0.21	-0.42
92	GFF	26.58	1.37	1.88	0.10	23.23	5.74	2.35	0.58	-0.47
93	VCE	25.30	8.80	1.79	0.62	22.93	0.73	2.32	0.07	-0.53
94	KSY	21.90	4.63	1.55	0.33	20.68	3.35	2.09	0.34	-0.54
95	GWP	16.13	3.35	1.14	0.24	16.94	3.63	1.71	0.37	-0.57
96	CMK	14.99	1.19	1.06	0.08	16.24	0.91	1.64	0.09	-0.58
97	FAS	14.78	0.99	1.05	0.07	16.29	6.96	1.65	0.70	-0.60
98	SRC	17.92	6.42	1.27	0.45	20.42	2.13	2.07	0.22	-0.80
99	PGC	19.17	4.94	1.36	0.35	21.56	1.70	2.18	0.17	-0.83
100	HGF	20.96	3.36	1.48	0.24	23.09	2.06	2.34	0.21	-0.85
101	SCL	22.13	3.00	1.57	0.21	24.03	2.07	2.43	0.21	-0.87
102	ISR	19.71	4.66	1.39	0.33	23.10	3.19	2.34	0.32	-0.94
103	YSF	19.83	2.78	1.40	0.20	23.41	2.99	2.37	0.30	-0.97
104	FWL	17.93	3.62	1.27	0.26	22.24	1.03	2.25	0.10	-0.98
105	SYW	18.09	3.81	1.28	0.27	22.64	1.82	2.29	0.18	-1.01
106	PFI	14.29	1.58	1.01	0.11	20.09	4.19	2.03	0.42	-1.02
107	RND	15.92	4.30	1.13	0.30	21.50	1.31	2.18	0.13	-1.05
108	GFG	34.86	2.75	2.47	0.19	35.44	17.65	3.59	1.79	-1.12
109	CNI	13.52	0.84	0.96	0.06	21.28	7.08	2.15	0.72	-1.20
110	EAP	13.79	3.59	0.98	0.25	21.91	2.80	2.22	0.28	-1.24
111	HSQ	14.92	2.98	1.06	0.21	23.10	2.47	2.34	0.25	-1.28
112	EGF	15.53	0.59	1.10	0.04	24.16	2.93	2.45	0.30	-1.35
113	SLW	14.29	0.58	1.01	0.04	24.43	2.03	2.47	0.21	-1.46
114	DGY	19.08	2.17	1.35	0.15	30.00	3.94	3.04	0.40	-1.69
	RGD	45.24	14.16	3.20	1.00	22.65	8.26	2.29	0.84	0.91

Table S3. List of cell-selective tripeptides

Positional area from N-terminus [%]*	COL4A1		COL4A2		COL4A3		COL4A4		COL4A5		COL4A6	
	EC-selective peptides	SMC-selective peptides	EC-selective peptides	SMC-selective peptides	EC-selective peptides	SMC-selective peptides	EC-selective peptides	SMC-selective peptides	EC-selective peptides	SMC-selective peptides	EC-selective peptides	SMC-selective peptides
0 - 10	2	1	4	1	3	1	1	0	2	2	4	1
10 - 20	0	0	0	1	0	0	0	0	1	0	1	0
20 - 30	2	2	2	0	2	2	1	0	0	0	1	0
30 - 40	0	0	0	1	0	0	0	0	0	1	0	0
40 - 50	0	0	2	2	2	0	1	2	0	0	1	0
50 - 60	0	1	1	0	0	0	1	0	0	0	0	0
60 - 70	0	0	2	1	1	0	4	2	0	0	0	0
70 - 80	0	1	0	0	0	1	1	2	0	2	0	0
80 - 90	1	3	1	2	1	2	1	5	0	4	0	2
90 - 100	6	16	4	15	6	13	5	13	5	18	5	16

* Length percentage in total protein. 0% = N-terminus. 100% = C-terminus.

Table S4. Cell adhesion results of fCOL4-peptides

Number	Sequence	EC				SMC				Cell-selectivity rate [-]
		Average of fluorescent intensity [-]	S.D. of fluorescent intensity	rRATIO [-]	S.D. of rRATIO	Average of fluorescent intensity [-]	S.D. of fluorescent intensity	rRATIO [-]	S.D. of rRATIO	
1	GQA	47.73	12.79	3.38	0.91	6.50	1.48	0.66	0.15	2.72
2	QGD	46.37	4.41	3.28	0.31	9.47	1.33	0.96	0.13	2.32
3	EKG	40.27	3.20	2.85	0.23	8.68	1.36	0.88	0.14	1.97
4	QGF	33.95	4.58	2.40	0.32	6.43	2.38	0.65	0.24	1.75
5	GMK	50.78	2.42	3.59	0.17	18.33	3.13	1.86	0.32	1.74
6	GLS	50.60	4.65	3.58	0.33	18.54	1.73	1.88	0.18	1.70
7	KGT	37.63	7.95	2.66	0.56	10.29	1.88	1.04	0.19	1.62
8	PLG	31.56	9.61	2.23	0.68	6.08	0.71	0.62	0.07	1.62
9	LGL	32.04	1.36	2.27	0.10	7.25	1.09	0.73	0.11	1.53
10	GIS	47.50	3.98	3.36	0.28	20.00	3.48	2.02	0.35	1.34
11	GEK	40.50	1.14	2.87	0.08	15.36	4.64	1.56	0.47	1.31
12	QGE	33.09	6.93	2.34	0.49	10.19	2.57	1.03	0.26	1.31
13	FPG	33.29	0.52	2.36	0.04	10.36	1.07	1.05	0.11	1.31
14	LPG	36.31	7.48	2.57	0.53	13.35	5.55	1.35	0.56	1.22
15	GDV	46.09	3.64	3.26	0.26	20.71	4.33	2.10	0.44	1.17
16	GTP	28.68	5.09	2.03	0.36	9.15	2.07	0.93	0.21	1.10
17	GIT	40.12	8.55	2.84	0.60	17.44	2.70	1.77	0.27	1.07
18	GFL	41.56	13.37	2.94	0.95	18.51	5.65	1.87	0.57	1.07
19	SGL	32.89	10.11	2.33	0.72	12.57	3.81	1.27	0.39	1.06
20	GLK	29.79	7.17	2.11	0.51	10.78	2.05	1.09	0.21	1.02
21	MKG	34.89	7.84	2.47	0.55	15.73	1.21	1.59	0.12	0.88
22	IGL	29.70	6.59	2.10	0.47	12.36	3.35	1.25	0.34	0.85
23	DGL	22.23	7.48	1.57	0.53	7.21	2.50	0.73	0.25	0.84
24	YPG	23.77	4.40	1.68	0.31	8.68	3.41	0.88	0.35	0.80
25	GDP	24.57	1.91	1.74	0.14	9.75	2.88	0.99	0.29	0.75
26	GEM	38.58	2.94	2.73	0.21	19.75	4.79	2.00	0.49	0.73
27	GPD	20.09	7.46	1.42	0.53	6.89	0.79	0.70	0.08	0.72
28	LRG	24.31	2.94	1.72	0.21	10.87	4.04	1.10	0.41	0.62
29	DGI	31.87	6.32	2.26	0.45	16.30	5.19	1.65	0.53	0.61
30	GPL	21.26	8.89	1.50	0.63	9.40	2.15	0.95	0.22	0.55
31	GYP	19.15	8.45	1.36	0.60	8.01	0.66	0.81	0.07	0.54
32	KGD	23.00	1.96	1.63	0.14	11.22	1.94	1.14	0.20	0.49
33	GQP	26.03	1.33	1.84	0.09	13.67	2.18	1.38	0.22	0.46
34	KGF	23.80	6.46	1.68	0.46	12.24	1.56	1.24	0.16	0.45
35	PGF	17.10	3.04	1.21	0.22	9.89	1.13	1.00	0.11	0.21
36	DKG	20.94	3.73	1.48	0.26	12.83	1.64	1.30	0.17	0.18
37	PGI	16.95	3.38	1.20	0.24	10.17	0.81	1.03	0.08	0.17
38	PGL	17.91	3.09	1.27	0.22	11.27	1.97	1.14	0.20	0.13
39	GSS	35.61	4.61	2.52	0.33	24.34	2.74	2.46	0.28	0.06
40	GTK	40.82	4.55	2.89	0.32	28.12	4.80	2.85	0.49	0.04
41	DPG	14.89	2.83	1.05	0.20	10.04	2.41	1.02	0.24	0.04
42	PGS	19.06	3.34	1.35	0.24	12.99	4.85	1.31	0.49	0.03
43	TKG	25.81	4.29	1.83	0.30	17.73	5.11	1.79	0.52	0.03
44	GIK	46.11	4.11	3.26	0.29	32.11	0.92	3.25	0.09	0.01
45	QPG	17.42	2.37	1.23	0.17	12.58	2.71	1.27	0.27	-0.04
46	TPG	17.28	3.15	1.22	0.22	12.95	0.56	1.31	0.06	-0.09
47	PGM	21.87	5.61	1.55	0.40	16.47	1.52	1.67	0.15	-0.12
48	SKG	27.33	3.35	1.93	0.24	20.68	11.84	2.09	1.20	-0.16
49	DQG	21.66	1.52	1.53	0.11	16.83	4.30	1.70	0.44	-0.17
50	VPG	16.54	4.12	1.17	0.29	13.38	0.86	1.35	0.09	-0.18
51	LGP	24.70	2.08	1.75	0.15	19.49	1.69	1.97	0.17	-0.22
52	LDG	19.05	4.18	1.35	0.30	15.97	3.92	1.62	0.40	-0.27
53	GYS	33.84	6.52	2.39	0.46	26.40	1.21	2.67	0.12	-0.28
54	IPG	32.55	1.64	2.30	0.12	25.51	7.54	2.58	0.76	-0.28
55	KGS	18.72	0.79	1.32	0.06	15.91	0.75	1.61	0.08	-0.29
56	QKG	24.67	3.59	1.75	0.25	20.11	3.75	2.04	0.38	-0.29
57	IKG	29.41	4.81	2.08	0.34	23.52	6.00	2.38	0.61	-0.30
58	PGV	20.92	2.09	1.48	0.15	17.69	4.81	1.79	0.49	-0.31
59	PGY	24.31	4.93	1.72	0.35	20.24	5.54	2.05	0.56	-0.33
60	LSG	20.04	3.43	1.42	0.24	17.35	3.60	1.76	0.36	-0.34
61	KGL	26.87	1.23	1.90	0.09	22.23	1.62	2.25	0.16	-0.35
62	EGP	22.74	1.06	1.61	0.07	19.36	2.02	1.96	0.20	-0.35
63	GIP	37.12	2.65	2.63	0.19	29.41	2.46	2.98	0.25	-0.35
64	KGN	31.27	2.22	2.21	0.16	26.09	6.44	2.64	0.65	-0.43
65	GQK	37.65	6.72	2.66	0.48	30.63	2.92	3.10	0.30	-0.44
66	GFP	35.69	5.16	2.53	0.37	29.40	4.12	2.98	0.42	-0.45
67	KGQ	28.50	3.57	2.02	0.25	24.48	3.01	2.48	0.30	-0.46
68	GEL	29.64	3.26	2.10	0.23	25.73	5.71	2.60	0.58	-0.51
69	GLP	37.40	4.76	2.65	0.34	31.29	3.61	3.17	0.37	-0.52
70	LKG	20.53	1.16	1.45	0.08	19.64	5.11	1.99	0.52	-0.54
71	GDK	19.94	5.23	1.41	0.37	19.71	5.21	2.00	0.53	-0.58
72	GLD	36.99	1.12	2.62	0.08	32.56	5.19	3.30	0.53	-0.68
73	KGI	26.23	1.64	1.86	0.12	25.09	1.68	2.54	0.17	-0.68
74	GVP	22.01	6.21	1.56	0.44	22.48	4.15	2.28	0.42	-0.72
75	PGR	16.67	1.64	1.18	0.12	18.99	2.97	1.92	0.30	-0.74
76	SRC	17.92	6.42	1.27	0.45	20.42	2.13	2.07	0.22	-0.80
77	GSK	35.27	4.26	2.50	0.30	32.63	0.94	3.30	0.10	-0.81
78	PGC	19.17	4.94	1.36	0.35	21.56	1.70	2.18	0.17	-0.83
79	PGT	20.66	3.14	1.46	0.22	22.95	5.12	2.32	0.52	-0.86
80	SCL	22.13	3.00	1.57	0.21	24.03	2.07	2.43	0.21	-0.87
81	YSF	19.83	2.78	1.40	0.20	23.41	2.99	2.37	0.30	-0.97
82	KGE	22.96	2.55	1.62	0.18	26.48	3.97	2.68	0.40	-1.06
83	GDQ	32.71	2.76	2.31	0.20	33.78	4.12	3.42	0.42	-1.10
84	PGD	18.82	2.55	1.33	0.18	25.17	1.96	2.55	0.20	-1.22
85	HSQ	14.92	2.98	1.06	0.21	23.10	2.47	2.34	0.25	-1.28
86	PGQ	16.94	1.44	1.20	0.10	24.64	3.56	2.49	0.36	-1.30
87	GSC	31.93	2.42	2.26	0.17	35.51	1.40	3.59	0.14	-1.33
	RGD	45.24	14.16	3.20	1.00	22.65	8.26	2.29	0.84	0.91

4.6. Summary

To reduce life-threatening risks from medical implants, material modification with cell-selective peptides derived from extracellular matrix (ECM) is one approach for managing rapid recovery and proper reorganization of surrounding cells. Since each ECM has its characteristic cell-selectivity, we focused our investigation on short peptides that contribute to the ECM-specific cell-selectivity. Our underlying hypothesis is that ECM cellular selectivity is regulated not only by discrete ligand-like sequences in the protein, but also by motifs (short as peptides) that are uniquely found within a specific ECM type (designated as ECM-specific peptides). *In silico* comparison of five collagen types (I, II, III, IV, and V), allowed us to focus on tripeptides uniquely found in collagen type IV, since collagen type IV is enriched in the basement membrane and is primarily responsible for separating endothelial cells (ECs) and smooth muscle cells (SMCs). Preferential adhesion of ECs and SMCs to collagen type IV-specific tripeptides was evaluated *in vitro* by peptide array. Among 114 candidates, 21 peptides (18%) were found to indicate strong cell adhesion selectivity, simultaneously promoting adhesion of one cell type while inhibiting adhesion of the other. This result indicates that there are multiple cell-selective peptides that contribute to the ECM's cell selectivity. We chose to further evaluate the Cys-Ala-Gly (CAG) peptide, which was the best performing EC-selective tripeptide, as a practical application example. To demonstrate the utility of CAG in a practical setting, we simply incorporated the peptide into poly-ε-caprolactone fine-fibers, which is a type of material used for artificial small-caliber vascular grafts. The CAG containing fine-fiber surface was found to enhance adhesion of ECs (+190%) while limiting SMCs (-10%) compared to the native, unmodified surface. These findings support the idea that peptides uniquely found in specific ECM types play an important role in establishing that ECM's cell-selectivity.

4.7. Acknowledgements

The authors deeply thank Dr. Yoshikazu Fujita, Nagoya University School of Medicine, for help in obtaining SEM images, Ms. Tomoko Yoshida, Mr. Hiroki Kondo and Mr. Takuya Takeuchi, Nagoya University, for help in obtaining XPS data, Mr. Daisuke Suzuki, Nagoya University, for help in obtaining CHN coder data.

4.8. References

[1] Vamvakopoulos JE, Petrov L, Aavik S, Lehti S, Aavik E, Hayry P. Synergistic suppression of rat neointimal hyperplasia by rapamycin and imatinib mesylate: implications for the prevention of accelerated arteriosclerosis. J Vasc Res 2006;43:184-92.

[2] Fitzgibbon GM, Kafka HP, Leach AJ, Keon WJ, Hooper GD, Burton JR. Coronary bypass graft fate and patient outcome: angiographic follow-up of 5,065 grafts related to survival and reoperation in 1,388 patients during 25 years. J Am Coll Cardiol 1996;28:616-26.

[3] Shuhaiber JH, Evans AN, Massad MG, Geha AS. Mechanisms and future directions for prevention of vein graft failure in coronary bypass surgery. Eur J Cardiothorac Surg 2002;22:387-96.

[4] Bourassa MG. Fate of venous grafts: the past, the present and the future. J Am Coll Cardiol 1991;17:1081-3.

[5] Bhoday J, de Silva S, Xu Q. The molecular mechanisms of vascular restenosis: Which genes are crucial? Curr Vasc Pharmacol 2006;4:269-75.

[6] Sumpio BE, Riley JT, Dardik A. Cells in focus: endothelial cell. Int J Biochem Cell Biol 2002;34:1508-12.

[7] Popowich DA, Varu V, Kibbe MR. Nitric oxide: what a vascular surgeon needs to know. Vascular 2007;15:324-35.

[8] Engler RL, Dahlgren MD, Morris DD, Peterson MA, Schmid-Schonbein GW. Role of leukocytes in response to acute myocardial ischemia and reflow in dogs. Am J Physiol 1986;251:H314-23.

[9] Verrier ED, Boyle EM, Jr. Endothelial cell injury in cardiovascular surgery. Ann Thorac Surg 1996;62:915-22.

[10] McCormick C, Wadsworth RM, Jones RL, Kennedy S. Prostacyclin analogues: the next drug-eluting stent? Biochem Soc Trans 2007;35:910-1.

[11] LoGerfo FW, Quist WC, Cantelmo NL, Haudenschild CC. Integrity of vein grafts as a function of initial intimal and medial preservation. Circulation 1983;68:II117-24.

[12] Kraitzer A, Kloog Y, Zilberman M. Approaches for prevention of restenosis. J Biomed Mater Res B Appl Biomater 2008;85:583-603.

[13] Kushwaha M, Anderson JM, Bosworth CA, Andukuri A, Minor WP, Lancaster JR, Jr., et al. A nitric oxide releasing, self assembled peptide amphiphile matrix that mimics native endothelium for coating implantable cardiovascular devices. Biomaterials 2009;31:1502-8.

[14] Tang C, Kligman F, Larsen CC, Kottke-Marchant K, Marchant RE. Platelet and endothelial adhesion on fluorosurfactant polymers designed for vascular graft modification. J Biomed Mater Res A 2009;88:348-58.

[15] Rodenberg EJ, Pavalko FM. Peptides derived from fibronectin type III connecting segments promote endothelial cell adhesion but not platelet adhesion: implications in tissue-engineered vascular grafts. Tissue Eng 2007;13:2653-66.

[16] Larsen CC, Kligman F, Tang C, Kottke-Marchant K, Marchant RE. A biomimetic peptide fluorosurfactant polymer for endothelialization of ePTFE with limited platelet adhesion. Biomaterials 2007;28:3537-48.

[17] Blindt R, Vogt F, Astafieva I, Fach C, Hristov M, Krott N, et al. A novel drug-eluting stent coated with an integrin-binding cyclic Arg-Gly-Asp peptide inhibits neointimal hyperplasia by recruiting endothelial progenitor cells. J Am Coll Cardiol 2006;47:1786-95.

[18] Yin M, Yuan Y, Liu C, Wang J. Development of mussel adhesive polypeptide mimics coating for in-situ inducing re-endothelialization of intravascular stent devices. Biomaterials 2009;30:2764-73.

[19] Yin M, Yuan Y, Liu C, Wang J. Combinatorial coating of adhesive polypeptide and anti-CD34 antibody for improved endothelial cell adhesion and proliferation. J Mater Sci Mater Med 2009;20:1513-23.

[20] Hubbell JA, Massia SP, Desai NP, Drumheller PD. Endothelial cell-selective materials for tissue engineering in the vascular graft via a new receptor. Biotechnology (N Y) 1991;9:568-72.

[21] Gobin AS, West JL. Val-ala-pro-gly, an elastin-derived non-integrin ligand: smooth muscle cell adhesion and specificity. J Biomed Mater Res A 2003;67:255-9.

[22] Kato R, Kaga C, Kunimatsu M, Kobayashi T, Honda H. Peptide array-based interaction assay of solid-bound peptides and anchorage-dependant cells and its effectiveness in cell-adhesive peptide design. J Biosci Bioeng 2006;101:485-95.

[23] Kanie K, Kato R, Zhao Y, Narita Y, Okochi M, Honda H. Amino acid sequence preferences to control cell-specific organization of endothelial cells, smooth muscle cells, and fibroblasts. J Pept Sci. in press.

[24] Frank R. SPOT-Synthesis: An easy technique for the positionally addressable, parallel chemical synthesis on a membrane support. Tetrahedron 1992;48:9917-32.

[25] Kaga C, Okochi M, Tomita Y, Kato R, Honda H. Computationally assisted screening and design of cell-interactive peptides by a cell-based assay using peptide arrays and a fuzzy neural network algorithm. Biotechniques 2008;44:393-402.

[26] Suzuki S, Narita Y, Yamawaki A, Murase Y, Satake M, Mutsuga M, et al. Effects of extracellular matrix on differentiation of human bone marrow-derived mesenchymal stem cells into smooth muscle cell lineage: utility for cardiovascular tissue engineering. Cells Tissues Organs 2009;191:269-80.

[27] Domingos M, Chiellini F, Cometa S, De Giglio E, Grillo-Fernandes E, Bartolo P, et al. Evaluation of *in vitro* degradation of PCL scaffolds fabricated via EioExtrusion. Part 1:

Influence of the degradation environment. Virtual and Pysical Prototyping 2010;5:65-73.

[28] Ju YM, Choi JS, Atala A, Yoo JJ, Lee SJ. Bilayered scaffold for engineering cellularized blood vessels. Biomaterials 2010;31:4313-21.

[29] Zhang X, Thomas V, Xu Y, Bellis SL, Vohra YK. An *in vitro* regenerated functional human endothelium on a nanofibrous electrospun scaffold. Biomaterials 2010;31:4376-81.

[30] Kagami H, Agata H, Satake M, Narita Y. Considerations on designing scaffolds for soft and hard tissue engineering. Singapore: Pan Stanford Publishing Pte. Ltd.; 2011.

Chapter 5

Development of novel small-caliber vascular grafts with tripeptide for accelerationof endothelialization and prevention of intimal hyperplasia

5.1. Introduction

Cardiovascular surgeons have used artificial vascular grafts with various diameters for vascular surgery including aortic replacement and an arterial bypass procedure. While artificial vascular grafts were developed more than 50 years ago, large-caliber synthetic vascular grafts have been used at the clinical level with satisfactory results for patency rate, durability, and safety. On the other hand, small-caliber synthetic vascular grafts (less than 4 mm in diameter) have low patency rates resulting in a far from clinically acceptable performance [1], since their reaction to foreign bodies causes intimal hyperplasia and thrombosis resulting in occlusion. Autologous arterial or venous grafts thus remain the most optimal vascular graft substitutes. However, we sometimes encountered patients with diseased venous graft such as varicose vein at coronary artery bypass surgery, lack of grafts at redo bypass surgery and repeatedly failed blood access for chronic

hemodialysis [2]. Hence, the development of alternative artificial small caliber vascular grafts (SCVGs) is eagerly anticipated.

Recently, the research on tissue-engineered small-caliber vascular grafts (TE-SCVGs) appears promising. Although tissue-engineered venous grafts can be used clinically for patients suffering from congenital heart defects (during Fontan-type procedure) [3], satisfactory tissue-engineered arterial grafts including a small-diameter prosthesis cannot be made in a clinical situation. One of the reasons for failed TE-SCVG is that no suitable or appropriate scaffold substitute has yet been developed. The requirements for an ideal scaffold substitute for TE-SCVG are: (1) it must induce rapid endothelialization [4], (2) shows a minimal foreign body reaction or good biocompatibility and, (3) has excellent mechanical properties (equivalent to those of native artery in terms of pressure resistance, elasticity, and compliance) [5]. It is well known that a foreign body reaction and/or a compliance mismatch can lead to intimal hyperplasia, which is one of the causes of graft failure.

Kagami at al., who is our co-investigator, have investigated a TE-SCVG using an electrospinning biodegradable polymer [6]. Simultaneously, we have also developed the technology to apply peptides to medical devices to improve their biocompatibility. Using our original peptide array technology, we discovered a short-chain tripeptide with a high affinity for endothelial cells (ECs) and a low affinity for smooth muscle cells (SMCs) derived from collagen type IV. Furthermore, we fabricated a small tube (inner diameter 0.7 mm), comprised of a short-chain peptide together with a biodegradable polymer using the electrospinning technique. In the present study, the efficacy of our novel TE-SCVGs was investigated using a rat carotid arterial replacement model. Particularly, rapid endothelialization and intimal hyperplasia of the grafts were evaluated.

5.2. Materials and Methods

5.2.1. Cell-selective adhesion peptide

To achieve rapid endothelialization and inhibit the over-growth of SMCs, a CAG (Cys-Ala-Gly) tripeptide sequence, which enhanced the selective cell adhesion of ECs while limiting SMCs adhesion, was incorporated into the fine-fiber sheet. The method of revealing such a cell-selective peptide was described previously [7]. Briefly, tripeptides that are found only in human collagen type IV (not in collagen types I, II, III, and V) were searched, and peptides with a high redundancy rate in collagen type IV (114 sequences) were screened with their cell adhesion effects using the peptide array-based cell assay method [8]. Collagen type IV was screened as the target protein since it is one of the main ECM components in the basement membrane that separates the ECs and SMCs in vascular tissue. By comparing the relative cell adhesion rate of ECs and SMCs on a peptide array, CAG peptide was found to show the highest selective performance for enhancing ECs and rejecting SMCs. Although the RGD (Arg-Gly-Asp) peptide (the well-known cell adhesion peptide which has an integrin binding sequence) exhibited a high cell-adhesion effect, it does not possess adherent cell selectivity. **Fig. 1A** showed the difference of the subtracted average adhesion ratio of SMCs from the average adhesion ratio of ECs in CAG and RGD. This graph indicated that CAG has a high selectivity for EC adhesion and a strong resistance to SMC adhesion.

5.2.2. Preparation of small-caliber vascular grafts

SCVGs 0.7 mm in diameter were fabricated by a biodegradable polymer mixed with the peptide (CAG) using the electrospinning procedure. We used poly-ε-caprolactone (PCL) for the biodegradable polymer. A solution consisting of PCL and methylene chloride was drawn into a syringe with a needle which used the positive electrode of the electrospinning apparatus and a

voltage range of 10–15 kV. The charged polymer was spun toward a circular cylinder-like counter electrode at 60 rpm. The fibrous material collected on the counter electrode formed a tube-like structure (**Fig. 1B**).

5.2.3. Operative procedure

We used Sprague Dawley rats (males 9.9±1.4 weeks old: body weight: 322±27 g, purchased from Chubu Kagaku Shizai Corporation, Nagoya, Japan) anesthetized by inhalation of diethyl ether (Wako Pure Chemical Industries Ltd., Osaka, Japan) and an intraperitoneal administration of 20-30 mg/kg sodium pentobarbital (Somnopentyl, Kyoritsu Seiyaku Corp., Tokyo, Japan), 0.15-0.20 mg/kg atropine sulfate (Mitsubishi Tanabe Pharma Corp., Osaka, Japan). Sodium heparin (Novo-heparin, Mochida Pharmaceutical Co. Ltd., Tokyo, Japan) was used for anti-coagulation. The rats underwent a common carotid arterial replacement using (1) our developed peptide containing SCVGs (group CAG, **Fig. 1C**, **Fig. 1D**) which was about 7 mm in length or (2) non-peptide containing SCVGs (group C **Fig. 1E**) as a control. The method of anastomosis was end-to-end, interrupted suture technique using 10-0 nylon (Crownjun, Kono Seisakusyo Co., Ltd., Chiba, Japan) (**Fig. 1F**).

The grafts were removed 1 week, 2 weeks, and 6 weeks after the operation in each group (**Fig. 1G**). We eliminated cases which were obviously technical errors, then investigated 17 patent grafts (patency rate 77.3%) in group CAG among the 22 implanted group CAG grafts and 19 patent grafts (patency rate 79.2%) in group C among the 24 implanted group C grafts. From time-points in both groups, 1 graft of each time-point was assessed by scanning electron microscopy (SEM), while the other grafts were cut in half, with one frozen section used for staining and another piece of extracted protein for Western blotting.

We conformed to the Regulations for Animal Experiments in Nagoya University and to the

legally-established criteria for animal experiments. All procedures involving animal experiments were approved by the Animal Experimentation Committee of the Nagoya University School of Medicine.

5.2.4. Immunofluorescent staining and proportion of endothelialization

To determine expressions of EC- or SMC-selective protein in each replaced graft, immunofluorescent staining for the von Willebrand factor (vWF) and α-smooth muscle actin (ASMA) was performed. Removed grafts were fixed in 7.5% buffered formaldehyde sodium. After overnight dehydration using 20% sucrose, the samples were embedded in Tissue-Tek™ O.T.C. compound (Sakura Finetec Japan Co. Ltd., Tokyo, Japan) cut into 5-μm slices. The frozen slices were blocked with 5% bovine serum albumin (Sigma, Saint Louis, MO) for 30 minutes at room temperature. After blocking, the slices were immunostained for 30 minutes with the following primary antibodies; vWF (Dako, Glostrup, Denmark) and ASMA (1:500, Sigma). After washing with 1% phosphate-buffered saline, the primary antibodies were detected by secondary antibodies for 30 minutes（1:500, Alexa Fluor 488, Invitrogen, Carlsbad, CA, 1:500, Alexa Fluor 546, Invitrogen. After washing, 4',6-diamidine-2-phenylindole (DAPI, VECTASHIELD, Vector Laboratories Inc., Burlingame, CA) was mounted and examined under a fluorescent microscope.

To determine the degree of endothelialization for the inner surface of the grafts, we examined the proportion of the vWF-positive part to the total inner surface circumference of the graft (so-called “ratio of endothelialization”) using graphic software (Image-J, Research Services Branch, National Institutes of Mental Health, Bethesda, MD). The ratios were calculated at 8 randomly selected parts of the grafts at all time points and in all groups. The data were expressed as the mean ± standard deviation.

5.2.5. Scanning electron microscopy

To examine the structure of the vascular grafts before and after implantation, we observed them with SEM. The grafts were fixed by 2.5% glutaraldehyde for 24 hours. After fixation in 1% osmium tetroxide, the samples were dehydrated with a graded ethanol series. Using the t-butyl-alcohol freeze-drying method, the dried grafts were coated using the Osmium Plasma Coater (Nippon Laser & Electronics Lab., Nagoya, Japan). The inner cavity and cross-section of the coated grafts were observed with SEM (S-800S, Hitachi Ltd., Tokyo, Japan) and the images were acquired using an Image Photographer2000 (COMELE Corporation, Tokyo, Japan).

5.2.6. Western blot analysis

Western blot analysis was performed to assess the expressions of EC- and SMC-selective proteins. The removed grafts were homogenized by an ultrasonic disintegrator (Sonic & Materials Inc., Newtown, CT) in a protein-extraction buffer (CytoBuster™, Merck KGaA, Darmstadt, Germany) with 20 mM ethylenediaminetetraacetic acid (EDTA) and 1 mM phenylmethylsulfonyl fluoride (PMSF). The protein concentration of the lysate was measured with BCA Protein Assay Kit (Pierce Biotechnology, Rockford, IL). The proteins were denatured by boiling with sodium dodecyl sulfate (SDS) and 2-mercaptoethanol solution. Equal concentration proteins were applied in 7.5-12.5% SDS-polyacrylamide gel (Atto Corp., Tokyo, Japan) to perform electrophoresis. The proteins were transferred to the blotting membrane (polyvinyliden difluoride) by iBlot™ (Invitrogen). The membrane was blocked with 4% skim milk (Snow Brand Milk Products Co. Ltd., Tokyo, Japan) in T-TBS (Tween-20 added Tris buffer saline) for 1 hour at room temperature. The membrane was immunoblotted using endothelial nitric oxide synthase (eNOS, 1:250, Thermo Fisher Scientific Inc., Waltham, MA), thrombomodulin (TM, 1:200, Santa Cruz Biotechnology Inc., Santa Cruz, CA), ASMA (1:3000, Sigma), calponin (1:5000, Epitomics Inc., Burlingame, CA), and

β-actin（1:5000, Sigma）as an internal control. Horseradish peroxidase (HRP)-conjugated goat anti-mouse/rabbit IgG (1:5000, Cell Signaling Technology Inc., Danvers, MA) was used for secondary antibodies to detect the bands using enhanced chemoluminescence ECL Plus Detection Reagents (Amersham, Buckinghamshire, UK). To quantitatively assess the intensity of the bands, densitometric analysis was performed using ChemiDoc XRS System (Bio-Rad Laboratories, Hercules, CA) with imaging software (Quantity One; Bio-Rad). In order to be standardized, the intensity levels of the bands were divided by the intensity level of β-actin.

5.2.7. Statistical analysis

The statistical analyses were performed using the PASW Statistics 18.0 software program (SPSS Inc., Chicago, IL). The data were analyzed by unpaired Student's t-test. All results were expressed as the mean ± standard deviation, with a P-value of less than 0.05 considered to be statistically significant.

5.3. Results

5.3.1. Ratio of Endothelialization

Immunofluorescent staining for vWF was shown in **Fig. 2A** to **Fig. 2F**. The ratio of endothelialization was increased time dependently in both groups. In addition, the ratio of endothelialization of group CAG was significantly higher than that of group C at all time-points (CAG vs C at 1 week; 64.4 ± 20.0% vs 42.1 ± 8.9%, P=0.012, CAG vs C at 2 weeks; 98.2 ± 2.3% vs 72.7 ± 12.9%, P<0.001, and CAG vs C at 6 weeks; 97.4 ± 4.6% vs 76.7 ± 5.4%, P<0.001) (**Fig. 2G**). It was suggested that the adhesion and growth of vascular ECs would be better observed on the CAG-treated graft in comparison with the non-treated graft.

5.3.2. SEM Findings of Surface of the Graft

The direct appearance of the inner surface of grafts with SEM showed that the adherence and extension of the ECs were superior in group CAG compared to group C during the observation period. Configuration of the cells in group CAG was also different from that in group C. ECs in group CAG were wide and adhere well to the surface of the graft (**Fig. 3A** to **Fig. 3F**).

5.3.3. Endothelial Function

To assess the function of adherent ECs, Western blotting for eNOS and TM were performed. Expressions of eNOS and TM increased over time in both groups. These results were similar to those for the ratio of endothelialization. The intensity of eNOS and TM showed a higher tendency toward group CAG compared with group C (**Fig. 4A**); in particular, the intensity of eNOS at 1 week in group CAG was significantly higher than that in group C (CAG vs C: 1.20 ± 0.37 vs 0.34 ± 0.16, P=0.012) (**Fig. 4B**).

5.3.4. Penetration and Growth of SMCs in the Graft Wall

To evaluate the behavior of the mesenchymal cells including SMCs in the graft, immunofluorescent staining and Western blotting of mesenchymal-cell specific proteins such as ASMA and calponin were performed. Immunofluorescent staining of ASMA revealed that the ASMA-positive area of group C was similar to that of group CAG (**Fig. 5A** to **Fig. 5F**). In addition, the intensity of ASMA 6 weeks after implant in the Western blot analysis was significantly higher in group C than in group CAG (CAG vs C: 0.89±0.06 vs 1.25±0.22, P=0.04). Though the intensity of calponin showed no significant difference, group C tended to show somewhat higher intensity than group CAG (**Fig. 5G**, **Fig. 5H**).

5.4. Discussion

Early endothelialization of grafts is absolutely imperative for achieving a desirable patency of SCVGs after replacement. Many ingenious attempts have been made to achieve the successful engraftment of ECs, and several that obtained early endothelialization were published (using autologous cells, biodegradable scaffold, and various other methods) [9-11]. Meanwhile, the inhibition of intimal hyperplasia is also involved in long-term patency rates of SCVGs. The sustained release of agents able to inhibit cell proliferation prevents anastomotic intimal hyperplasia [12]. However, the adverse effects of these drugs on ECs are a matter of concern. Our developed SCVGs could achieve not only early endothelialization but also inhibition of intimal hyperplasia by the inhibition of mesenchymal cell adhesion, using tripeptide. To our knowledge, this study is the first to report both early endothelialization and the inhibition of intimal hyperplasia for SCVG by tripeptide.

RGD peptide is widely known as a short-chain peptide with high affinity for vessel-composed cells. Some studied have established the efficacy of RGD peptide for its improvement of endothelialization for prostheses [13-15]. However, concurrently, RGD has the potential to adhere to mesenchymal cells, including synthetic SMCs that produce abundant ECM [16]. Since it is well known that excessive production of ECM by synthetic SMCs could cause intimal hyperplasia [17-19], thus, RGD may induce intimal hyperplasia. On the other hand, our prior *in vitro* study revealed that the affinity for the ECs in the CAG peptide is similar to RGD peptide, although the affinity for the SMCs in CAG peptide is lower than RGD (data not shown). We considered that these results would work favorably toward early endothelialization and the inhibition of intimal hyperplasia.

Although early endothelialization is important for the regeneration of small-diameter blood vessels, it is also essential for normal endothelial function. Anti-coagulation is the most important function of ECs, and it directly influences graft patency. In this study, we evaluated the function of EC by immunostaining for vWF (the coagulation factor in the blood clotting cascade), Western blot analysis for eNOS which has the function of a vasodilator property [20] and inhibits platelet aggregation [21], and for TM which is an inhibitor of the coagulant function [22]. Our results revealed that expressions of these factors (vWF, eNOS and TM) in group CAG were greater than those in the control group. Therefore, these results also suggested that a prosthesis which contains CAG could expect to achieve long-term patency.

To assess the status of a replaced arterial graft wall, a specimen of the removed graft was evaluated by immunostaining and Western blotting for ASMA and calponin. Unfortunately, tunica media of the stratified SMC layer was not formed, and fiber of the biodegradable polymer remained for at least 6 weeks. However, no overgrowth of the mesenchymal cells was observed (including dedifferentiated SMCs which had the synthetic ability of ECM). Excessive synthesis of ECM is a potential cause of intimal hyperplasia that progresses to vascular stenosis and occlusion [23]. Our results showed that expressions of the ASMA and calponin of group CAG were lower than those of group C, suggesting that intimal hyperplasia was controlled by CAG.

It is recognized that CAG can be applied to various medical devices that can be used for intravascular problems. In this study, we developed TE-SCVG using a biodegradable polymer (PCL) with peptide, so that the entire prosthesis will finally be dissolved to become an autologous artery. If we attach the CAGs to existing artificial blood vessels (made of polyester or PTFE), the long-term patency rate of an existing prosthesis may be improved. Similarly, if we use CAG in a stent for percutaneous coronary intervention, stent-induced re-stenosis may be reduced. Further study will be necessary to apply CAGs to these devices, e.g., in the development of an effective

procedure for coating CAGs to the devices or determine the appropriate CAG concentrations and the contact angle.

There are some limitations in the current study. (1) The short observation period is one. The PCL fiber had not completely disappeared at least 6 weeks into the follow-up. We were interested in the tissue strength of the regenerated vessel once the scaffold had disappeared completely, as well as in the long-term patency rate of this prosthesis. However, in fact, we were unable to observe any difference in the patency rates between both groups over a 6-week follow-up period. Such results supported the need for a long-term observation study in the future. (2) Since we based our study on a small animal (rodent) carotid-arterial replaced model, the vascular remodeling or healing process of rat vessels may differ from those in large animal including humans. The reproducibility of CAG effects on large animal arterial replacement or bypass surgery need to be verified. (3) Our study was also based on a rat carotid artery only 0.7 mm in diameter. The operative procedure called for a high-quality anastomosis technique. Therefore, although the operation was performed by one surgeon, a learning curve is needed to achieve satisfactory anastomosis. Our study, thus, could not completely avoid such a learning curve.

In conclusion, we developed a novel SCVG comprised of a biodegradable polymer with a short-chain tripeptide. Our results suggest that the SCVG with CAG peptide may improve the long-term patency rate of SCVG.

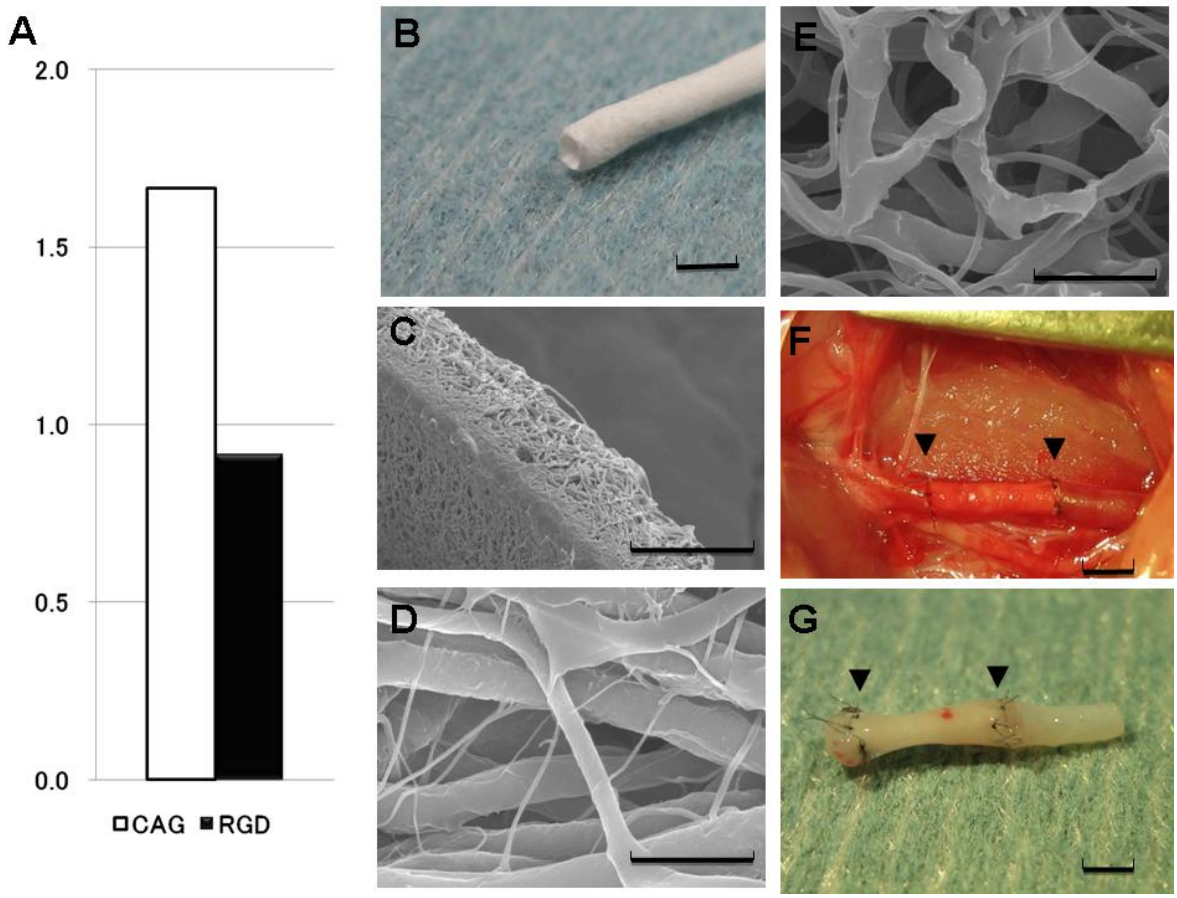

Figure 1. The EC-selectivity of CAG peptide and the morphology of CAG containing graft. The values express the EC-selective adhesion, attract ECs and rejects SMCs (Cell adhesion ratio of EC minus SMC (no peptide as 1.0, N=3)) *in vitro* study. The RGD peptide is indicated as a reference. This graph shows that CAG peptide has more selectivity to ECs than to RGD peptide [A]. Gross view of the scaffold (0.7 mm in diameter) [B] and scanning electron micrographs (SEM) of group CAG cross-section surface [C] and luminal surface in group CAG [D] and group C [E] (original magnification of [C]: 2000×, [D and [E]: 10000×). The micrographic findings of these grafts showed no difference between group CAG and group C. An operative view of the implantation [F] and removed graft [G] was shown (the arrows in these figures denote the site of anastomosis). Scale bar in [A], [F], and [G] = 1 mm, [C] = 60 μm, [D] and [E] = 3 μm.

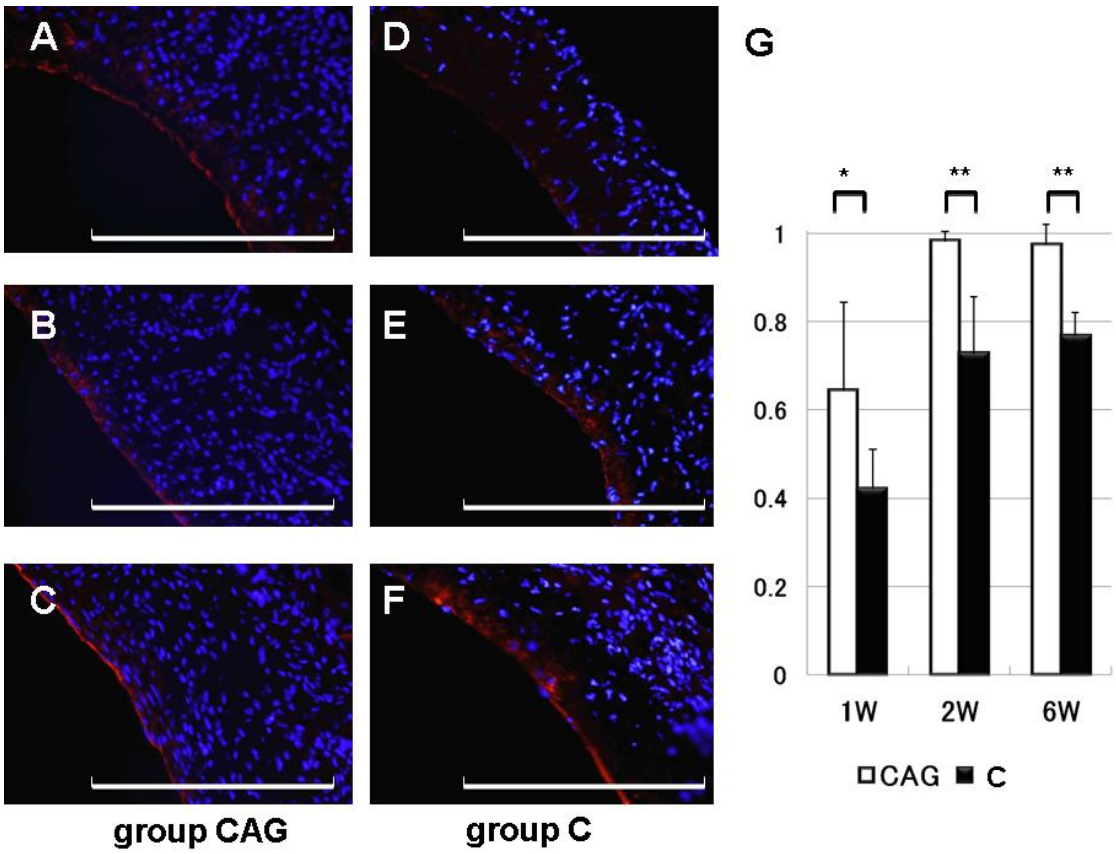

Figure 2. Immnofluorescene for von Willebrand factor (vWF). At 1 week [A], 2 weeks [B], and 6 weeks [C] after implantation in group CAG and at 1 week [D], 2 weeks [E], and 6 weeks [F] in group C. Scale bar = 200 μm, and results of ratios of endothelialization [G], (*P<0.05, **P<0.01) In both staining, the endothelial cells were observed in the lumen of the scaffold. Endothelial regeneration was better in group CAG than in group C at each time point

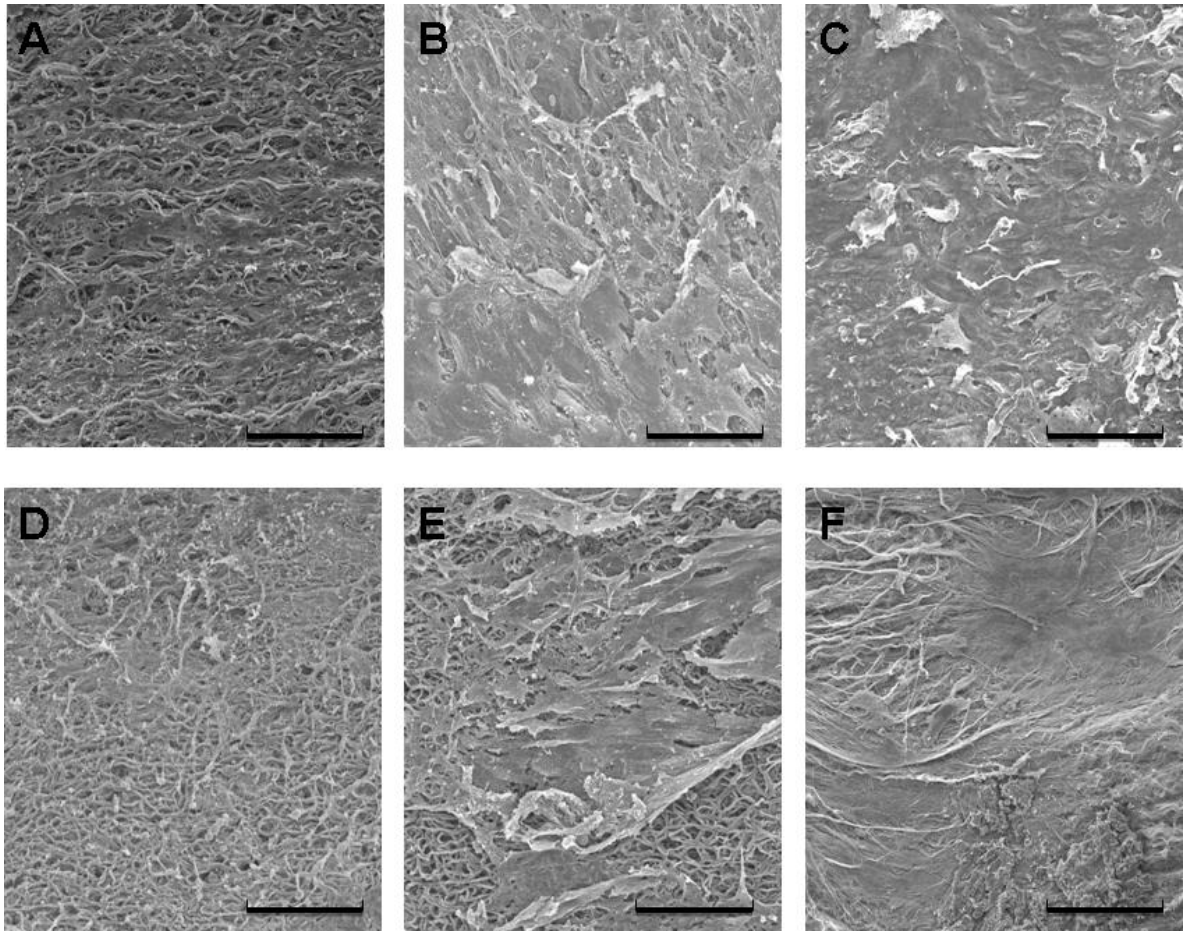

Figure 3. Scanning electron microscopy image of endothelialization. At 1 week [A], 2 weeks [B], and 6 weeks [C] after implantation in group CAG, and 1 week [D], 2 weeks [E], and 6 weeks [F] in group C. Scale bar = 60 μm. Endothelium on the poly-caprolacton fiber was shown. At all timepoints, the endothelial structures in CAG grafts were more numerous than in the control.

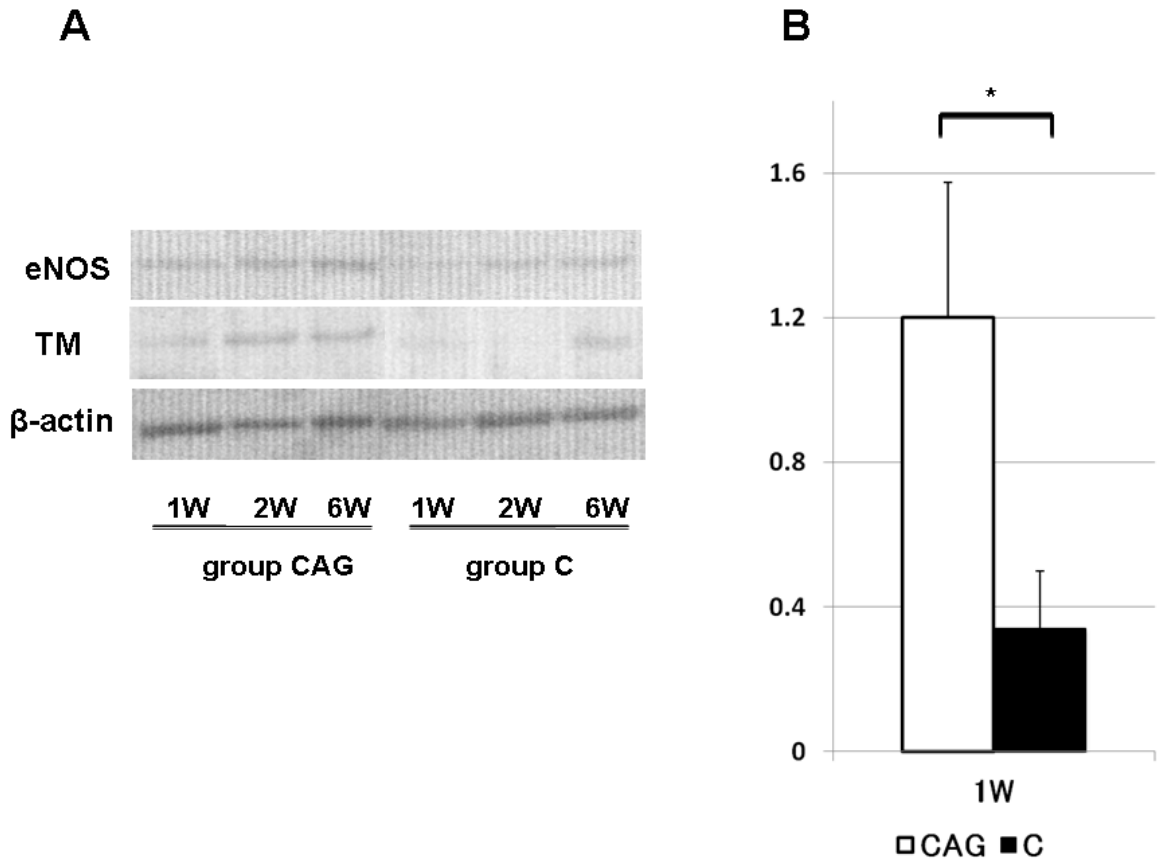

Figure 4. Western blot analysis of the grafts with and without CAG peptide. Each data was obtained 1, 2, and 6 weeks after implantation for eNOS (upper line), thrombomodulin (middle line), and β-actin was used as an internal standard of the Western blot (lower line)[A]. Moreover, intensity of eNOS which was standardized in that of β-actin showed a significant difference about 1 week after implantation between group CAG and group C (n=4, *P<0.05) [B].

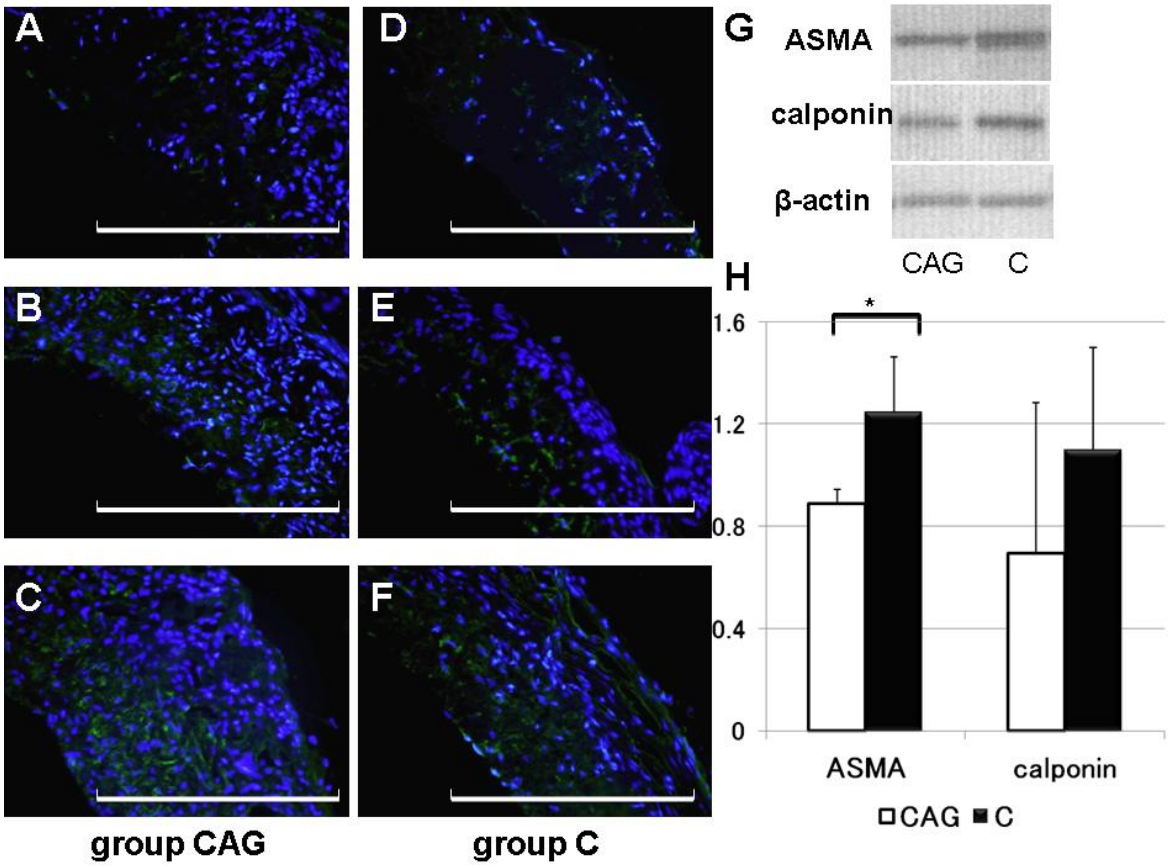

Figure 5. Immunofluorescence for α-smooth muscle actin (ASMA). At 1 week [A], 2 weeks [B], and 6 weeks [C] after implantation in group CAG, and 1 week [D], 2 weeks [E], and 6 weeks [F] in group C. Scale bar = 200 μm. The results of Western blot analysis of the grafts with and without CAG peptide retrieved 6 weeks after implantation for ASMA (upper line), calponin (middle line), and β-actin were used as an internal standard of Western blot (lower line) [G]; results of the intensity of ASMA and calponin which was standardized in that of β-actin (n=4, *P<0.05) [H]

5.5. Summary

Both rapid endothelialization and the prevention of intimal hyperplasia are essential to improve the patency of small-caliber vascular grafts (SCVGs). Using the peptide array-based screening system, we identified the peptide "CAG (Cysteine-Alanine-Glycine)," which has a high affinity for endothelial cells and a low adhesive property for smooth muscle cells. In this study, we report an *in vivo* analysis of the novel SCVGs that were constructed with a biodegradable polymer (poly-ε-caprolactone) containing CAG peptide.

The novel SCVG, which measured 0.7 mm in diameter and 7 mm in length, was fabricated using the electrospinning technique. The carotid arterial replacement was performed on SD rats using the SCVGs with (group CAG) or without CAG (group C). Histological and biochemical assessments were performed at 1, 2 and 6 weeks after implantation.

The ratio of endothelialization was significantly higher in group CAG compared to group C (CAG vs C: 64.4±20.0% vs 42.1±8.9% at 1 week, 98.2±2.3% vs 72.7±12.9% at 2 weeks, and 97.4±4.6% vs 76.7±5.4% at 6 weeks, $P<0.05$). Additionally, Western blot analysis showed that the endothelial nitric oxide synthase at 1 week of group CAG was significantly higher than that of group C (CAG vs C: 1.20±0.37 vs 0.34±0.16, $P=0.01$), and that α-smooth muscle actin at 6 weeks in group CAG was significantly lower than that of group C (CAG vs C: 0.89±0.06 vs 1.25±0.22, $P=0.04$). Intimal hyperplasia was not observed in group CAG.

The graft with CAG promoted rapid endothelialization and regulated intimal hyperplasia.

5.6. Acknowledgements

The authors deeply thank Mr. Fumiaki Kuwabara and Ms. Aika Ogata, Department of Cardiac Surgery, Nagoya University Graduate School of Medicine, for his many and grateful *in vivo* experiments.

5.7. References

[1] Faries PL, Logerfo FW, Arora S, Hook S, Pulling MC, Akbari CM, et al. A comparative study of alternative conduits for lower extremity revascularization: all-autogenous conduit versus prosthetic grafts. J Vasc Surg. 2000;32:1080-90.

[2] Papanikolaou V, Papagiannis A, Vrochides D, Imvrios G, Gakis D, Fouzas I, et al. The natural history of vascular access for hemodialysis: a single center study of 2,422 patients. Surgery. 2009;145:272-9.

[3] Shin'oka T, Matsumura G, Hibino N, Naito Y, Watanabe M, Konuma T, et al. Midterm clinical result of tissue-engineered vascular autografts seeded with autologous bone marrow cells. J Thorac Cardiovasc Surg. 2005;129:1330-8.

[4] van der Zijpp YJ, Poot AA, Feijen J. Endothelialization of small-diameter vascular prostheses. Arch Physiol Biochem. 2003;111:415-27.

[5] Chan-Park MB, Shen JY, Cao Y, Xiong Y, Liu Y, Rayatpisheh S, et al. Biomimetic control of vascular smooth muscle cell morphology and phenotype for functional tissue-engineered small-diameter blood vessels. J Biomed Mater Res A. 2009;88:1104-21.

[6] Kagami H, Agata H, Satake M, Narita Y. Considerations on designing scaffolds for soft and hard tissue engineering. Singapore: Pan Stanford Publishing; 2010.

[7] Kato R, Kaga C, Kanie K, Kunimatsu M, Okochi M, Honda H. Peptide array-based peptide-cell interaction analysis. Mini-Reviews in Organic Chemistry. 2010:in press.

[8] Kato R, Kaga C, Kunimatsu M, Kobayashi T, Honda H. Peptide array-based interaction assay of solid-bound peptides and anchorage-dependant cells and its effectiveness in cell-adhesive peptide design. J Biosci Bioeng. 2006;101:485-95.

[9] Kaushal S, Amiel GE, Guleserian KJ, Shapira OM, Perry T, Sutherland FW, et al. Functional

small-diameter neovessels created using endothelial progenitor cells expanded *ex vivo*. Nat Med. 2001;7:1035-40.

[10] Zhou M, Liu Z, Wei Z, Liu C, Qiao T, Ran F, et al. Development and validation of small-diameter vascular tissue from a decellularized scaffold coated with heparin and vascular endothelial growth factor. Artif Organs. 2009;33:230-9.

[11] Rotmans JI, Heyligers JM, Verhagen HJ, Velema E, Nagtegaal MM, de Kleijn DP, et al. *In vivo* cell seeding with anti-CD34 antibodies successfully accelerates endothelialization but stimulates intimal hyperplasia in porcine arteriovenous expanded polytetrafluoroethylene grafts. Circulation. 2005;112:12-8.

[12] Mutsuga M, Narita Y, Yamawaki A, Satake M, Kaneko H, Suematsu Y, et al. A new strategy for prevention of anastomotic stricture using tacrolimus-eluting biodegradable nanofiber. J Thorac Cardiovasc Surg. 2009;137:703-9.

[13] Hersel U, Dahmen C, Kessler H. RGD modified polymers: biomaterials for stimulated cell adhesion and beyond. Biomaterials. 2003;24:4385-415.

[14] de Mel A, Punshon G, Ramesh B, Sarkar S, Darbyshire A, Hamilton G, et al. In situ endothelialization potential of a biofunctionalised nanocomposite biomaterial-based small diameter bypass graft. Biomed Mater Eng. 2009;19:317-31.

[15] Hsu SH, Sun SH, Chen DC. Improved retention of endothelial cells seeded on polyurethane small-diameter vascular grafts modified by a recombinant RGD-containing protein. Artif Organs. 2003;27:1068-78.

[16] Beamish JA, Fu AY, Choi AJ, Haq NA, Kottke-Marchant K, Marchant RE. The influence of RGD-bearing hydrogels on the re-expression of contractile vascular smooth muscle cell phenotype. Biomaterials. 2009;30:4127-35.

[17] Jevon M, Ansari TI, Finch J, Zakkar M, Evans PC, Shurey S, et al. Smooth muscle cells in

porcine vein graft intimal hyperplasia are derived from the local vessel wall. Cardiovasc Pathol. 2010.

[18] Hillebrands JL, Klatter FA, van den Hurk BM, Popa ER, Nieuwenhuis P, Rozing J. Origin of neointimal endothelium and alpha-actin-positive smooth muscle cells in transplant arteriosclerosis. J Clin Invest. 2001;107:1411-22.

[19] Wang CH, Cherng WJ, Yang NI, Kuo LT, Hsu CM, Yeh HI, et al. Late-outgrowth endothelial cells attenuate intimal hyperplasia contributed by mesenchymal stem cells after vascular injury. Arterioscler Thromb Vasc Biol. 2008;28:54-60.

[20] Shapira OM, Xu A, Aldea GS, Vita JA, Shemin RJ, Keaney JF, Jr. Enhanced nitric oxide-mediated vascular relaxation in radial artery compared with internal mammary artery or saphenous vein. Circulation. 1999;100:II322-7.

[21] Radomski MW, Palmer RM, Moncada S. An L-arginine/nitric oxide pathway present in human platelets regulates aggregation. Proc Natl Acad Sci U S A. 1990;87:5193-7.

[22] Van de Wouwer M, Collen D, Conway EM. Thrombomodulin-protein C-EPCR system: integrated to regulate coagulation and inflammation. Arterioscler Thromb Vasc Biol. 2004;24:1374-83.

[23] Dzau VJ, Braun-Dullaeus RC, Sedding DG. Vascular proliferation and atherosclerosis: new perspectives and therapeutic strategies. Nat Med. 2002;8:1249-56.

Chapter 6

Concluding remarks

Biomaterials play a key role in creating a suitable environment for cells, and many biomaterials are used as scaffolds for many types of medical devices that are implanted in body. Many kinds of materials have been investigated and used in different manners. However, more suitable biomaterials are desired for the improvement of the patient's quality of life.

ECM, the natural scaffold and the peptides derived from ECM protein, is useful molecules for giving ideal features such as cell adhesion, proliferation and differentiation to biomaterials. The suitable biomaterial is important to construct the tissues that are composed of certain cells. Hence, cell-selective molecule is required as new biomaterials.

Peptide is one of the most attractive molecules to mimic the ECM and several peptide materials are investigated and reported. But there is little report that focuses on the cell-selectivity for the effective regeneration of the proper tissues. Therefore, the screening of cell-selective peptide using peptide array method was conducted, and the screened peptides were applied as the biomaterial.

In the Chapter 1, general introduction covering the importance of biomimetic materials including from ECMs to peptides and their applications for tissue engineering was discussed.

Considering these backgrounds, the objective and the strategy of this thesis were described.

In the Chapter 2, standardization scheme for datasets obtained from peptide array was established. Using standardizing datasets, the several cell-selective peptides could be effectively screened, and its applicability is applied in Chapter 3 and Chapter 4.

In the Chapter 3, single amino acid sequence preferences to control cell-selectivity were screened by peptide array method was described. Considering the application of cardiovascular medical devices, three kinds of cell, EC, SMC and FB, were compared. This study suggested that hydrophobic preference has the selectivity for EC adhesion and proliferation than the other cell types. Combinational effect of the physicochemical properties of the residues indicated that hydrophobic preference has similarly the EC selectivity.

In the Chapter 4, cell-selective peptides from collagen type IV-specific peptides were screened by peptide array method was described. Two kinds of cell, EC and SMC were chosen and several EC-selective and SMC-selective peptides were obtained by comparing the adhesion rate. EC-selective peptides were found to have some sequence flexibility, but maintain certain physiochemical rules. This sequence flexibility can be described as a C-X-G motif, where X is either A, N, S or D. One of the best EC-selective peptide, CAG peptide, was used for PCL polymer as the one example for the application of biomaterial. The evaluation of this polymer suggested that the EC-selectivity of the peptide existed on the surface of PCL fine-fiber sheet. This result suggested that cell-selective peptide screened from peptide array method could have the ability to apply for the construction of biomaterials.

In the Chapter 5, *in vivo* study using the small-caliber vascular grafts including the EC-selective peptide, CAG, in PCL polymer was examined. From immunofluorescent staining, the endothelialization of CAG group was significantly higher than of control group. From the examination of SEM, ECs were wide and adhere well to the surface of the CAG containing graft than the surface of control graft. Additionally, Western blot analysis showed that the endothelial nitric oxide synthase of CAG group was significantly higher than that of control group, and α-smooth muscle actin of CAG group was significantly lower than that of control group. Intimal hyperplasia was not observed in CAG group.

Thus the concept of cell-selective peptide screening was established and one of the peptide was able to apply for constructing the biomaterials *in vitro* and *in vivo*. In addition, ECMs has the cell-selectivity not only as strict peptide sequence, but also flexible peptide sequence of physicochemical preferences. And these data would be the support to understand the function of EMCs.

In the further work, the exhaustive investigation of wider varieties of cell-selective peptides to understand the function of ECMs is expected. Such concept could be achieved by constructing "clustered" peptide library *in silico* using amino acid physicochemical indices, and massively and effectively screen abundant types of cell-selective peptides (Idea is illustrated in **Fig. 1**).

Although we performed the *in vivo* experiment by using biomaterial that contains cell-selective peptide in Chapter 5, it should also be further examined. This is one example to apply the cell-selective peptide for constructing biomaterials. More varieties of cell-selective peptides should be applied as vascular graft material for long term implantation effect. I hope that my proposing type of "cell-selective peptides" will be used for a significant advance in the field of tissue engineering and biomaterial, and contribute to the improvement for human grateful life.

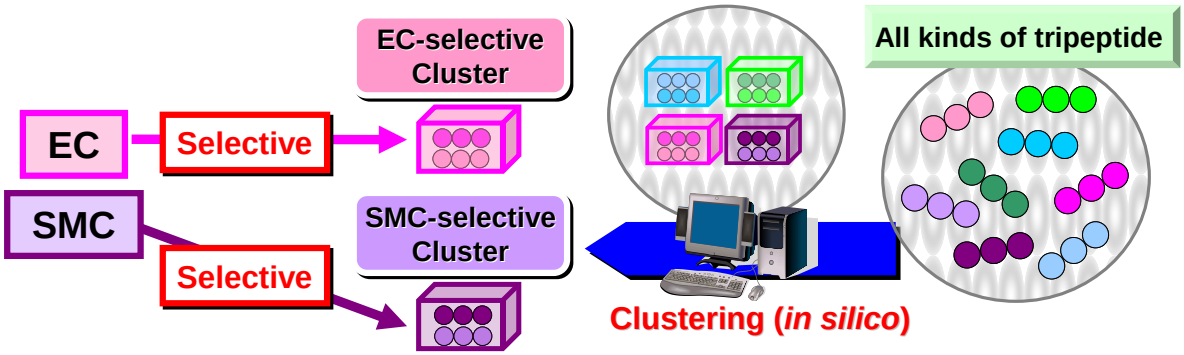

Figure 1 Exhaustive cell-selective peptide screening method by clustering analysis

List of publications

List of publications for dissertation

[1] Ryuji Kato, Chiaki Kaga, **Kei Kanie**, Mitoshi Kunimatsu, Mina Okochi and Hiroyuki Honda: Peptide array-based peptide-cell interaction analysis. *Mini-Reviews in Organic Chemistry*, (2011) in press

[2] **Kei Kanie**, Ryuji Kato, Zhao Yingzi, Yuji Narita, Mina Okochi and Hiroyuki Honda: Amino acid sequence preferences to control cell-specific organization of endothelial cells, smooth muscle cells, and fibroblasts. *Journal of Peptide science*, (2011) in press

[3] **Kei Kanie**, Yuji Narita, Junki Owaki, Yingzi Zhao, Fumiaki Kuwabara, Makoto Satake, Susumu Honda, Hiroaki Kaneko, Tomohiko Yoshioka, Mina Okochi, Hiroyuki Honda and Ryuji Kato: Specific tripeptides that contribute the cell-selectivity of extracellular matrixes. *Acta Biomaterialia* (submitting)

Other publications

[1] Mina Okochi, **Kei Kanie**, Masaki Kurimoto, Masafumi Yohda, and Hiroyuki Honda: Overexpression of prefoldin from the hyperthermophilic archaeum *Pyrococcus horikoshii* OT3 increased organic solvent tolerance of *Escherichia coli*. *Applied Microbiology and Biotechnology*, 79(3), 443-449 (2008)

[2] Katsutoshi Hori, Naoto Hiramatsu, Mari Nannbu, **Kei Kanie**, Mina Okochi, Hiroyuki Honda and Hisami Watanabe: Drastic change in cell surface hydrophobicity of a new bacterial strain, *Pseudomonas sp.* TIS1-127, induced by growth temperature and its effects on the toluene-conversion rate. *Journal of Bioscience and Bioengineering*, 107(3), 250-255 (2009)

[3] Rui Gan, Seiji Furuzawa, Takaaki Kojima, **Kei Kanie**, Ryuji Kato, Mina Okochi, Hiroyuki Honda and Hideo Nakano: Proposal of pumpless, valveless, and flowless miniaturized reactor using mangetic beads for the portable analysis device. *Journal of Bioscience and Bioengineering*, 109(4), 411-417 (2010)

Books

[1] 加藤 竜司, **蟹江 慧**, 加賀 千晶, 大河内 美奈, 長岡 利, 本多 裕之 『コレステロール低下機能性食品開発のためのカタログペプチドアレイによる胆汁酸結合ペプチド探索法』New Food Industry, 51(4), 67-74 (2009)

[2] **蟹江 慧**, 加藤 竜司, 成田 裕司, 本多 裕之『医療機器コーティングのためのペプチドマテリアル』バイオサイエンスとインダストリー, 解説, 68(6), 404-408 (2010)

Conference

International 12 times, Domestic 15 times

(The international conferences related this thesis are described below)

[1] Ryuji Kato, **Kei Kanie**, Chiaki Kaga, Mina Okochi, and Hiroyuki Honda: Effective Informatic Peptide Design Methodology for Short Cell Adhesive Peptides. *The Third International Conference on the Science and Technology for Advanced Ceramics (STAC-3)*, Yokohama, Japan, June, 17pP087 (p.168) (2009) (poster)

[2] **Kei Kanie**, Yingzi Zhao, Ryuji Kato, Yuji Narita, Mina Okochi, and Hiroyuki Honda: Discovering Cell Specific Preference on Short Peptides from ECM for Regenerative Stent. *2nd TERMIS World Congress*, Seoul, Korea, August, 951 (p.249) (2009) (poster)

[3] **Kei Kanie**, Yingzi Zhao, Ryuji Kato, Yuji Narita, Mina Okochi, Hiroyuki Honda: Screening for the functionality peptide for coating the medical device. *The 15th Symposium of Young Asian Biochemical Engineers' Community (YABEC)*, Xiamen, China, December, OP-D-4 (p.37) (2009) (oral)

[4] **Kei Kanie**, Ryuji Kato, Yuji Narita, Yingzi Zhao, Fumiaki Kuwabara, Makoto Satake, Hiroaki Kaneko, and Hiroyuki Honda: Screening of cell-specific adhesion peptides for medical device coating. *31th European Peptide Symposium (EPS)*, Copenhagen, Denmark, August, P177 (p.102) (2010) (poster)

[5] **Kei Kanie**, Ryuji Kato, Yuji Narita, Yingzi Zhao, Fumiaki Kuwabara, Makoto Satake, Susumu

Honda, Hiroaki Kaneko, and Hiroyuki Honda: Screening of cell-specific adhesion peptides for medical device coating. *The 16th Symposium of Young Asian Biochemical Engineers' Community (YABEC)*, Taiwan, China, November, D-14 (p.48) (2010) (poster)

[6] **Kei Kanie**, Ryuji Kato, Yuji Narita, Yingzi Zhao, Junki Owaki, Fumiaki Kuwabara, Makoto Satake, Susumu Honda, Hiroaki Kaneko, and Hiroyuki Honda: Screening of cell-specific adhesion peptides for medical device coating. *5th International Peptide Symposium (IPS)*, Kyoto, Japan, December, P1-170 (p. 178) (2010) (poster)

[7] Fumiaki Kuwabara, Yuji Narita, Aika Ogata, **Kei Kanie**, Ryuji Kato, Makoto Satake, Hideki Oshima, Akihiko Usui, and Yuichi Ueda: Novel small caliber vascular prosthesis with specific trimmer peptide. *The Society of Thoracic Surgeons (STS) 47th Annual Meeting*, San Diego, USA, January, 35 (pp. 136-137) (2011) (oral)

[8] Ryuji Kato, **Kei Kanie**, Yuji Narita, Fumiaki Kuwabara, Makoto Satake, Susumu Honda, Hiroaki Kaneko, Mina Okochi and Hiroyuki Honda: Enhancing regeneration of vascular graft using cell-specific peptide. *International Conference on Biomaterials Science (ICBS) 2011*, Tsukuba, Japan, March, (2011) (poster)

Award

[1] 化学工学会 第 41 回秋季大会 バイオ部会優秀ポスター賞, 『医療機器被覆のための機能性ペプチドの探索』, 広島, 2009 年 9 月

[2] 材料バックキャストテクノロジー研究センター 平成 21 年度 若手研究奨励賞, 2009 年 11 月

[3] 材料バックキャストテクノロジー研究センター 平成 22 年度 若手研究奨励賞, 2010 年 12 月

Acknowledgments

This study has been carried out in Bioprocess Engineering laboratory, Department of Biotechnology, School of Engineering, Nagoya University, Japan.

First of all, the author expresses his sincerest gratitude to his supervisor, Professor HONDA Hiroyuki, Department of Biotechnology, Graduate School of Engineering, Nagoya University, for his supreme leading, support and assistance for this research and also his human empathy. The author has been given a multiplicity of opportunities and encouragements to grow as a researcher and member of society by Professor HONDA.

The author expresses deep gratefulness to Professor IIJIMA Shinji and Associate Professor OKOCHI Mina, Department of Biotechnology, Graduate School of Engineering, Nagoya University, and Professor Hideo Nakano, Department of Bioengineering Sciences, Graduate School of Bioagricultural Science, Nagoya University, for their thoughtful advises to this research.

The author expresses deep appreciation to Assistant Professor KATO Ryuji, Department of Biotechnology, Graduate School of Engineering, Nagoya University, for his precise leading and a multiplicity of his thoughtful advises and encouragements. This research could never be completed without his helpful suggestions and precise thesis direction.

The author is most grateful to Associate Professor ITO Akira, Department of Chemical Engineering, Faculty of Engineering, Kyushu University, for his thoughtful advices and many encouragements.

The author expresses deep appreciation to Associate Professor NARITA Yuji, Department of Cardiac Surgery, Nagoya University Graduate School of Medicine, for his precise leading with the view point of medical science and a multiplicity of his thoughtful advises and encouragements.

This research could never be completed without his helpful suggestions and kind advices.

The author expresses deep appreciation to Dr. SATAKE Makoto, Mr. HONDA Susumu and Dr. KANEKO Hiroaki, Integrative Technology Research Institute, TEIJIN LIMITED. This research could never be completed without their helpful suggestions and techniques.

The author is most grateful to Assistant Professor YOSHIOKA Tomohiko, Department of Metallurgy and Ceramics Science, Tokyo Institute of Technology, for his thoughtful advices and many encouragements.

The author also expresses his sincere thanks to his collaborator, Mr. KUWABARA Fumiaki and Ms. Ogata Aika, Department of Cardiac Surgery, Nagoya University Graduate School of Medicine, for their many and grateful *in vivo* experiments.

The author appreciates deeply to his juniors in Bioprocess Engineering laboratory: Ms. ZHAO Yingzi support the study of Chapter 3 and Chapter 4, Mr. OWAKI Junki support the study of Chapter 4. The author is very glad to learn, discuss and prove this study together through his doctor course.

The author appreciates deeply to the member of “Baiyou” team, Dr. SHIMIZU Kazunori (presently Assistant Professor in Institute for Innovative NanoBio Drug Discovery and Development, Graduate School of Pharmaceutical Sciences, Kyoto University), Ms. NAKAGAWA Izumi and Mr. KURIMOTO Masaki, in Bioprocess Engineering laboratory for teaching the basic of research.

The author also appreciates deeply to the member of “Cell” team, Mr. ARINOBE Manabu, Ms. KAWASUMI Tamayo, Mr. TAKANO Sho, Ms. YAMAMOTO Wakana, Mr. USHIDA Yasunori, Mr. NAGURA Yoshihide, Mr. KAJIURA Keiichi, Mr. KOJIMA Kenji, Mr. MUKAIYAMA Kazunori, Mr. SASAKI Hiroto, Ms. MIWA Asuka, Mr. KONDO Yuto, Mr. TSUBOI Taiki, Ms. MATSUMOTO Megumi, Ms. NONOGAKI Yurika and Ms. OKADA Mai, in Bioprocess

Engineering laboratory for their earnest cooperation, helpful discussions, and precious friendships. Many thanks are due to all the members of Bioprocess Engineering laboratory for their creative discussions, warmhearted assistance, and valuable friendships.

Furthermore, the author is most grateful to Dr. TOMITA Yasuyuki, Dr. INO Kosuke (presently Assistant Professor in Graduate School of Environmental Studies, Tohoku University), Dr. KAGA Chiaki, Dr. ITO Hiroshi and Mr. NAKATOCHI Masahiro, for their precise leading, thoughtful advises, and many encouragements, in addition to sharing precious experiences and time in the laboratory together.

Finally, the author is expressing the deepest appreciation to his parents, his family members, and all of people who have supported his life and mind for devoting everything through the doctor course.

January, 2011, Kei KANIE